Тонкие химические технологии | Fine Chemical Technologies
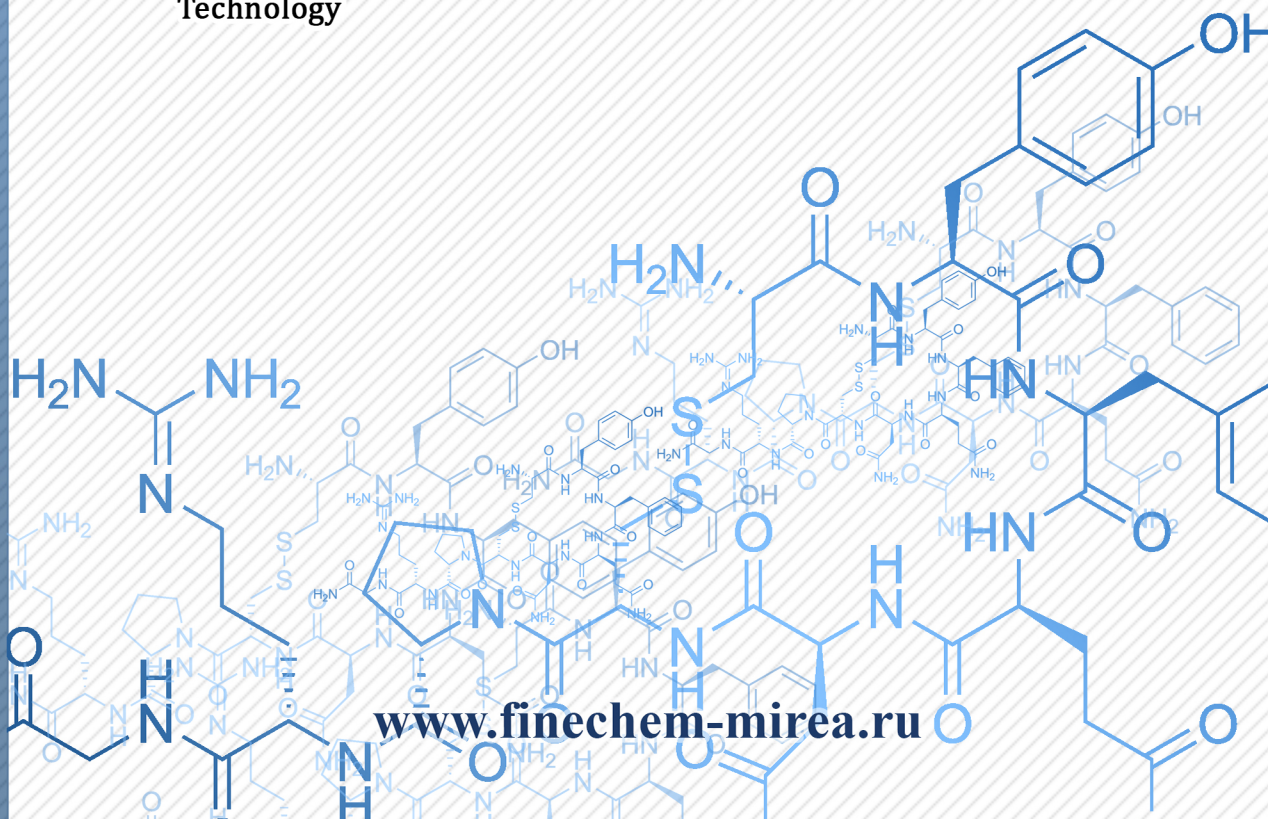
I Theoretical Bases of Chemical Technology

I Chemistry and Technology of Organic Substances

I Chemistry and Technology of Medicinal Compounds and Biologically Active Substances

I Biochemistry and Biotechnology

I Synthesis and Processing of Polymers and Polymeric Composites

I Chemistry and Technology of Inorganic Materials

I Analytical Methods in Chemistry and Chemical Technology

I Mathematical Methods and Information Systems in Chemical Technology

19(5)

2024

ТОНКИЕ ХИМИЧЕСКИЕ ТЕХНОЛОГИИ | Fine Chemical Technologies

Theoretical Bases of Chemical Technology

Chemistry and Technology of Organic Substances

Chemistry and Technology of Medicinal Compounds
and Biologically Active Substances

Biochemistry and Biotechnology

Synthesis and Processing of Polymers and Polymeric
Composites

Chemistry and Technology of Inorganic Materials

Analytical Methods in Chemistry and Chemical Technology

Mathematical Methods and Information Systems
in Chemical Technology

Tonkie Khimicheskie Tekhnologii =
Fine Chemical Technologies
2024, Vol. 19, No. 5

The peer-reviewed scientific and technical journal Fine Chemical Technologies highlights the modern achievements of fundamental and applied research in the field of fine chemical technologies, including theoretical bases of chemical technology, chemistry and technology of medicinal compounds and biologically active substances, organic substances and inorganic materials, biochemistry and biotechnology, synthesis and processing of polymers and polymeric composites, analytical and mathematical methods and information systems in chemistry and chemical technology.

Founder and Publisher

Federal State Budget
Educational Institution of Higher Education
"MIREA – Russian Technological University"
78, Vernadskogo pr., Moscow, 119454, Russian Federation.
Publication frequency: bimonthly.
The journal was founded in 2006. The name was Vestnik MITHT until 2015 (ISSN 1819-1487).

The journal is included into the List of peer-reviewed science press of the State Commission for Academic Degrees and Titles of the Russian Federation.

The journal is indexed: SCOPUS, DOAJ, Chemical Abstracts, Science Index, RSCI, Ulrich's International Periodicals Directory

Editor-in-Chief:

Andrey V. Timoshenko – Dr. Sci. (Eng.), Cand. Sci. (Chem.), Professor, MIREA – Russian Technological University, Moscow, Russian Federation. Scopus Author ID 56576076700, ResearcherID Y-8709-2018, https://orcid.org/0000-0002-6511-7440, *timoshenko@mirea.ru*

Deputy Editor-in-Chief:

Valery V. Fomichev – Dr. Sci. (Chem.), Professor, MIREA – Russian Technological University, Moscow, Russian Federation. Scopus Author ID 57196028937, http://orcid.org/0000-0003-4840-0655, *fomichev@mirea.ru*

Executive Editor:

Sergey A. Durakov – Cand. Sci. (Chem.), Associate Professor, MIREA – Russian Technological University, Moscow, Russian Federation, Scopus Author ID 57194217518, ResearcherID AAS-6578-2020, http://orcid.org/0000-0003-4842-3283, *durakov@mirea.ru*

Editorial staff:

Managing Editor	Cand. Sci. (Eng.) Galina D. Seredina
Editor	Sofya M. Mazina
Science editors	Dr. Sci. (Chem.), Prof. Tatyana M. Buslaeva
	Dr. Sci. (Chem.), Prof. Anatolii A. Ischenko
	Dr. Sci. (Eng.), Prof. Anatolii V. Markov
	Dr. Sci. (Chem.), Prof. Vladimir A. Tverskoy
Desktop publishing	Sergey V. Trofimov

86, Vernadskogo pr., Moscow, 119571, Russian Federation.
Phone: +7 (499) 600-80-80 (#31288)
E-mail: *seredina@mirea.ru*

Ivan A. Novakov – Academician at the RAS,
Dr. Sci. (Chem.), Professor, President of the Volgograd
State Technical University, Volgograd,
Russian Federation.
Scopus Author ID 7003436556, ResearcherID I-4668-2015,
http://orcid.org/0000-0002-0980-6591,
president@vstu.ru.

Alexander N. Ozerin – Corresponding Member of the RAS,
Dr. Sci. (Chem.), Professor, Enikolopov Institute
of Synthetic Polymeric Materials of the RAS,
Moscow, Russian Federation.
Scopus Author ID 7006188944, ResearcherID J-1866-2018,
https://orcid.org/0000-0001-7505-6090,
ozerin@ispm.ru.

Tapani A. Pakkanen – PhD, Professor, Department
of Chemistry, University of Eastern Finland, Joensuu,
Finland.
Scopus Author ID 7102310323,
tapani.pakkanen@uef.fi.

Armando J.L. Pombeiro – Academician at the Academy
of Sciences of Lisbon, PhD, Professor, President of the
Center for Structural Chemistry of the Higher Technical
Institute of the University of Lisbon, Lisbon, Portugal.
Scopus Author ID 7006067269, ResearcherID I-5945-2012,
https://orcid.org/0000-0001-8323-888X,
pombeiro@ist.utl.pt.

Dmitrii V. Pyshnyi – Corresponding Member of the RAS,
Dr. Sci. (Chem.), Professor, Institute of Chemical
Biologyand Fundamental Medicine, Siberian Branch
of the RAS, Novosibirsk, Russian Federation.
Scopus Author ID 7006677629, ResearcherID F-4729-2013,
https://orcid.org/0000-0002-2587-3719,
pyshnyi@niboch.nsc.ru.

Alexander S. Sigov – Academician at the RAS,
Dr. Sci. (Phys. and Math.), Professor, President
of MIREA – Russian Technological University, Moscow,
Russian Federation.
Scopus Author ID 35557510600, ResearcherID L-4103-2017,
sigov@mirea.ru.

Alexander M. Toikka – Dr. Sci. (Chem.), Professor,
Institute of Chemistry, Saint Petersburg State University,
St. Petersburg, Russian Federation.
Scopus Author ID 6603464176, ResearcherI D A-5698-2010,
http://orcid.org/0000-0002-1863-5528,
a.toikka@spbu.ru.

Andrzej W. Trochimczuk – Dr. Sci. (Chem.),
Professor, Faculty of Chemistry, Wrocław University
of Science and Technology, Wrocław, Poland.
Scopus Author ID 7003604847,
andrzej.trochimczuk@pwr.edu.pl.

Aslan Yu. Tsivadze – Academician at the RAS, Dr. Sci. (Chem.),
Professor, A.N. Frumkin Institute of Physical Chemistry
and Electrochemistry of the RAS, Moscow, Russian Federation.
Scopus Author ID 7004245066, ResearcherID G-7422-2014,
tsiv@phyche.ac.ru.

Новаков Иван Александрович – академик РАН,
д.х.н., профессор, президент Волгоградского
государственного технического университета,
Волгоград, Российская Федерация.
Scopus Author ID 7003436556, ResearcherID I-4668-2015,
http://orcid.org/0000-0002-0980-6591,
president@vstu.ru.

Озерин Александр Никифорович – член-корр. РАН,
д.х.н., профессор, Институт синтетических
полимерных материалов им. Н.С. Ениколопова РАН,
Москва, Российская Федерация.
Scopus Author ID 7006188944, ResearcherID J-1866-2018,
https://orcid.org/0000-0001-7505-6090,
ozerin@ispm.ru.

Пакканен Тапани – PhD, профессор, Департамент
химии, Университет Восточной Финляндии, Йоенсуу,
Финляндия.
Scopus Author ID 7102310323,
tapani.pakkanen@uef.fi.

Помбейро Армандо – академик Академии наук
Лиссабона, PhD, профессор, президент Центра
структурной химии Высшего технического института
Университета Лиссабона, Португалия.
Scopus Author ID 7006067269, ResearcherID I-5945-2012,
https://orcid.org/0000-0001-8323-888X,
pombeiro@ist.utl.pt.

Пышный Дмитрий Владимирович – член-корр. РАН,
д.х.н., профессор, Институт химической биологии
и фундаментальной медицины Сибирского отделения РАН,
Новосибирск, Российская Федерация.
Scopus Author ID 7006677629, ResearcherID F-4729-2013,
https://orcid.org/0000-0002-2587-3719,
pyshnyi@niboch.nsc.ru.

Сигов Александр Сергеевич – академик РАН,
д.ф.-м.н., профессор, президент МИРЭА – Российского
технологического университета, Москва,
Российская Федерация.
Scopus Author ID 35557510600, ResearcherID L-4103-2017,
sigov@mirea.ru.

Тойкка Александр Матвеевич – д.х.н., профессор,
Институт химии, Санкт-Петербургский государственный
университет, Санкт-Петербург, Российская Федерация.
Scopus Author ID 6603464176, Researcher ID A-5698-2010,
http://orcid.org/0000-0002-1863-5528,
a.toikka@spbu.ru.

Трохимчук Андржей – д.х.н., профессор, Химический
факультет Вроцлавского политехнического университета,
Вроцлав, Польша.
Scopus Author ID 7003604847,
andrzej.trochimczuk@pwr.edu.pl.

Цивадзе Аслан Юсупович – академик РАН, д.х.н.,
профессор, Институт физической химии и электрохимии
им. А.Н. Фрумкина РАН, Москва, Российская Федерация.
Scopus Author ID 7004245066, ResearcherID G-7422-2014,
tsiv@phyche.ac.ru.

Contents

СОДЕРЖАНИЕ

RESEARCH ARTICLE

Identification of hypoxene metabolites in urine samples using gas chromatography–tandem mass spectrometry for anti-doping control

Pavel V. Postnikov[1, ✉], Andrey V. Polosin[1], Nadezhda B. Savelieva[1], Sergey A. Kurbatkin[2], Yulia A. Efimova[2], Elena S. Mochalova[1]

[1] *National Anti-Doping Laboratory (Institute), M.V. Lomonosov Moscow State University (NADL MSU), Moscow, 105005 Russia*

[2] *MIREA – Russian Technological University (M.V. Lomonosov Institute of Fine Chemical Technologies), Moscow, 119571 Russia*

✉ *Corresponding author, e-mail: pletneva@mirea.ru*

Abstract

Objectives. Hypoxen is a drug which possesses antioxidant and antihypoxic effects. It achieves this by increasing the utilization of oxygen by mitochondria, intensifying oxidative phosphorylation, and as a result, improving tissue respiration. Athletes take it during prolonged exercise, in order to increase efficiency and reduce physical overwork. Since 2023, the World Anti-Doping Agency has included the drug in the monitoring program, in the belief that it can be used to gain a competitive advantage. It is thus a candidate for inclusion in the Prohibited List as a potential regulator of the human metabolism. Currently, there are no studies or scientific publications focusing on the identification of hypoxene in biofluids for the purpose of anti-doping control. The aim of this study is to determine the possible metabolites of the drug and their chromato-mass spectrometric characteristics in urine samples using gas chromatography–tandem mass spectrometry (GC–MS/MS) for doping control screening purposes.

Methods. Sample preparation of urine samples was carried out using enzymatic hydrolysis, liquid–liquid extraction and derivatization. The GC–MS/MS method was used for analysis. Screening of hypoxene metabolites was carried out in the mode of total ion current after fragmentation of selected parent ions.

Results. Three specific metabolites of hypoxene (m/z 342, 300, and 346, including trimethylsilyl derivatives) were identified in urine samples of volunteers ($n = 3$). They can act as markers for taking the target antihypoxant, and their possible structural formulas are given. The excretion curves of two metabolites with an m/z of 300 and 346 respectively in urine were studied. The maximum concentration is reached after 8–14 and 1.5–6 h, respectively. It was established, that these metabolites are reliably identified in urine 90 h or more after a single dose of the drug.

Conclusions. Possible structures of hypoxene metabolites in urine samples from volunteers were determined for the first time and their chromato-mass spectrometric characteristics were established. The approach developed in this study can be used for screening analysis of hypoxene for the purpose of anti-doping control.

Identification of hypoxene metabolites in urine samples using gas chromatography–tandem mass spectrometry for anti-doping control

Pavel V. Postnikov, *et al.*

НАУЧНАЯ СТАТЬЯ

Идентификация метаболитов гипоксена в образцах мочи методом газовой хроматографии – тандемной масс-спектрометрии с целью антидопингового контроля

П.В. Постников[1, ✉], А.В. Полосин[1], Н.Б. Савельева[1], С.А. Курбаткин[2], Ю.А. Ефимова[2], Е.С. Мочалова[1]

[1] *Национальная антидопинговая лаборатория (Институт), Московский государственный университет им. М.В. Ломоносова (НАДЛ МГУ), Москва, 105005 Россия*

[2] *МИРЭА – Российский технологических университет (Институт тонких химических технологий им. М.В. Ломоносова), Москва, 119571 Россия*

✉ *Автор для переписки, e-mail: drpavelpostnikov@gmail.com*

Аннотация

Цели. Гипоксен — лекарственный препарат, обладающий антиоксидантным и антигипоксическим эффектами за счет увеличения утилизации митохондриями кислорода, интенсификации окислительного фосфорилирования и, как следствие, улучшения тканевого дыхания. Спортсмены принимают его при длительных нагрузках для увеличения работоспособности и уменьшения физического переутомления. Всемирное антидопинговое агентство с 2023 г. внесло препарат в мониторинговую программу на основании того, что он является потенциальным регулятором метаболизма, т.е. может использоваться для получения конкурентного преимущества и быть претендентом на включение в Запрещенный список. В настоящее время отсутствуют какие-либо исследования и научные публикации по идентификации гипоксена в биожидкостях для антидопингового контроля. В связи с этим, целью работы было определение возможных метаболитов препарата и их хромато-масс спектрометрических характеристик в образцах мочи методом газовой хроматографии – тандемной масс-спектрометрии (ГХ–МС/МС) для скрининг-процедуры допинг-контроля.

Методы. Пробоподготовку образцов мочи проводили с применением ферментативного гидролиза, жидкость-жидкостной экстракции и дериватизации. Для анализа использовали метод ГХ–МС/МС. Скрининг метаболитов гипоксена осуществлялся в режиме полного ионного тока после фрагментации выбранных парент-ионов.

Результаты. В образцах мочи добровольцев ($n = 3$) идентифицированы три специфичных метаболита гипоксена (m/z 342, 300 и 346, включая триметилсилил-производные), которые могут выступать в качестве маркеров приема целевого антигипоксанта; приведены их возможные структурные формулы. Изучены кривые выведения двух метаболитов с m/z 300 и m/z 346 с мочой, максимальная концентрация которых достигается спустя 8–14 и 1.5–6 ч соответственно. Установлено, что данные метаболиты надежно идентифицируются в моче спустя 90 ч и более после однократного приема препарата.

Выводы. Впервые определены возможные структуры метаболитов гипоксена в образцах мочи добровольцев и установлены их хромато-масс-спектрометрические характеристики. Разработанный подход может быть применен для скринингового анализа с целью антидопингового контроля.

Identification of hypoxene metabolites in urine samples using gas chromatography–tandem mass spectrometry for anti-doping control

Pavel V. Postnikov,
et al.

INTRODUCTION

Hypoxen (sodium polydihydroxyphenylene thiosulfonate) is a group of synthetic quinone derivatives with a pronounced antihypoxic effect. The drug was created by Soviet scientists in the 1970s, and has been authorized for medical use since 1997 under the name *Olyphenum* [1]. The mechanism of its action is not fully understood, but an important role in this mechanism may be played by the following factors: a reduction of the damaging effect of reactive oxygen species on biomembranes; a reduction of lactate acidosis concentration in hypoxia conditions due to correction of the disturbed electrotransport function of mitochondrial enzyme complex (MEC-1) [1] and a reduction of calcium load in mitochondria. Hypoxene is able to lay an additional channel bypassing the damaged first and second complexes of the mitochondrial respiratory chain, which contributes to the restoration of the formation of adenosine triphosphate and creatine phosphate, disturbed by a variety of factors [1]. In addition to the antihypoxic effect, the drug has pronounced pro- and antioxidant properties [2–3]. Thus, it can activate adrenaline autooxidation by 213%[1] and also suppresses the formation of superoxide anion O^{2-}. Its antioxidant properties are due to the fact that hydroxyl groups of polyhydrophenylene structure easily give up the hydrogen atom and can bind free radicals.

The clinical efficacy of the drug has been demonstrated in many scientific studies [4–8]. It is used in complex treatment and in the recovery period after pneumonias and acute bronchitis. It can also be used in alcohol intoxication [7], for the prevention of heart attacks, angina pectoris and strokes [4], in increased physical exertion and hypoxia, and it has a gastroprotective effect [8]. Hypoxene has been used in pharmacological training of athletes for more than a decade as a means of increasing the body's resistance to hypoxia and increasing performance by restoring the disturbed processes of adenosine triphosphoric acid formation [9]. Nevertheless, certain aspects of its effect on a number of body systems of athletes remain unexplored.

As of 2023, the World Anti-Doping Agency (WADA) has placed hypoxene on the monitoring program as a potential metabolic regulator with the wording "to assess inappropriate in- and out-of-competition use

in sport"[2]. The drug may end up on the Prohibited List[3] as early as 2025. In this regard, the anti-doping community is faced with the task of its identification in biological fluids. There is no information in scientific literature regarding the identification of the drug for the purpose of anti-doping control in human biofluids, or on the study of its metabolism and pharmacokinetics. The only information given concerns the confirmation of the synthesized structure by matrix activated laser desorption/ionization (MALDI) [10], electron paramagnetic resonance and IR spectroscopy [10, 11]. For the first time, our article proposes an analytical approach based on the gas chromatography-triple quadrupole tandem mass spectrometry (GC–MS/MS) method for the detection of possible metabolites of hypoxene in urine samples of volunteers for the purpose of anti-doping control.

EXPERIMENTAL

Reagents and objects of analysis

For the experiments we used hypoxene, purchased in the pharmacy network, produced by the *Olifen Corporation* (Moscow, Russia), and urine samples of several volunteers ($n = 3$) who had not previously taken hypoxene, quinone derivatives or any dietary supplements at the age of 35 ± 7 years. The volunteers' gender was not taken into account. The drug is sold through pharmacy chains and is authorized for use as an over-the-counter product. In order to search for possible metabolites, volunteers took the drug according to the following scheme: Day 1 — 5 capsules, Day 2 — 6 capsules, Day 3 — 7 capsules, at the same time in the afternoon, having previously passed a blank urine before the course of intake. Urine samples were collected in sterile 80 mL urine containers, labeled, stored at +4°C and analyzed the next day.

To study the excretion of hypoxene, three other volunteers took a single therapeutic dose of the drug (8 capsules), after which urine samples were collected daily for a period of 7 days according to the following scheme: on the first two days every 3–5 h, the following days—once in the morning on an empty stomach. Samples with the date and time of collection were also stored at +4°C or frozen at −20°C until sample

---

[1]   Study of the mechanism of antihypoxic action of artificial quinone derivatives. Grant No. 04-04-97279. 2004. URL: https://www.elibrary.ru/item.asp?edn=cwevtp. Accessed January 21, 2024.

[2]   The 2024 Monitoring Program. URL: https://www.wada-ama.org/sites/default/files/2023-09/2024_list_monitoring_program_en_final_22_september_2023.pdf. Accessed January 29, 2024.

[3]   The 2024 List of prohibited substances. URL: http://rusada.ru/upload/iblock/836/drtkaf3eckdo1jrnjxacdwqkbm054m1n/Запрещенный%20список%202024%20(1).pdf. Accessed January 29, 2024.

Identification of hypoxene metabolites in urine samples using gas chromatography–tandem
mass spectrometry for anti-doping control

Pavel V. Postnikov,
et al.

preparation. The work was performed in accordance with the WADA Code of Ethics (WADA Code of Ethics)[4]: written permission was obtained from volunteers to use their biological material for research.

As an internal standard, 17α-methyltestosterone (certified standard, 1 mg/mL solution, *NMI*, Australia) was used. Also used in the experiment were diethyl ether and *n*-pentane from *JT Baker* (Netherlands); anhydrous sodium sulfate, carbonate, potassium hydrogen carbonate, DL-dithiothreitol, ammonium iodide, potassium dihydrophosphate, sodium phosphate bivalent dihydrate, sodium azide from *Sigma-Aldrich* (USA); compressed argon 5.0 with a purity of at least 99.999% and helium compressed 6.0 with a purity of at least 99.999% (Russia). *N*-methyl-*N*-(trimethyl)trifluoroacetamide from *Macherey-Nagel* (Germany) was used for derivatization. For hydrolysis, β-glucuronidase from *E. Coli* K12 (*Roche Diagnostics*, Germany). Deionized water, with a specific resistance of 18.2 MOhm·cm, was used for preparation of buffer solutions.

Auxiliary equipment

Solid-state heater with programmable temperature (*Thermo*, USA); crimper, decapper, polypropylene vials with silanized inserts of 0.2 mL (*Macherey-Nagel*, Duren, Germany); automatic variable volume pipettes 500–5000 µL, 10–200 µL (*Eppendorf*, Germany) and tips for them; tabletop centrifuge with horizontal rotor Rotixa 50 RS (*Hettich*, Germany); automatic shaker; OHaus Discovery DV215CD analytical scales (5 digit accuracy) (*OHaus Corp*, Switzerland); glass tubes with screw caps 16 × 125 mm; Vortex liquid shaker (*Scientific industries Inc.*, USA); low-temperature liquid thermostat (−30 ± 5°C) (*Grant Instruments*, United Kingdom); incubator thermostat (55 ± 3°C) (*Binder*, Germany); HP Ultra-1 gas chromatography column 17 m × 0.2 mm, 0.11 µm (*Agilent*, USA).

Sample preparation

For the sample preparation of urine samples of the volunteers before (negative control) and after drug administration, 16 mL glass tubes were used and 3 mL urine samples were taken for analysis [10]. A buffer mixture of 1 mL for hydrolysis was added to each tube. The buffer mixture for hydrolysis was prepared as follows: 54 g Na_2HPO_4-$2H_2O$, 68 g K_2HPO_4 and 1 g sodium azide were brought to 1000 mL with deionized water (pH 6.2–6.5). Next, the contents of

2 vials of β-glucuronidase (2 × 15 mL) were transferred into a 1000 mL measuring flask, 150 µL of 1-mg/mL methyltestosterone solution (internal standard) was added. Then a freshly prepared phosphate buffer solution was brought to the mark. The tubes were then shaken on a Vortex type apparatus and incubated for 60 ± 10 min in a thermostat at 55 ± 3°C. After that, 1–2 g of anhydrous sodium sulfate was added to each tube, shaken for 10 s, 1 mL of carbonate buffer solution was added, and shaken again for 5–10 s. The carbonate buffer solution was added to each tube (carbonate buffer solution was prepared as follows: 60 g each of K_2CO_3 and $KHCO_3$ were weighed and the solution was brought to 800 mL with deionized water (pH 9.6–9.9). The resulting solution was stored in a dark glass bottle). After cooling, 5 mL of diethyl ether (or *n*-pentane) was added and stirred for 20 ± 5 min on a rotary shaker for liquid–liquid extraction. The solution was centrifuged for 3–4 min at 3000 rpm and the tubes were placed in a low-temperature liquid thermostat. The organic solvent was then transferred to derivatization tubes and evaporated to dryness at 70 ± 5°C for 20–30 min. Derivatization reagent of 50 µL was added to each tube and heated at 70 ± 5°C for 25 min. Subsequently, the reaction mixture was cooled and transferred to vials with silanized glass inserts, tightly closed and analyzed.

Parameters of instrumental analysis by gas chromatography–triple quadrupole tandem mass spectrometry

A GC–MS/MS analysis was performed using a Trace 1310 gas chromatograph coupled to a TSQ Quantum XLS triple quadrupole mass spectrometer and a TriPlus RSH autosampler (*Thermo Fisher Scientific*, USA). The chromatographic column was Agilent HP Ultra 1 (20 m × 0.18 mm, film thickness 0.18 µm). The carrier gas was helium (purity 6.0), flow rate 1.1 mL/min. The injector temperature and at the interface line device was 280°C, and the ion source (Trace GC Ultra) temperature was 270°C. The interface temperature is 300°C. Sample injection was carried out in flow division mode (1 : 20), and the volume of injected sample was 2 µL. Temperature program: the initial starting temperature is 179°C; next rise to 235°C at a rate of 4°C/min and rise to 310°C at a rate of 20°C/min; delay time is 4.25 min. The signal-to-noise (S/N) ratio was considered to be 3 : 1. Mass spectrometer: onset of ion current registration is 2.9 min; emission current 35–100 µA; scan rate 3.3 scans/min; and target gas—argon with

---

Identification of hypoxene metabolites in urine samples using gas chromatography–tandem mass spectrometry for anti-doping control

Pavel V. Postnikov,
et al.

the pressure 1 mTorr. Ion transmission width at the first and third quadrupoles is 0.7. Metabolites were detected in the scanning mode of total ion current from specific precursor ions.

RESULTS AND DISCUSSION

According to the information given in [13], hypoxene (*Olyphenum*) may consist of a polymer chain of hydroquinone links (2 to 6 links) linked covalently with each other in meta-positions, and is the sodium salt of poly-(2,5-dihydroxyphenylene)-4-thiosulfonic acid. It has been previously shown [10] that there may be more hydroquinone links in such compounds, and its molecular mass ranges from 352 to 784 g/mol. The structural formula of the active substance of the medicinal product is presented in Fig. 1.

As stated earlier, there is no information or scientific publications in the public domain about possible metabolites of the drug and their identification in human biological fluids. We compared for the first time chromatograms of urine samples of volunteers before and after administration of maximum daily doses of hypoxen. As a result, 4 compounds were detected (Figs. 2–5), three of which are absent in blank urine and may be specific metabolites of sodium hypoxene (polydihydroxyphenylene thiosulfonate) ingestion (indicated by red arrows in Figs. 3–5). The intensity of the peaks of these substances correlates with the doses of the drug taken.

The two substances found with retention times of 5.27 min (*m/z* 254) and 5.44 min (*m/z* 182) correspond to trimethylsilyl derivatives (TMS-derivatives) of hydroquinone. However, they cannot be used for doping control purposes, as hydroquinone is naturally present in the body and is used in food production as an antioxidant.

After appropriate sample preparation, TMS-derivatives of hydroquinone were detected both in the blank urine of volunteers and in the aqueous solution of the drug and urine samples after its administration. In addition, hydroquinone itself can presumably also act as a byproduct in the synthesis of the drug.

Three other substances with retention times of 8.99, 9.55, and 13.41 min were not detected in blank urine, although they were present in the aqueous solution of the drug and samples after administration of different doses of the drug. Thus, they can be deemed substances of exogenous origin. Figures 3–5 compares the chromatogram sections of blank urine samples and samples after hypoxene administration. They show the mass spectra of possible substances-metabolites of hypoxene which can be used as markers of antihypoxant administration. No interfering peaks were observed
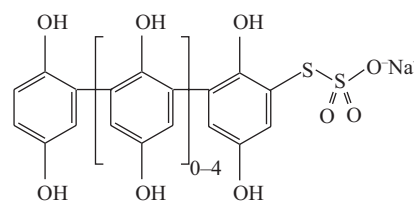
Fig. 1. Structural formula of hypoxene

when comparing the chromatograms of urine samples from volunteers before and after drug administration. In order to confirm the exogenous origin of each of these substances, a sample preparation of a solution of hypoxene in water was performed. We assumed that three ions determined in the full ion current scan mode from specific precursor ions, an *m/z* of 300, 342, and 346, could be characteristic for the determination of drug metabolites (Figs. 3c, 4c, and 5c). The inferred fragmentation patterns of these ions are shown in Fig. 6. Thus, the substance with an *m/z* of 342 may contain three hydroquinone fragments in its structure, and the thiosulfonate group may be replaced by –OH (Fig. 6a), corresponding to the information given [10]. In addition, the reason for this substitution may be the instability of the latter group to heating and the use of alkaline carbonate buffer with pH 9.6–9.9 during sample preparation. Also, this substance, presumably, can be formed as a byproduct during the synthesis of the drug.

Closest in structure to the metabolite of hypoxene is a substance with an *m/z* of 346 (Fig. 5). It is a silylated derivative of sodium dihydroxyphenylene thiosulfonate consisting of two hydroquinone links.

Also, one of the metabolites (*m/z* 300) may contain a mercapto group instead of thiosulfonate (Fig. 6b).

In general, the presence of closely related structures in urine samples of volunteers after administration of the drug with or without any of the –SH, –OH, –S–SO$_2$–ONa, or –CH$_3$ functional groups cannot be ruled out (Fig. 6).

When studying the excretion of the drug from the body, it was found that hypoxene is a mixture of homologs with a different number of hydroquinone links in their structure. The composition of the drug is heterogeneous and may differ from series to series. Thus, the metabolite with an *m/z* of 342 was present in urine samples of all volunteers taking the drug of series 170522 (Serial number Y9aYRMYBoBe6c), but was absent after taking series 220622 (Serial number ApfKe3z2WOmo3). The presence of metabolites with an *m/z* of 300 and 346 respectively was confirmed in urine samples after ingestion of both the above mentioned hypoxene series.

Identification of hypoxene metabolites in urine samples using gas chromatography–tandem
mass spectrometry for anti-doping control

Pavel V. Postnikov,
et al.
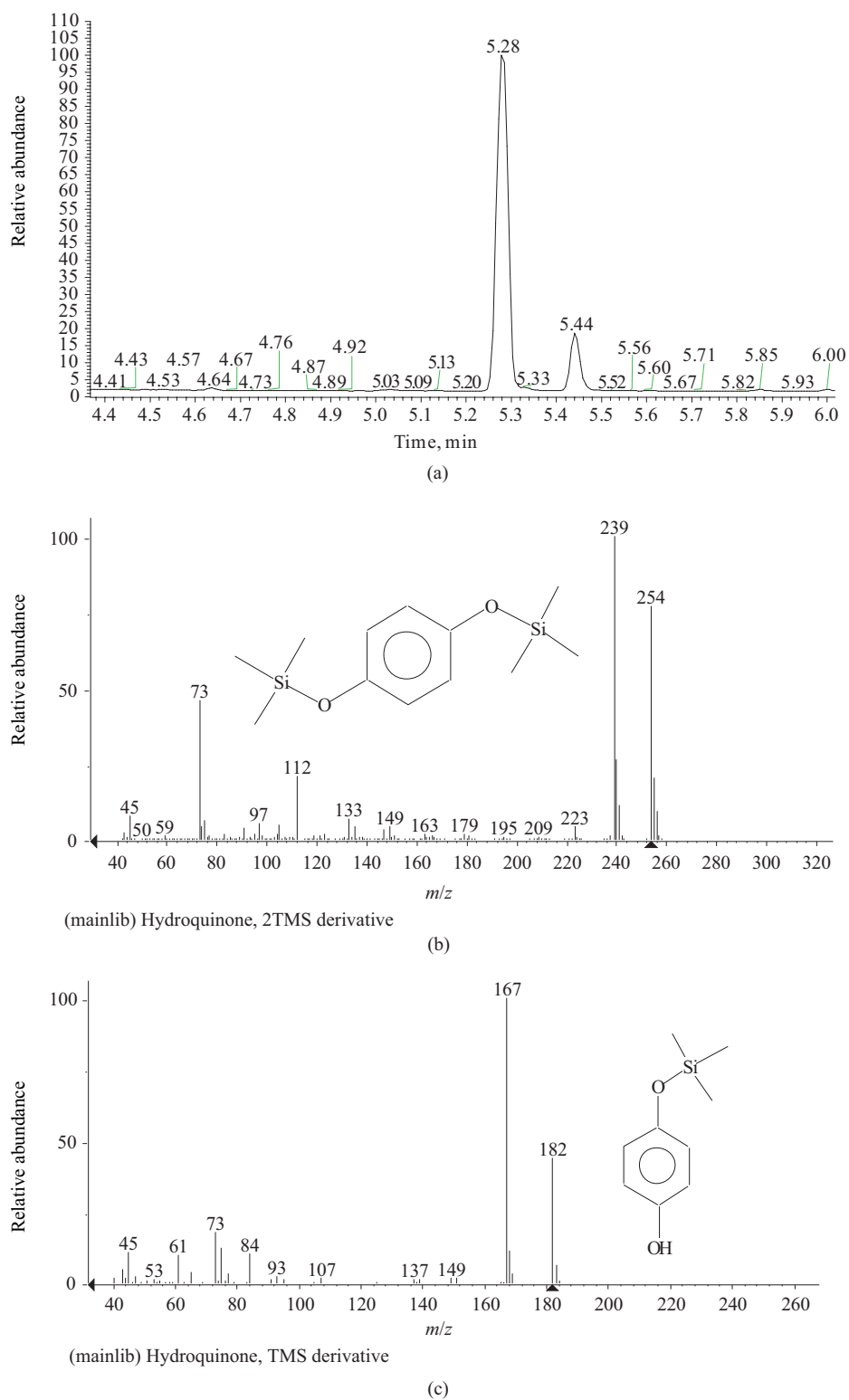
Fig. 2. Chromatogram (a) and mass spectra (b, c) of TMS derivatives of hydroquinone

Identification of hypoxene metabolites in urine samples using gas chromatography–tandem
mass spectrometry for anti-doping control

Pavel V. Postnikov,
et al.
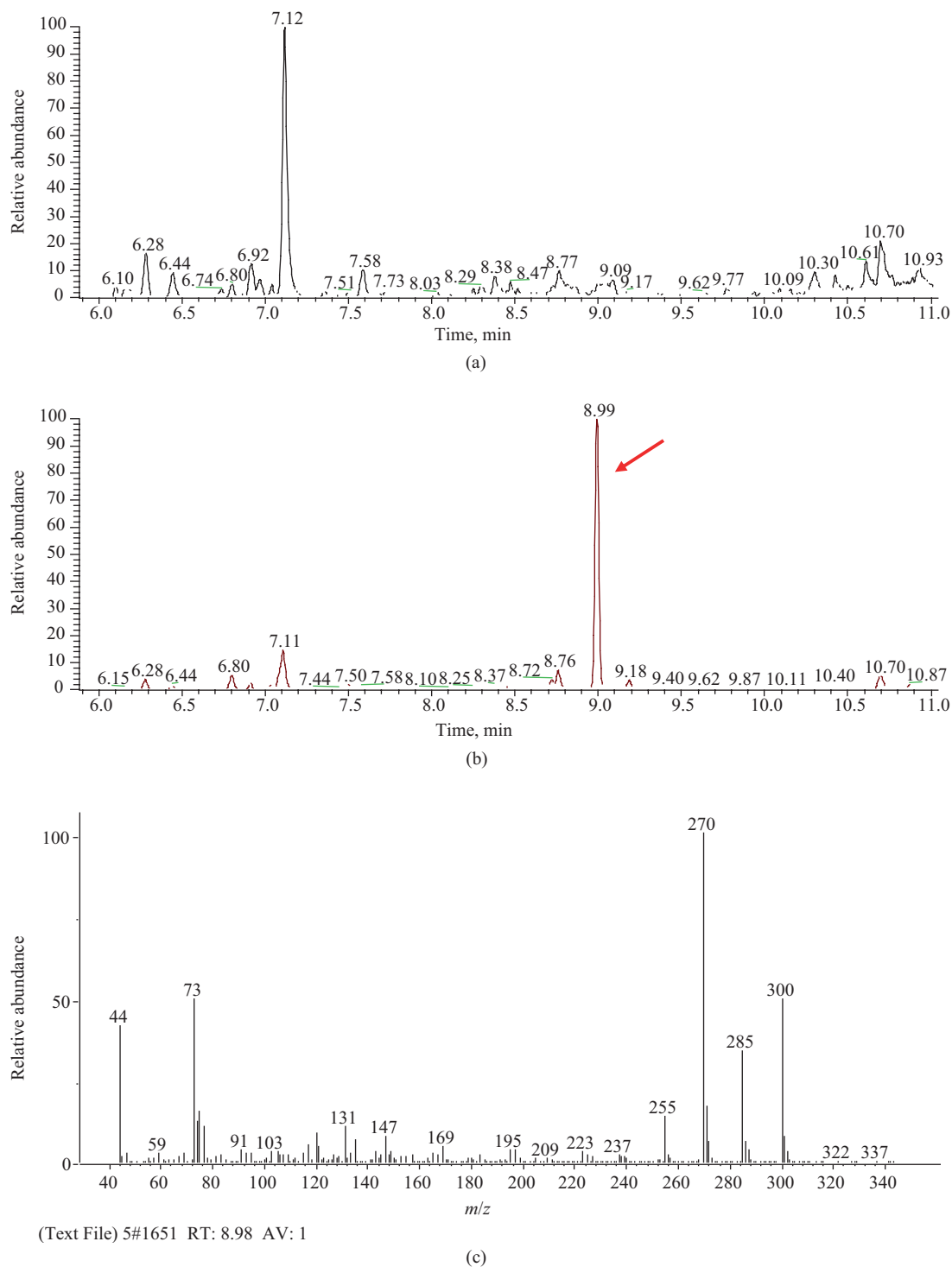
Fig. 3. Chromatogram of a urine sample of a volunteer before (a), after (b) drug administration and mass spectrum (c) of the detected substance with a retention time of 8.99 min. The red arrow indicates the peak of hypoxene metabolite.

Identification of hypoxene metabolites in urine samples using gas chromatography–tandem
mass spectrometry for anti-doping control

Pavel V. Postnikov,
et al.
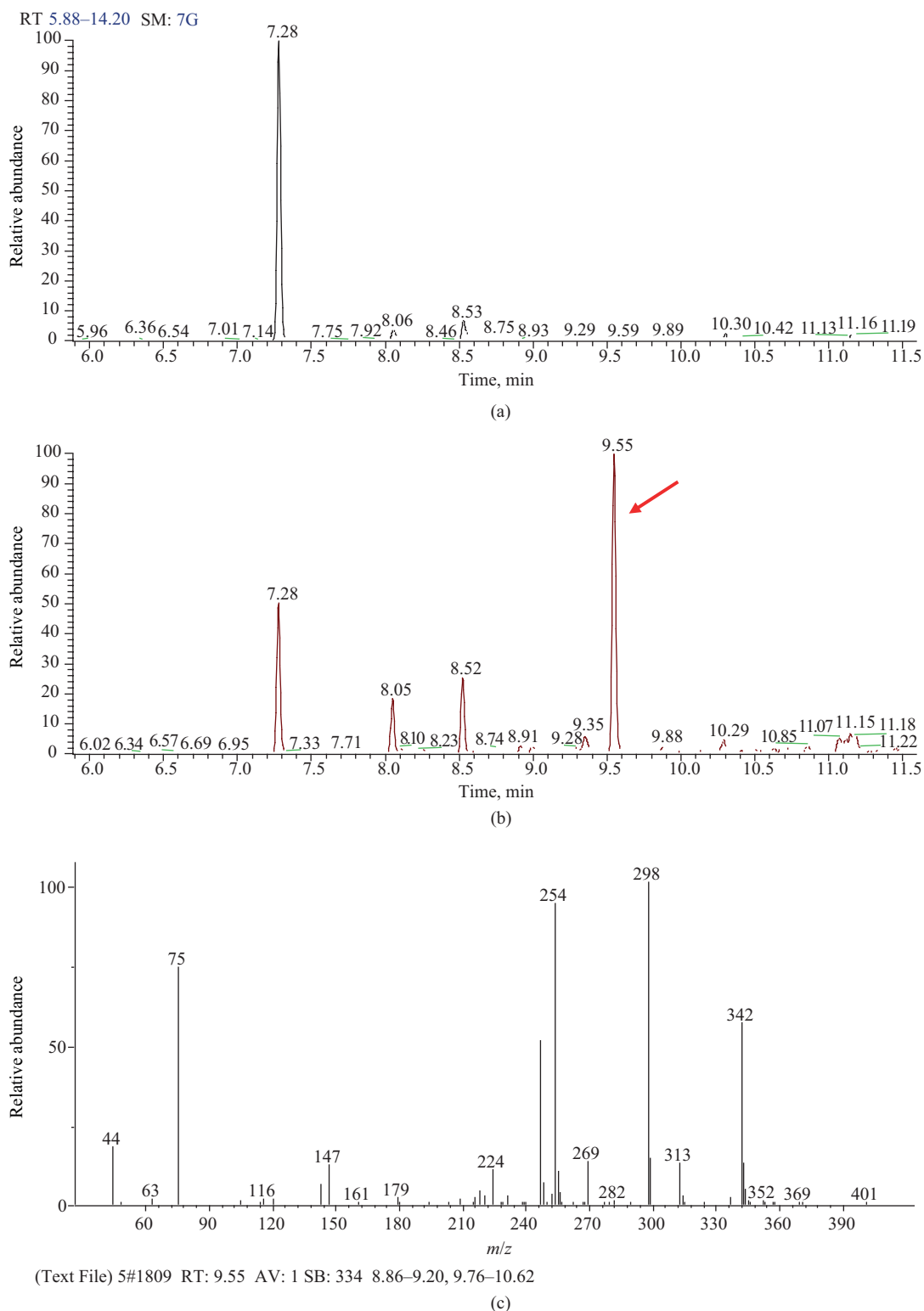
Fig. 4. Chromatogram of a urine sample of a volunteer before (a), after (b) drug administration and mass spectrum (c) of the detected substance with a retention time of 9.55 min. The red arrow indicates the peak of hypoxene metabolite

Identification of hypoxene metabolites in urine samples using gas chromatography–tandem
mass spectrometry for anti-doping control

Pavel V. Postnikov,
et al.
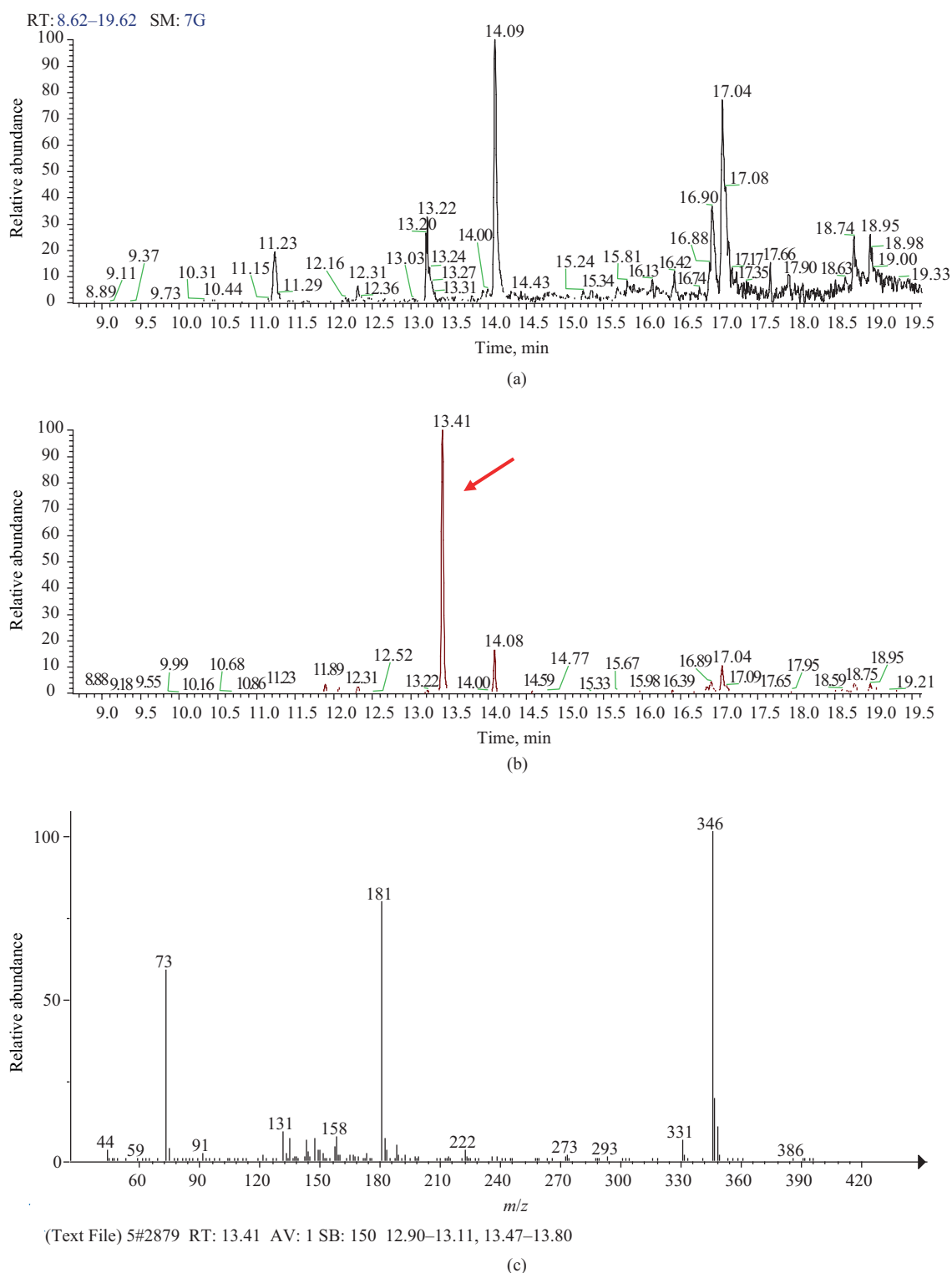
Fig. 5. Chromatogram of a urine sample of a volunteer before (a), after (b) drug administration and mass spectrum (c) of the detected substance with a retention time 13.41 min. The red arrow indicates the peak of hypoxene metabolite

Identification of hypoxene metabolites in urine samples using gas chromatography–tandem
mass spectrometry for anti-doping control

Pavel V. Postnikov,
et al.
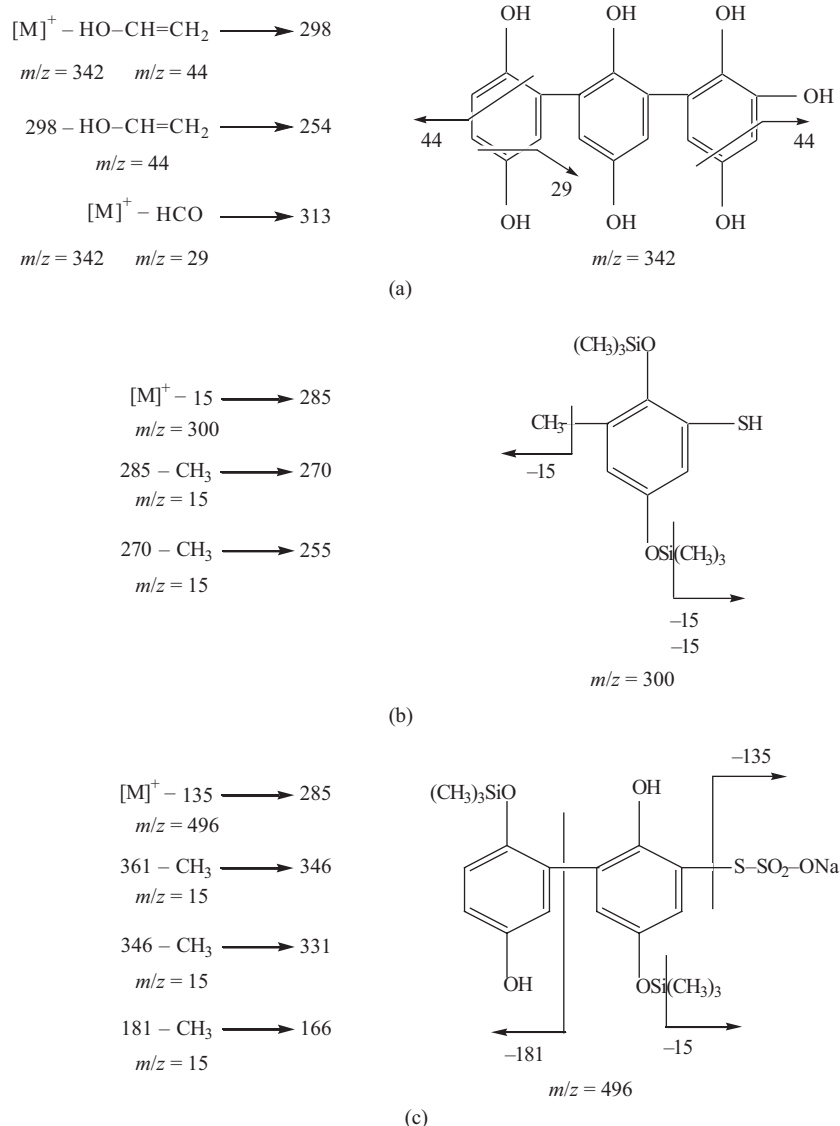
Fig. 6. Proposed fragmentation patterns of ions with m/z of 342 (a), 300 (b), and 346 (c) and proposed structural formulas of hypoxene metabolites (including TMS derivatives)
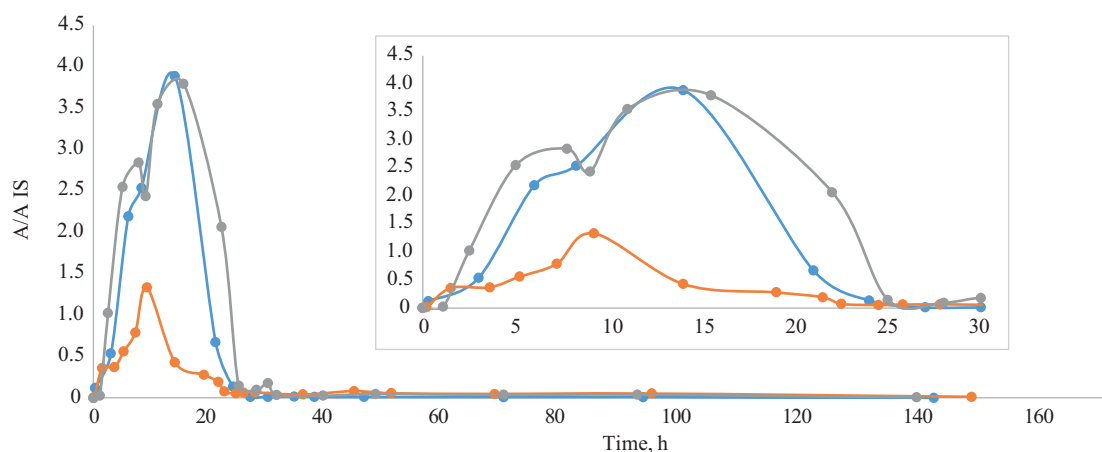
Fig. 7. Urinary excretion curves of hypoxene metabolite with an m/z of 300 for three volunteers. The first 30 h after a single administration of hypoxene (2 g, 8 capsules) are plotted separately. A/A IS is the ratio of the substance peak area to the internal standard peak area

Identification of hypoxene metabolites in urine samples using gas chromatography–tandem
mass spectrometry for anti-doping control

Pavel V. Postnikov,
et al.
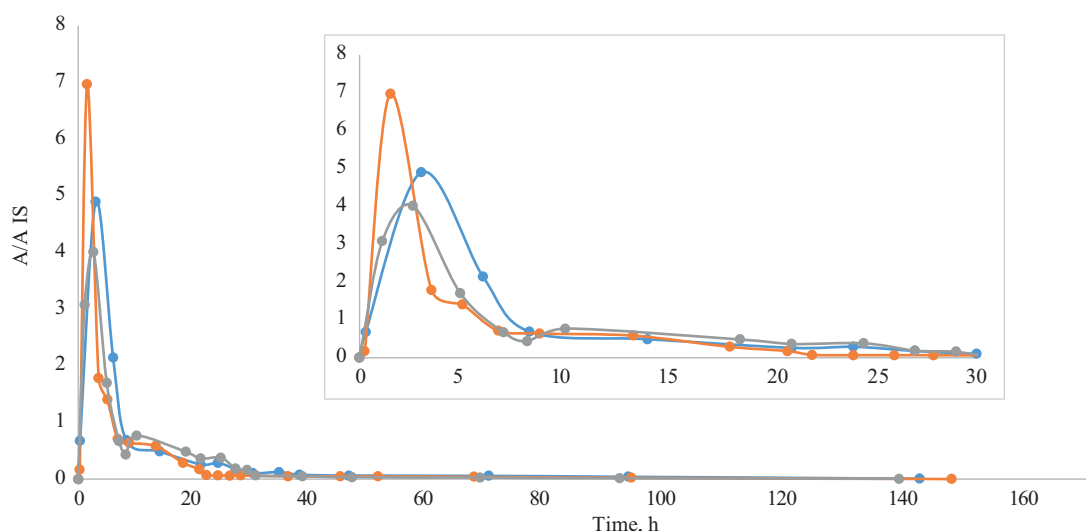
Fig. 8. Urinary excretion curves of hypoxene metabolite with *m/z* of 346 in three volunteers. The first 30 h after a single administration of hypoxene (2 g, 8 capsules) are plotted separately. A/A IS is the ratio of the peak area of the substance to the peak area of the internal standard

Figures 7 and 8 show the excretion curves of metabolites with an *m/z* of 300 and 346 of hypoxene.

The above data shows that for the metabolite with an *m/z* of 300, the maximum concentration in the urine of volunteers is reached 8–14 h after the drug administration (8 capsules once). Moreover, even after 90 h or more, this metabolite can be reliably detected. However, in a urine sample taken 2 weeks after a single dose of hypoxene, it is no longer present (data not shown). For the metabolite with an *m/z* of 346, the maximum concentration in urine can be determined as early as 1.5–6.0 h after administration, and it is reliably detected in urine more than 90 h after administration. However, it too cannot be identified after 2 weeks or more (data not shown). It is possible that hypoxene has a cumulative effect, and if multiple doses or courses of administration are administered, its excretion time may be significantly increased. However, this is an area for further investigation. When taking a single dose, the volunteers did not feel any sudden onset of strength, vigor or other effect. One experienced slight dizziness which passed after a few hours.

The main candidates for inclusion in the WADA banned list are primarily substances from the monitoring program. Hypoxene, which has been included in this program since 2023, may be banned as early as 2025. This is similar to meldonium which was previously included in the training regimens of Russian and CIS[5] athletes. This sulfur-containing oligoquinone can be

classified under Item 4 "Metabolic Modulators" of Article S4 "Hormones and Metabolic Modulators," including AMP[6]-activated protein kinase activators, mildronate and trimetazidine, which are antihypoxants of direct energizing action. Post-load reoxygenation due to increasing oxidative stress is a major component of post-hypoxic cell damage [11, 12]. In view of this, various antioxidants, including hypoxene, are actively used for antihypoxic therapy by activating oxidative phosphorylation and reducing the formation of reactive oxygen species. As mentioned earlier, hypoxene is used in sports medicine to restore the body after prolonged physical exertion and increase performance capacity.

Murzaeva *et al.* [13] conducted experiments on the effect of hypoxene on the bioenergetic processes in rat liver and heart mitochondria. They concluded that in the concentration of 0.05–10 μg/mL the drug increases the conjugation of respiratory chain work, stimulates respiration and partially reduces the accumulation of H_2O_2. Ignatiev *et al.* [14] studied the effect of this polyquinone on gas exchange parameters, exercise tolerance, and dyspnea severity in chronic obstructive pulmonary disease of moderate and severe course. Clinically significant changes were obtained in the assessment of dyspnea severity. The number of patients with clinically significant improvement reached 46% after a 6-month course of hypoxene administration. The authors also stress that on-demand salbutamol use decreased by 0.5 doses per patient during hypoxene when

---

[5]   CIS— Commonwealth of Independent States.

[6]   AMP—adenosine monophosphate.

Identification of hypoxene metabolites in urine samples using gas chromatography–tandem mass spectrometry for anti-doping control

Pavel V. Postnikov,
et al.

compared with data at the start of therapy. Improvement of patients' exercise tolerance was also noted: saturation increased and recovery period was shortened.

CONCLUSIONS

During the first pilot studies on the identification of possible metabolites of hypoxene by GC–MS/MS method, we identified 5 substances, 3 of which are specific for the drug administration and can indicate its presence in biological fluids of volunteers (*m/z* 300, 342, and 346). It was found that hypoxene is a mixture of homologues with a differing number of hydroquinone links in its structure. The composition of the drug is heterogeneous and may differ from series to series. The article presents structural formulas and fragmentation schemes of metabolites, two of which (with an *m/z* of 300 and 346, respectively) can be unambiguously identified from series to series. Their excretion curves with urine are given. It was found that the maximum concentration of these metabolites in urine is reached after 8–14 h and 1.5–6 h, respectively. It was also observed that they were reliably detected by GC–MS/MS for a period of more than 90 h after a single dose of 2 g (8 capsules). Hydroquinone derivatives are present in the urine of almost every human being. Therefore, for the purposes of doping control, the monitored substance needs to be distinguished from substances with a similar structure, possibly ingested with food. At the moment, the selection of optimal selective reaction monitoring transitions is underway to determine hypoxene metabolites and obtain more accurate data on the time of their elimination from the body.

The search for markers of the presence of new substances from the WADA monitoring program has undoubted practical significance for the purposes of modern anti-doping control, since hypoxene is a potential candidate for inclusion in the Prohibited List in 2025, and the methods of its determination and identification criteria have not yet been developed.

Authors' contributions

P.V. Postnikov—writing the text of the article, formulation of aims and objectives, development of a plan for conducting experiments, conducting experimental research, discussion of experiments and results, editing the manuscript, editing the final version of the article, and preparing materials for publication.

A.V. Polosin—conducting experimental research, discussion of experiments and results.

N.B. Savelieva—discussion of experiments and results, preparing materials for publication.

S.A. Kurbatkin—preparing materials for publication.

Yu.A. Efimova—editing the manuscript and preparing materials for publication.

E.S. Mochalova—preparing materials for publication.

The authors declare no conflicts of interest.

REFERENCES

1. Levchenkova O.S., Novikov V.E., Pozhilova E.V. Pharmacodynamics of antihypoxants and their clinical use. *Obzory po klinicheskoi farmakologii i lekarstvennoi terapii = Reviews on Clinical Pharmacology and Drug Therapy.* 2012;10(3):3–12 (in Russ.). https://doi.org/10.17816/RCF1033-12

2. Shatalin Yu.V., Naumov A.A., Potselueva M.M. A comparison of antioxidant properties of hypoxen and duroquinone by the method of chemiluminescence. *Biofizika.* 2008;53(1):100–106 (in Russ.).

3. Murzaeva S.V., Belova S.P., Mironova G.D. Determination of the antioxidant properties of activators of mitochondrial ATP-dependent potassium channels with the Amplex Red fluorescent indicator. *Appl. Biochem. Microbiol.* 2013;49(4): 333–340. https://doi.org/10.1134/S0003683813040108 [Original Russian Text: Murzaeva S.V., Belova S.P., Mironova G.D. Determination of the antioxidant properties of activators of mitochondrial ATP-dependent potassium channels with the Amplex Red fluorescent indicator. *Prikladnaya biokhimiya i mikrobiologiya.* 2013;49(4):345–352 (in Russ.). https://doi.org/10.7868/s0555109913040107]

4. Semigolovskii N.Yu. Use of antihypoxants in the acute period of myocardial infarction. *Anesteziol. Reanimatol.* 1998;(2):56–59 (in Russ.).

СПИСОК ЛИТЕРАТУРЫ

1. Левченкова О.С., Новиков В.Е., Пожилова Е.В. Фармако-динамика и клиническое применение антигипоксантов. *Обзоры по клинической фармакологии и лекарственной терапии.* 2012;10(3):3–12. https://doi.org/10.17816/RCF1033-12

2. Шаталин Ю.В., Наумов А.А., Поцелуева М.М. Сравни-тельная характеристика антиоксидантных свойств ги-поксена и дурохинона методом хемилюминисценции. *Биофизика.* 2008;53(1):100–106.

3. Мурзаева С.В., Белова С.П., Миронова Г.Д. Определение антиоксидантных свойств активаторов митохондриально-го АТФ-зависимого калиевого канала с помощью флуо-ресцентного индикатора Amplex Red. *Прикладная био-химия и микробиология.* 2013;49(4):345–352. https://doi.org/10.7868/s0555109913040107

4. Семиголовский Н.Ю. Применение антигипоксантов в остром периоде инфаркта миокарда. *Анестезиология и реаниматология.* 1998;(2):56–59.

5. Иванова Л.А., Павлова М.В., Арчакова Л.И. Антиокси-данты в комбинированной терапии больных хроническим деструктивным туберкулезом легких. *Терапевтический архив.* 1994;66(11):54–56.

6. Ганапольский В.П., Шабанов П.Д. Метеоадаптогенные свойства антигипоксантов. *Экспериментальная и клини-ческая фармакология.* 2009;72(6):36–41.

Identification of hypoxene metabolites in urine samples using gas chromatography–tandem
mass spectrometry for anti-doping control

Pavel V. Postnikov
et al.

5. Ivanova L.A., Pavlova M.V., Archakova L.I. Antioxidants in the combined therapy of patients with chronic destructive pulmonary tuberculosis. *Therapeutic Archive.* 1994;66(11):54–56 (in Russ.).

6. Ganapolskii V.P., Shabanov P.D. Meteoadaptogenic properties of antihypoxic drugs. *Eksperimental'naya i Klinicheskaya Farmakologiya.* 2009;72(6):36–41 (in Russ.).

7. Dolgareva S.A., Sorokin A.V., Konoplya N.A., Bushmina O.N., Bystrova N.A., Ovod A.I. The use of immunomodulators, antioxidants and hepatoprotectors for the correction of the liver, erythrocites and the immune system disorders in chronic ethanol intoxication. *Biomed. Khim.* 2018;64(4):360–367 (in Russ.). https://doi.org/10.18097/pbmc20186404360

8. Novikov V.E., Kriukova N.O., Novikov A.S. Gastroprotective properties of mexidol and hypoxen. *Eksperimental'naya i Klinicheskaya Farmakologiya.* 2010;73(5):15–18 (in Russ.).

9. Churganov O.A., Gavrilova E.A. Influence of gipoksen supplement on some values of psychological, immune, biochemical and functional status of athletes. *Vestnik sportivnoi nauki = Sports Science Bulletin.* 2009;(1):36–38 (in Russ.).

10. Zagorsky A.L., Kalninsh K.K., Toropov D.K. *Mixture of poly-(1,4-dihydroxy)-phenylenes (polyhydroquinones)*: RF Pat. 2294918. Publ. 10.03.2007 URL: https://yandex.ru/patents/doc/RU2294918C1_20070310. Accessed January 29, 2024.

11. Zagorsky A.L., Kalninsh K.K., Toropov D.K. *Mixtures of poly(1,4-dihydroxy)-phenylenes (polyhydroquinones)*: Pat. WO2007073236. Publ. 28.06.2007. https://patentscope.wipo.int/search/en/detail.jsf?docId=WO2007073236. Accessed February 02, 2024.

12. Savelieva N.B., Ishutenko G.V., Polosin A.V., Radus F.V., Polyansky D.S., Kurbatkin S.A., Efimova Yu.A., Postnikov P.V. Validation of a method for the quantitative determination of narcotic and psychotropic substances in urine by UHPLC–MS/MS. *Fine Chem. Technol.* 2022;17(3): 253–267. https://doi.org/10.32362/2410-6593-2022-17-3-253-267

13. Shoibonov B.B., Ontoboev A.N., Zinchenko A.A., Aleshkin V.A. *Hypoxen is an Inhibitor of the c1q Subcomponent and c1 Component of the Human Complement System*: RF Pat. 2205002. Publ. 27.05.2003. https://patents.google.com/patent/RU2205002C1/ru. Accessed February 05, 2024.

14. James A.M., Cochemé H.M., Smith R.A.J., Murphy M.P. Interactions of mitochondria-targeted and untargeted ubiquinones with the mitochondrial respiratory chain and reactive oxygen species. Implications for the use of exogenous ubiquinones as therapies and experimental tools. *J. Biol. Chem.* 2005;280(22):21295–21312. https://doi.org/10.1074/jbc.M501527200

15. Grishina E.V., Khaustova Ya.V., Pogorelova V.G., *et al.* Accelerated utilization of lactate under the effect of hypoxen after intensive exercise. *Bull. Exp. Biol. Med.* 2008;145(2): 198–201. https://doi.org/10.1007/s10517-008-0049-y [Original Russian Text: Grishina E.V., Khaustova Ya.V., Pogorelova V.G., Pogorelov A.G., Kuz'mich M.K., Maevskii E.I. Accelerated utilization of lactate under the effect of hypoxen after intensive exercise. *Zhurnal eksperimental'noi biologii i meditsiny.* 2008;145(2):158–161 (in Russ.).]

16. Murzaeva S.V., Abramova M.B., Popova I.I., *et al.* Effect of hypoxenum on bioenergetic processes in mitochondria and the activity of ATP-sensitive potassium channel. BIOPHYSICS. 2010;55(5):727–732. https://doi.org/10.1134/S0006350910050076

7. Долгарева С.А., Сорокин А.В., Конопля Н.А., Бушмина О.Н., Быстрова Н.А., Овод А.И. Использование иммуномодуляторов, антиоксидантов и гепатопротекторов для коррекции нарушений в печени, эритроцитах и иммунной системе при хронической интоксикации этанолом. *Биомедицинская химия.* 2018;64(4):360–367. http://dx.doi.org/10.18097/PBMC20186404360

8. Новиков В.Е., Крюкова Н.О., Новиков А.С. Гастропротекторные свойства мексидола и гипоксена. *Экспериментальная и клиническая фармакология.* 2010;73(5):15–18.

9. Чурганов О.А., Гаврилова Е.А. Влияние препарата гипоксен на некоторые показатели психологического, иммунного, биохимического и функционального статуса спортсменов. *Вестник спортивной науки.* 2009;(1):36–38.

10. Загорский А.Л., Калниньш К.К., Торопов Д.К. *Смесь поли (1,4-дигидрокси)-фениленов (полигидрохинонов)*: пат. 2294918 РФ. Заявка № 2005139599/04; заявл. 20.12.2005; опубл. 10.03.2007. https://yandex.ru/patents/doc/RU2294918C1_20070310. Дата обращения 29.01.2024 г.

11. Zagorsky A.L., Kalninsh K.K., Toropov D.K. *Mixtures of poly(1,4-dihydroxy)-phenylenes (polyhydroquinones)*: Pat. WO2007073236. Publ. 28.06.2007. https://patentscope.wipo.int/search/en/detail.jsf?docId=WO2007073236. Дата обращения 02.02.2024 г.

12. Савельева Н.Б., Ишутенко Г.В., Полосин А.В., Радус Ф.В., Полянский Д.С., Курбаткин С.А., Ефимова Ю.А., Постников П.В. Валидация методики количественного определения наркотических и психотропных веществ в моче методом СВЭЖХ-МС/МС. *Тонкие химические технологии.* 2022;17(3): 253–267. https://doi.org/10.32362/2410-6593-2022-17-3-253-267

13. Шойбонов Б.Б., Онтобоев А.Н., Зинченко А.А., Алёшкин В.А. *Гипоксен – ингибитор c1q субкомпонента и c1 компонента системы комплемента человека*: пат. 2205002 РФ. Заявка № 2002118468/14; заявл. 11.07.2002; опубл. 27.05.2003. https://patents.google.com/patent/RU2205002C1/ru. Дата обращения 05.02.2024 г.

14. James A.M., Cochemé H.M., Smith R.A.J., Murphy M.P. Interactions of mitochondria-targeted and untargeted ubiquinones with the mitochondrial respiratory chain and reactive oxygen species. Implications for the use of exogenous ubiquinones as therapies and experimental tools. *J. Biol. Chem.* 2005;280(22):21295–21312. https://doi.org/10.1074/jbc.M501527200

15. Гришина Е.В., Хаустова Я.В., Погорелова В.Г., Погорелов А.Г., Кузьмич М.К., Маевский Е.И. Ускорение утилизации лактата под влиянием гипоксена после напряженной мышечной работы. *Журнал экспериментальной биологии и медицины.* 2008;145(2):158–161.

16. Мурзаева С.В., Абрамова М.Б., Попова И.И., Гриценко Е.Н., Миронова Г.Д., Лежнев Э.И. Влияние гипоксена на биоэнергетические процессы в митохондриях и активность АТФ-чувствительного калиевого канала. *Биофизика.* 2010;55(5):814–821.

17. Игнатьев В.А., Петрова И.В., Цветкова Л.Н. Опыт применения гипоксена (Олифена) в лечении пациентов с хронической обструктивной болезнью легких среднетяжелого и тяжелого течения. *Terra Medica.* 2010;3(62):19–24.

Identification of hypoxene metabolites in urine samples using gas chromatography–tandem mass spectrometry for anti-doping control

Pavel V. Postnikov, *et al.*

[Original Russian Text: Murzaeva S.V., Abramova M.B., Popova I.I., Gritsenko E.N., Mironova G.D., Lezhnev E.I. Effect of hypoxenum on bioenergetic processes in mitochondria and the activity of ATP-sensitive potassium channel. *Biofizika.* 2010;55(5):814–821 (in Russ.).]

17. Ignat'ev V.A., Petrova I.V., Tsvetkova L.N. Experience with the use of hypoxen (*Olyphenum*) in the treatment of patients with moderate and severe chronic obstructive pulmonary disease. *Terra Medica.* 2010;3(62):19–24 (in Russ.).

About the authors

Pavel V. Postnikov, Cand. Sci. (Chem.), Head of the Doping Control Department, National Anti-Doping Laboratory (Institute), Lomonosov Moscow State University (10-1, Elizavetinskii per., Moscow, 105005, Russia). E-mail: drpavelpostnikov@gmail.com. Scopus Author ID 57021610900, RSCI SPIN-code 7251-9937, https://orcid.org/0000-0003-3424-0582

Andrey V. Polosin, Chief Specialist of the Doping Control Department, National Anti-Doping Laboratory (Institute), Lomonosov Moscow State University (10-1, Elizavetinskii per., Moscow, 105005, Russia). E-mail: polosin@dopingtest.ru. https://orcid.org/0000-0002-0009-7362

Nadezhda B. Savelieva, Chief Specialist of the Doping Control Department, National Anti-Doping Laboratory (Institute), Lomonosov Moscow State University (10-1, Elizavetinskii per., Moscow, 105005, Russia). E-mail: savelieva@dopingtest.ru. https://orcid.org/0000-0002-3988-6043

Sergey A. Kurbatkin, Assistant, I.P. Alimarin Department of Analitical Chemistry, M.V. Lomonosov Institute of Fine Chemical Technologies, MIREA – Russian Technological University (86, Vernadskogo pr., Moscow, 119571, Russia). E-mail: kurbatkins@mail.ru. https://orcid.org/0000-0002-2984-2178

Yuliya A. Efimova, Cand. Sci. (Chem.), Assistant Professor, I.P. Alimarin Department of Analitical Chemistry, M.V. Lomonosov Institute of Fine Chemical Technologies, MIREA – Russian Technological University (86, Vernadskogo pr., Moscow, 119571, Russia). E-mail: efimova_yulia@bk.ru. Scopus Author ID 25228417800, https://orcid.org/0000-0002-3582-0012

Elena S. Mochalova, Acting Director, National Anti-Doping Laboratory (Institute), Lomonosov Moscow State University (10-1, Elizavetinskii per., Moscow, 105005, Russia). E-mail: mochalova@dopingtest.ru

Identification of hypoxene metabolites in urine samples using gas chromatography–tandem mass spectrometry for anti-doping control

Pavel V. Postnikov,
et al.

Об авторах

Постников Павел Викторович, к.х.н., начальник отдела допингового контроля, Национальная антидопинговая лаборатория (Институт), Московский государственный университет им. М.В. Ломоносова (Россия, 105005, Москва, Елизаветинский пер., д. 10, стр. 1). E-mail: postnikov@dopingtest.ru, drpavelpostnikov@gmail.com. Scopus Author ID 57021610900, SPIN-код РИНЦ 7251-9937, https://orcid.org/0000-0003-3424-0582

Полосин Андрей Вячеславович, главный специалист отдела допингового контроля, Национальная антидопинговая лаборатория (Институт), Московский государственный университет им. М.В. Ломоносова (105005, Россия, Москва, Елизаветинский пер., д. 10, стр. 1). E-mail: polosin@dopingtest.ru. https://orcid.org/0000-0002-0009-7362

Савельева Надежда Борисовна, главный специалист отдела допингового контроля, Национальная антидопинговая лаборатория (Институт), Московский государственный университет им. М.В. Ломоносова (105005, Россия, Москва, Елизаветинский пер., д. 10, стр. 1). E-mail: savelieva@dopingtest.ru. https://orcid.org/0000-0002-3988-6043

Курбаткин Сергей Александрович, ассистент кафедры аналитической химии им. И.П. Алимарина, Институт тонких химических технологий им. М.В. Ломоносова, ФГБОУ ВО «МИРЭА – Российский технологический университет» (119571, Россия, Москва, пр-т Вернадского, д. 86). E-mail: kurbatkins@mail.ru. https://orcid.org/0000-0002-2984-2178

Ефимова Юлия Александровна, к.х.н., доцент кафедры аналитической химии им. И.П. Алимарина, Институт тонких химических технологий им. М.В. Ломоносова, ФГБОУ ВО «МИРЭА – Российский технологический университет» (119571, Россия, Москва, пр-т Вернадского, д. 86). E-mail: efimova_yulia@bk.ru. Scopus Author ID 25228417800, https://orcid.org/0000-0002-3582-0012

Мочалова Елена Сергеевна, исполняющий обязанности директора Национальной антидопинговой лаборатории (Института), Московский государственный университет им. М.В. Ломоносова (105005, Россия, Москва, Елизаветинский переулок, д. 10, стр. 1). E-mail: mochalova@dopingtest.ru

Translated from Russian into English by H. Moshkov
Edited for English language and spelling by Dr. David Mossop

Biochemistry and biotechnology

Биохимия и биотехнология

RESEARCH ARTICLE

Investigation of the substrate properties of fluorescently labeled pyrimidine triphosphates in recombinase polymerase amplification

Aleksei S. Epifanov✉, **Valeriy E. Shershov, Sergey A. Surzhikov, Alexander V. Chudinov, Sergey A. Lapa**

Engelhardt Institute of Molecular Biology, Russian Academy of Sciences, Moscow, 119991 Russia

✉ *Corresponding author, e-mail: alex.E.797@yandex.ru*

Abstract

Objectives. To study the substrate properties of Cy5-labeled deoxynucleoside triphosphates of various natures (dU and dC) in the process of incorporation in the DNA chain during recombinase polymerase amplification (RPA).

Methods. The work used the real-time RPA method. The method of horizontal electrophoresis was used to control the quality of the amplification products obtained.

Results. The influence of the fluorophore structure and linker lengths on the substrate properties for deoxynucleoside triphosphates Cy5-dUTP and Cy5-dCTP was studied. The following values of the substrate efficiency parameters were determined: amplification efficiency (kinetic indicator), normalized product yield, and embedding coefficient.

Conclusions. Modified deoxynucleoside triphosphates (dNTP) with long linkers between the fluorophore and the nitrogenous base, as well as between the quaternary ammonium group and the second heterocycle of the fluorophore, showed greater substrate efficiency than fluorescently labeled dNTP with short linkers. The modified dU in each pair demonstrated greater substrate efficiency compared to the modified dC.

For citation

Investigation of the substrate properties of fluorescently labeled pyrimidine triphosphates
in recombinase polymerase amplification

Aleksei S. Epifanov,
et al.

НАУЧНАЯ СТАТЬЯ

Исследование субстратных свойств флуоресцентно-меченых пиримидинтрифосфатов в рекомбиназной полимеразной амплификации

А.С. Епифанов⊠, В.Е. Шершов, С.А. Суржиков, А.В. Чудинов, С.А. Лапа

Институт молекулярной биологии им. В.А. Энгельгардта, Российская академия наук, Москва, 119991 Россия

⊠ *Автор для переписки, e-mail: alex.E.797@yandex.ru*

Аннотация

Цели. Изучить субстратные свойства трифосфатов дезоксинуклеозидов различной природы (dU и dC), флуоресцентно-меченых красителями цианинового ряда Cy5, при их встраивании в цепь ДНК в процессе рекомбиназной полимеразной амплификации (RPA).

Методы. В работе использовали метод RPA в режиме реального времени. Для контроля качества получаемых продуктов амплификации использовали метод горизонтального электрофореза.

Результаты. Исследовано влияние строения флуорофора и длин линкеров между красителем и азотистым основанием нуклеотида, а также вторым гетероциклом флуорофора и четвертичной аммониевой группой, на субстратные свойства для дезоксинуклеозидтрифосфатов Cy5-dUTP и Cy5-dCTP. Определены значения параметров субстратной эффективности: эффективности амплификации (кинетического показателя), а также нормированного выхода продукта и коэффициента встраивания.

Выводы. Модифицированные дезоксинуклеозидтрифосфаты (dNTP) с длинными линкерами между флуорофором и азотистым основанием нуклеотида, а также между четвертичной аммониевой группой и вторым гетероциклом флуорофора, показывали большую субстратную эффективность, в отличие от флуоресцентно-меченых dNTP с короткими линкерами. Модифицированные dU в каждой паре демонстрировали большую субстратную эффективность по сравнению с модифицированными dC.

INTRODUCTION

Fluorescent labeling of nucleic acids is currently widely used in molecular biology and medical diagnostics. Deoxynucleoside triphosphates (dNTPs) modified by fluorophore introduction [1–4], more often of pyrimidine nature, are used to introduce DNA directly in the process of amplification, which greatly simplifies the procedure of analysis of amplification products using the immobilized phase (on biological microarrays, various strip systems, etc.) [5]. The fluorophores used to obtain fluorescently labeled DNA need the following properties: chemical stability, low background fluorescence, and resistance to multiple irradiation (fluorescence). Such tags include deoxyribonucleoside triphosphate derivatives modified

with Cy5 cyanine dyes (Cy5-dNTP) [6], where the fluorophore is attached via a linker to the nitrogenous base of the nucleotide [7–9]. The wide application of fluorescently labeled nucleoside triphosphates in molecular biological diagnostic systems makes it extremely important for their compatibility with enzymatic systems [2, 3, 10] to be studied.

The aim of the study is to investigate the substrate properties of fluorescently labeled dNTPs of pyrimidine nature (dU and dC) in the enzymatic system of recombinase polymerase amplification (RPA) [11–13]. A fragment of the *ebpS* gene of the human pneumonia pathogen *Staphylococcus aureus* was selected as a bacterial genetic target to study the substrate efficiency of Cy5-dUTP and Cy5-dCTP.

Investigation of the substrate properties of fluorescently labeled pyrimidine triphosphates
in recombinase polymerase amplification

Aleksei S. Epifanov,
et al.

EXPERIMENTAL

DNA samples. Decontaminated DNA of *Staphylococcus aureus* obtained from the collection of the State Scientific Center of Applied Microbiology and Biotechnology (Obolensk, Moscow oblast) was used in the work.

PCR. The polymerase chain reaction (PCR) method was used to produce the target fragment of the *ebpS* gene. The reaction mixture (30 µL) contained a mixture of natural dNTPs at a concentration of 0.2 mM; species-specific primers: forward (5'-TTAGAAGCGTCTTTAGATGTGTC-3') and reverse (5'-GGAACAGCGGGGGGTGTTGTTGCAGGTGC-3'); 5U Taq-DNA polymerase (*Thermo Scientific*, USA). Its reaction buffer was in the amount recommended by the manufacturer. Amplification was performed on a Gentier 96E (*Tianlong*, China) using the following program: preheating at 95°C for 3 min, then 32 cycles: 95°C for 20 s, 60°C for 30 s, 72°C for 30 s. This was followed by final incubation at 72°C for 3 min. The resulting PCR product of 497 base pairs (bp) in length was purified and isolated according to the method described in [14] and then used in RPA to study the kinetic characteristics and substrate properties.

Real-time RPA. The reaction mixture (50 µL) contained the components of the TwistAmp Basic kit (*TwistDX*, United Kingdom) at the manufacturer's recommended concentrations; the kit reagents with the addition of a pair of primers: 5'-CTCCAAATATATCGCTAATGCACCGATAATTAGTACAGTACAGCTGC-3') and reverse (5'-ACTCGACTGAGGAGGAGGATAAAGCGTCTCTCTCAAGATAAGATAAGTCTAAGAAGA-3'). EvaGreen intercalating dye (*Biotium*, USA) and purified PCR product in the amount of 1 µL were included in the total mixture. After careful stirring it was poured into 200 µL reaction tubes with the lyophilizate from the kit. Fluorescently labeled triphostaphates were introduced into the reaction volume at a concentration of 8 µM. The reaction was carried out on a Gentier 96E DNA amplifier (*Tianlong*, China) in real time according to the program: 50 min at 40°C and fluorescence signal acquisition once per minute. The accumulation of reaction product was visualized using intercalating dye. The RPA product with a length of 282 bp obtained was purified and isolated according to the method described in [14].

Horizontal electrophoresis for RPA product control. RPA products were separated in 4% agarose gel Agarose LE (*Helicon*, Russia) for 5 min at 5 V/cm, then 50 min at 10 V/cm, SYBR Green I (*Molecular Probes*, USA) was used for staining. For DNA detection by SYBR Green I staining, visualization was performed on a ChemiScope 6200 Touch gel-documentation system (*Clinx Science Instruments*, China) using built-in LEDs, and "Green light excitation/emission" light filters with excitation spectrum corresponding to Cy3 dye ($\lambda_{max.excitation}$ = 550 nm, $\lambda_{max.emission}$ = 570 nm). For selective detection of the tag embedded in DNA, "Red light excitation/emission" light filters were used. Their excitation spectrum is similar to the Cy5 dye ($\lambda_{max.excitation}$ = 650 nm, $\lambda_{max.emission}$ = 670 nm).

RESULTS AND DISCUSSION

For a comparative analysis of the substrate efficiency of fluorescently labeled nucleotides, we used dNTPs (Fig. 1) containing zwitter-ionic indodicarbocyanine dyes in their structure. They differ in terms of the spatial structure of the fluorophore [7], the length of the linker between the dye and the nitrogenous base of the nucleotide, the second heterocycle of the fluorophore and the quaternary ammonium group.

Designations were introduced depending on the length of the two linkers for the fluorescently labeled derivatives in each pair (dU and dC). For the linker connecting the aromatic group of the dye to the nitrogenous base of the nucleotide, the following numbering was adopted: (1) for short and (2) for long. The linker connecting second heterocycle of the fluorophore to the quaternary ammonium group was designated as (a) for short and (b) for long.

The amplification kinetics in the presence of Cy5-dNTP were analyzed by means of real-time RPA.

The sample labeled as dU-K was taken as a comparison control. The choice was dictated by its wide application in gel biological microarray technology due to its good substrate efficiency [5]. Similar to the samples under study, it is characterized by the electroneutral structure of the fluorophore.

In order to analyze the kinetics of DNA fragment amplification, 8 µM was chosen as the working concentration of the tested labeled dNTPs. This was to ensure partial substitution of natural triphosphates during the formation of the growing DNA chain. Amplification was performed in the presence of all four natural dNTPs at a concentration of 200 µM in three repeats for each of the tested labeled dU and dC (Fig. 2). A reaction mixture containing only unmodified (natural) dNTPs at a concentration of 200 µM was used as a control sample.

The amplification efficiency in the RPA process (E_t) was determined using the slope of the straight line of the S-shaped signal accumulation curve on a logarithmic scale according to the methodology used for PCR [15]. The *t* letter implies plotting by reaction time due to the absence of cycles as in PCR (*E*).

The effect of linkers of different lengths on the inhibition of RPA enzyme system polymerases was studied, and the experimental data summarized in Table.
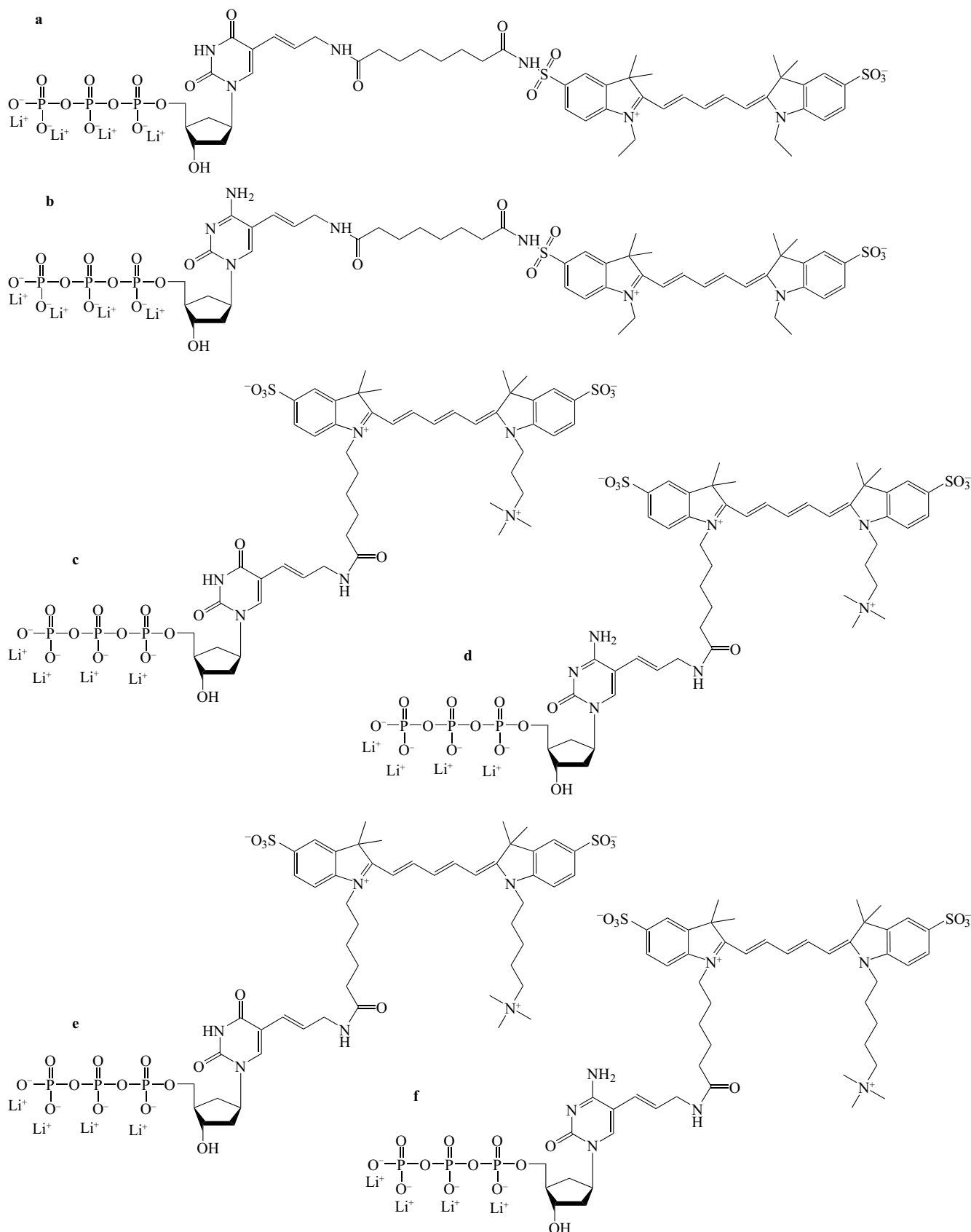
Investigation of the substrate properties of fluorescently labeled pyrimidine triphosphates
in recombinase polymerase amplification

Aleksei S. Epifanov,
et al.

Fig. 1. Structure of fluorescently labeled deoxyuridine and deoxycytidine triphosphates:
(**a**) dU-K, (**b**) dC-K, (**c**) U1a, (**d**) C1a, (**e**) U1b, (**f**) C1b
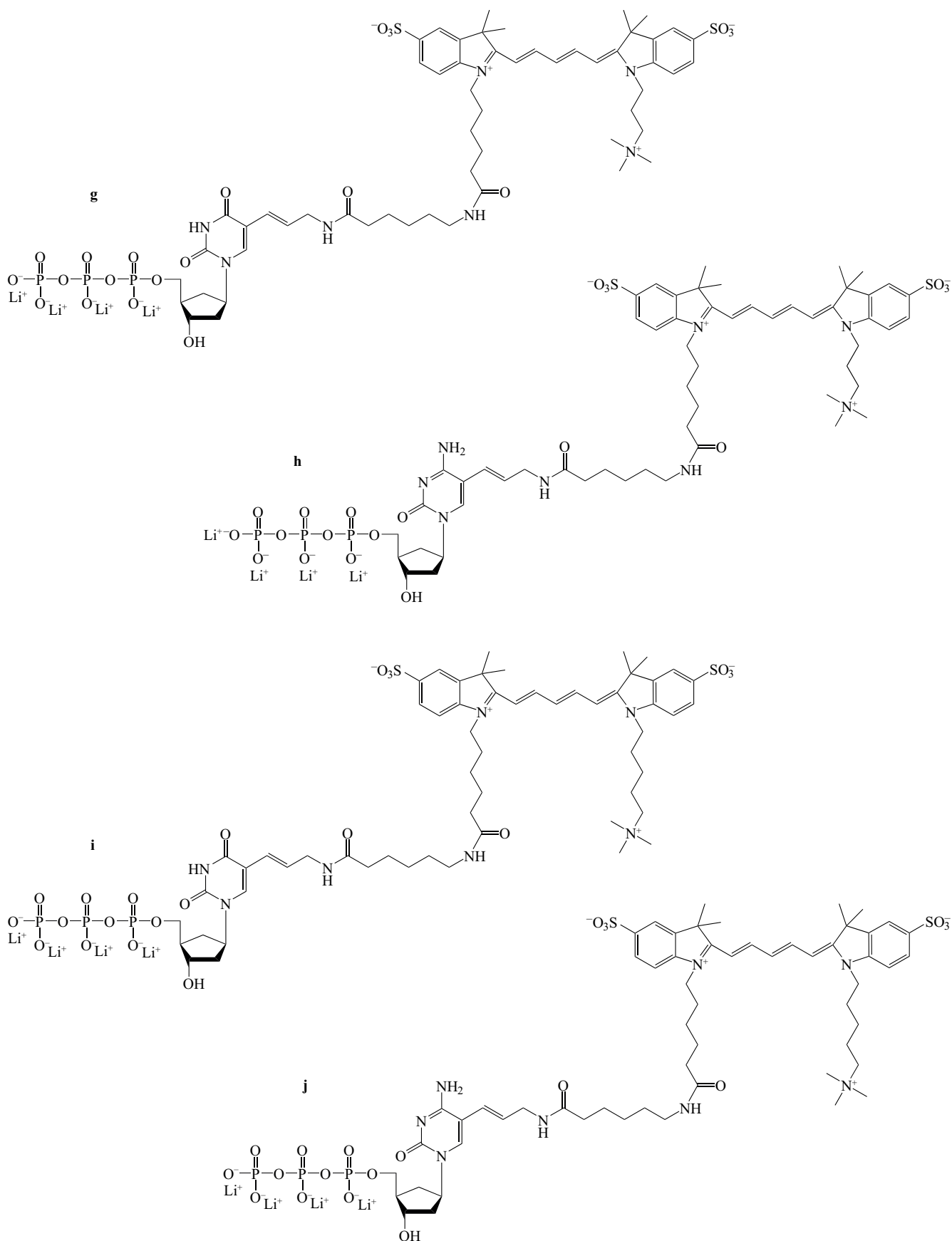
Investigation of the substrate properties of fluorescently labeled pyrimidine triphosphates
in recombinase polymerase amplification

Aleksei S. Epifanov,
et al.

Fig. 1. Structure of fluorescently labeled deoxyuridine and deoxycytidine triphosphates:
(**g**) U2a, (**h**) C2a, (**i**) U2b, (**j**) C2b

Investigation of the substrate properties of fluorescently labeled pyrimidine triphosphates
in recombinase polymerase amplification

Aleksei S. Epifanov,
et al.
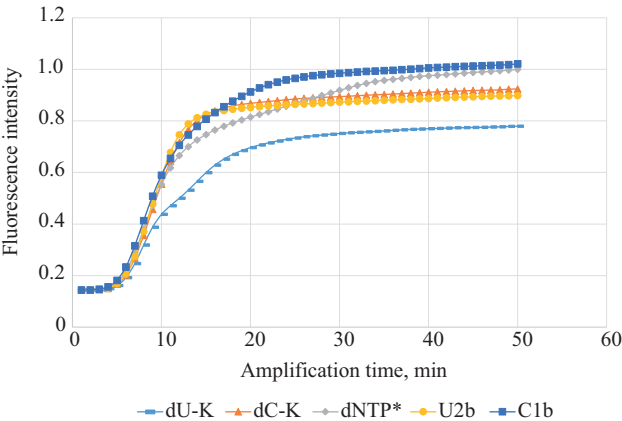
Fig. 2. Kinetics of fluorescence signal accumulation in the presence of modified dU and dC (case study of U2b and C1b).
*Unmodified deoxynucleoside triphosphates.

The data shows that the amplification efficiency for each of the Cy5-dNTPs was lower than when compared to natural dNTPs (except U1b, C2a), indicating inhibition. There was no significant effect of the length of the linker connecting the aromatic group of the dye to the nitrogenous base of the nucleotide on amplification efficiency. Increasing the length of the linker connecting the second heterocycle of the fluorophore to the quaternary amine resulted in a more pronounced inhibitory effect modified dC when compared to paired dU.

In order to estimate the yield of the amplification product, a normalized conditional product yield (η) was introduced according to the pixel brightness (pixel signal intensity of the analyzed image section) of the corresponding band in the electrophoregram. Normalization was performed, in order to visualize the effect of Cy5-(dU, dC) on the amplification process when compared to the control sample (natural dNTPs). The normalized conditional product yield was determined by means of the pixel brightness of the amplification product bands on an agarose gel in terms of the control band. The fluorescently labeled substrate under study had no significant effect on product yield (except for U1b).

Pixel brightness in conventional units (c.u.) was measured using ImageJ software (*NIH*, USA) (Table) and used to determine the normalized conditional product yield and label incorporation rate.

In order to evaluate the incorporation of fluorescently labeled dNTPs into the growing DNA strand, we introduced the incorporation coefficient (K_{in}). This is the ratio of the total pixel brightness of the area of the phoregram corresponding to the band of the labeled amplification product as captured on the Cy5 channel to the brightness of the same band as captured on the Cy3 channel (Table). Three RPA series were performed for each pair of fluorescently labeled triphosphates.

It is evident from the data obtained that all modified dU incorporate into DNA better compared to their Cy5-dC analogs. It was found that increasing the linker connecting the second heterocycle of the fluorophore to the quaternary ammonium group significantly increases the incorporation rate of fluorescently labeled dNTPs. Increasing the length of the linker connecting the aromatic group of the dye to the nitrogenous base of the nucleotide had a less significant effect on substrate characteristics.

Table. Amplification efficiency (E_t), normalized product yield (η), coefficient of incorporation (K_{in}) obtained for RPA with Cy5-dU and Cy5-dC

dNTP No.	Amplification efficiency $E_t \pm \sigma$**	Normalized product yield $\eta \pm \sigma$**	Coefficient of incorporation $K_{in} \pm \sigma$**
dNTP*	1.35 ± 0.02	1.00 ± 0.00	–
dU-K	1.27 ± 0.06	0.76 ± 0.25	1.74 ± 0.07
dC-K	1.29 ± 0.02	0.97 ± 0.17	0.50 ± 0.07
U1a	1.28 ± 0.01	0.96 ± 0.06	0.27 ± 0.05
C1a	1.28 ± 0.03	0.98 ± 0.11	0.17 ± 0.04

Investigation of the substrate properties of fluorescently labeled pyrimidine triphosphates
in recombinase polymerase amplification

Aleksei S. Epifanov,
et al.

Table. Continued

dNTP No.	Amplification efficiency $E_t \pm \sigma$**	Normalized product yield $\eta \pm \sigma$**	Coefficient of incorporation $K_{in} \pm \sigma$**
U1b	1.34 ± 0.06	0.77 ± 0.29	0.94 ± 0.13
C1b	1.33 ± 0.03	1.18 ± 0.58	0.35 ± 0.04
U2a	1.33 ± 0.04	0.99 ± 0.34	0.29 ± 0.10
C2a	1.35 ± 0.07	0.88 ± 0.14	0.23 ± 0.03
U2b	1.33 ± 0.03	0.84 ± 0.34	0.87 ± 0.21
C2b	1.28 ± 0.02	1.10 ± 0.51	0.68 ± 0.47

* Unmodified deoxynucleoside triphosphates.

** The mean square deviation.
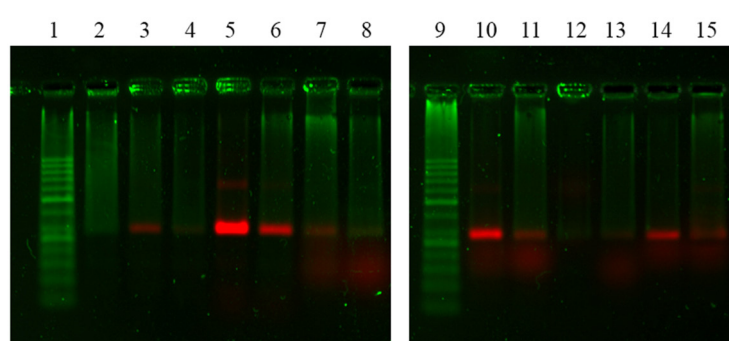
Fig. 3. Electrophoregram obtained in digital TIFF 24 format with saving pixel-by-pixel signal intensity data for measuring the embeddability coefficient (K_{in}) of the RPA product: (*1*) marker of the lengths of double-stranded DNA GeneRuler 50 bp (*Thermo Scientific*, USA); (*2*) dNTP; (*3*) laboratory control mod-U1, not considered in this study; (*4*) laboratory control mod-C1, not considered in this study; (*5*) dU-K; (*6*) dC-K; (*7*) U1a; (*8*) C1a; (*9*) marker of the lengths of double-stranded DNA GeneRuler 50 bp (*Thermo Scientific*, USA); (*10*) U2a; (*11*) C2a; (*12*) U1b; (*13*) C1b; (*14*) U2b; (*15*) C2b

CONCLUSIONS

The study showed that the spatial structure of the fluorophore and differences in linker lengths affect the substrate characteristics of the modified dNTPs. It was found that fluorescently labeled triphosphates with a long linker connecting the nitrogenous base of the nucleotide to the aromatic group of the dye, and a long linker connecting the second heterocycle of the fluorophore to the quaternary ammonium group were significantly better incorporated into the growing DNA strand and were characterized by high product yields.

Authors' contributions

A.S. Epifanov—conducting research, writing the text of the manuscript.

V.E. Shershov—synthesis of fluorescently labeled dNTPs.

S.A. Surzhikov—synthesis of primers.

A.V. Chudinov—academic advising.

S.A. Lapa—construction of primers for PCR and RPA, planning experiments, and editing the manuscript.

The authors declare no conflicts of interest.

Investigation of the substrate properties of fluorescently labeled pyrimidine triphosphates
in recombinase polymerase amplification

Aleksei S. Epifanov,
et al.

REFERENCES

1. Boháčová S., Ludvíková L., Poštová Slavětínská L., Vaníková Z., Klán P., Hocek M. Protected 5-(hydroxymethyl)-uracil nucleotides bearing visible-light photocleavable groups as building blocks for polymerase synthesis of photocaged DNA. *Org. Biomol. Chem.* 2018;16(9):1527–1535. https://doi.org/10.1039/c8ob00160j

2. Dziuba D., Pohl R., Hocek M. Bodipy-labeled nucleoside triphosphates for polymerase synthesis of fluorescent DNA. *Bioconjug. Chem.* 2014;25(11):1984–1995. https://doi.org/10.1021/bc5003554

3. Wynne S.A., Pinheiro V.B., Holliger P., Leslie A.G.W. Structures of an Apo and a Binary Complex of an Evolved Archeal B Family DNA Polymerase Capable of Synthesising Highly Cy-Dye Labelled DNA. *PLoS ONE.* 2013;8(8):e70892. https://doi.org/10.1371/journal.pone.0070892

4. Ramsay N., Jemth A.S., Brown A., Crampton N., Dear P., Holliger P. CyDNA: Synthesis and Replication of Highly Cy-Dye Substituted DNA by an Evolved Polymerase. *J. Am. Chem. Soc.* 2010;132(14):5096–5104. https://doi.org/10.1021/ja909180c

5. Shershov V.E., Lapa S.A., Kuznetsova V.E., Spitsyn M.A., Guseinov T.O., Polyakov S.A., Stomahin A.A., Zasedatelev A.S., Chudinov A.V. Comparative Study of Novel Fluorescent Cyanine Nucleotides: Hybridization Analysis of Labeled PCR Products Using a Biochip. *J. Fluoresc.* 2017;27(6):2001–2016. https://doi.org/10.1007/s10895-017-2139-6

6. Bertocchi F., Delledonne A., Vargas-Nadal G., Terenziani F., Painelli A., Sissa C. Aggregates of Cyanine Dyes: When Molecular Vibrations and Electrostatic Screening Make the Difference. *J. Phys. Chem. C.* 2023;127(21):10185–10196. https://doi.org/10.1021/acs.jpcc.3c01253

7. Shershov V.E., Lapa S.A., Levashova A.I., *et al.* Synthesis of Fluorescent-Labeled Nucleotides for Labeling of Isothermal Amplification Products. *Russ. J. Bioorg. Chem.* 2023;49(5):1115–1158. https://doi.org/10.1134/S1068162023050242
[Original Russian Text: Shershov V.E., Lapa S.A., Levashova A.I., Shishkin I.Yu., Shtylev G.F., Shekalova E.Yu., Vasiliskov V.A., Zasedatelev A.S., Kuznetsova V.E., Chudinov A.V. Synthesis of Fluorescent-Labeled Nucleotides for Labeling of Isothermal Amplification Products. *Bioorganicheskaya khimiya.* 2023;49(6):649–656 (in Russ.). https://doi.org/10.31857/S0132342323050056]

8. Telser J., Cruickshank K.A., Morrison L.E., Netzel T.L. Synthesis and characterization of DNA oligomers and duplexes containing covalently attached molecular labels: comparison of biotin, fluorescein, and pyrene labels by thermodynamic and optical spectroscopic measurements. *J. Am. Chem. Soc.* 1989;111(18):6966–6976. https://doi.org/10.1021/ja00200a011

9. Ren X., El-Sagheer A.H., Brown T. Efficient enzymatic synthesis and dual-colour fluorescent labelling of DNA probes using long chain azido-dUTP and BCN dyes. *Nucleic Acids Res.* 2016;44(8):e79. https://doi.org/10.1093/nar/gkw028

10. Lapa S.A., Volkova O.S., Spitsyn M.A., *et al.* Amplification Efficiency and Substrate Properties of Fluorescently Labeled Deoxyuridine Triphosphates in PCR in the Presence of DNA Polymerases without 3'-5' Exonuclease Activity. *Russ. J. Bioorg. Chem.* 2019;45(4):263–272 (in Russ.). https://doi.org/10.1134/S1068162019040046

СПИСОК ЛИТЕРАТУРЫ

1. Boháčová S., Ludvíková L., Poštová Slavětínská L., Vaníková Z., Klán P., Hocek M. Protected 5-(hydroxymethyl)-uracil nucleotides bearing visible-light photocleavable groups as building blocks for polymerase synthesis of photocaged DNA. *Org. Biomol. Chem.* 2018;16(9):1527–1535. https://doi.org/10.1039/c8ob00160j

2. Dziuba D., Pohl R., Hocek M. Bodipy-labeled nucleoside triphosphates for polymerase synthesis of fluorescent DNA. *Bioconjug. Chem.* 2014;25(11):1984–1995. https://doi.org/10.1021/bc5003554

3. Wynne S.A., Pinheiro V.B., Holliger P., Leslie A.G.W. Structures of an Apo and a Binary Complex of an Evolved Archeal B Family DNA Polymerase Capable of Synthesising Highly Cy-Dye Labelled DNA. *PLoS ONE.* 2013;8(8):e70892. https://doi.org/10.1371/journal.pone.0070892

4. Ramsay N., Jemth A.S., Brown A., Crampton N., Dear P., Holliger P. CyDNA: Synthesis and Replication of Highly Cy-Dye Substituted DNA by an Evolved Polymerase. *J. Am. Chem. Soc.* 2010;132(14):5096–5104. https://doi.org/10.1021/ja909180c

5. Shershov V.E., Lapa S.A., Kuznetsova V.E., Spitsyn M.A., Guseinov T.O., Polyakov S.A., Stomahin A.A., Zasedatelev A.S., Chudinov A.V. Comparative Study of Novel Fluorescent Cyanine Nucleotides: Hybridization Analysis of Labeled PCR Products Using a Biochip. *J. Fluoresc.* 2017;27(6):2001–2016. https://doi.org/10.1007/s10895-017-2139-6

6. Bertocchi F., Delledonne A., Vargas-Nadal G., Terenziani F., Painelli A., Sissa C. Aggregates of Cyanine Dyes: When Molecular Vibrations and Electrostatic Screening Make the Difference. *J. Phys. Chem. C.* 2023;127(21):10185–10196. https://doi.org/10.1021/acs.jpcc.3c01253

7. Шершов В.Е., Лапа С.А., Левашова С.А., Шишкин И.Ю., Штылев Г.Ф., Шекалова Е.Ю., Василисков В.А., Заседателев А.С., Кузнецова В.Е., Чудинов А.В. Синтез флуоресцентно-меченых нуклеотидов для маркирования продуктов изотермической амплификации. *Биоорганическая химия.* 2023;49(6):649–656. https://doi.org/10.31857/S0132342323050056

8. Telser J., Cruickshank K.A., Morrison L.E., Netzel T.L. Synthesis and characterization of DNA oligomers and duplexes containing covalently attached molecular labels: comparison of biotin, fluorescein, and pyrene labels by thermodynamic and optical spectroscopic measurements. *J. Am. Chem. Soc.* 1989;111(18):6966–6976. https://doi.org/10.1021/ja00200a011

9. Ren X., El-Sagheer A.H., Brown T. Efficient enzymatic synthesis and dual-colour fluorescent labelling of DNA probes using long chain azido-dUTP and BCN dyes. *Nucleic Acids Res.* 2016;44(8):e79. https://doi.org/10.1093/nar/gkw028

10. Лапа С.А., Волкова О.С., Спицын М.А., Шершов В.Е., Кузнецова В.Е., Гусейнов Т.О., Заседателев А.С., Чудинов А.В. Эффективность амплификации и субстратные свойства флуоресцентно-меченных трифосфатов дезоксиуридина в ПЦР с ДНК-полимеразами, не обладающими 3'-5'-экзонуклеазной. *Биоорганическая химия.* 2019;45(4):392–402. https://doi.org/10.1134/S0132342319040043

11. Piepenburg O., Williams C.H., Stemple D.L., Armes N.A. DNA detection using recombination proteins. *PLoS Biol.* 2006;4(7):e204. https://doi.org/10.1371/journal.pbio.0040204

Investigation of the substrate properties of fluorescently labeled pyrimidine triphosphates
in recombinase polymerase amplification

Aleksei S. Epifanov,
et al.

[Original Russian Text: Lapa S.A., Volkova O.S., Spitsyn M.A., Shershov V.E., Kuznetsova V.E., Guseinov T.O., Zasedatelev A.S., Chudinov A.V. Amplification Efficiency and Substrate Properties of Fluorescently Labeled Deoxyuridine Triphosphates in PCR in the Presence of DNA Polymerases without 3'-5' Exonuclease Activity. *Bioorganicheskaya khimiya.* 2019;45(4):392–402 (in Russ.). https://doi.org/10.1134/S0132342319040043]

11. Piepenburg O., Williams C.H., Stemple D.L., Armes N.A. DNA detection using recombination proteins. *PLoS Biol*. 2006;4(7):e204. https://doi.org/10.1371/journal.pbio.0040204

12. Bondareva O.S., Baturin A.A., Mironova A.V. Recombinase polymerase amplification: method's characteristics and applications in diagnostics of infectious diseases. *Zhurnal mikrobiologii, epidemiologii i immunobiologii = Journal of Microbiology, Epidemiology and Immunobiology*. 2024;101(2):270–280 (in Russ.). https://doi.org/10.36233/0372-9311-470

13. Lobato I.M., O'Sullivan C.K. Recombinase polymerase amplification: Basics, applications and recent advances. *Trends Analyt. Chem*. 2018;98:19–35. https://doi.org/10.1016/j.trac.2017.10.015.

14. Lapa S.A., Miftakhov R.A., Klochikhina E.S., *et al.* Development of Multiplex RT-PCR with Immobilized Primers for Identification of Infectious Human Pneumonia Pathogens. *Mol. Biol*. 2021;55(6):828–838. https://doi.org/10.1134/S0026893321040063
[Original Russian Text: Lapa S.A., Miftakhov R.A., Klochikhina E.S., Ammour Yu.I., Blagodatskikh S.A., Shershov V.E., Zasedatelev A.S., Chudinov A.V. Development of Multiplex RT-PCR with Immobilized Primers for Identification of Infectious Human Pneumonia Pathogens. *Molekulyarnaya biologiya*. 2021;55(6):944–955 (in Russ.). https://doi.org/10.31857/S0026898421050062]

15. Ramakers C., Ruijter J.M., Deprez R.H., Moorman A.F. Assumption – free analysis of quantitative real-time polymerase chain reaction (PCR) data. *Neurosci. Lett*. 2003;339(1):62–66. https://doi.org/10.1016/s0304-3940(02)01423-4

12. Бондарева О.С., Батурин А.А., Миронова А.В. Рекомбиназная полимеразная амплификация: характеристика метода и применение в диагностике инфекционных заболеваний. *Журнал микробиологии, эпидемиологии и иммунобиологии*. 2024;101(2):270–280. https://doi.org/10.36233/0372-9311-470

13. Lobato I.M., O'Sullivan C.K. Recombinase polymerase amplification: Basics, applications and recent advances. *Trends Analyt. Chem*. 2018;98:19–35. https://doi.org/10.1016/j.trac.2017.10.015

14. Лапа С.А., Мифтахов Р.А., Клочихина Е.С., Аммур Ю.И., Благодатских С.А., Шершов В.Е., Заседателев А.С., Чудинов А.В. Разработка мультиплексной ОТ-ПЦР с иммобилизованными праймерами для идентификации возбудителей инфекционной пневмонии человека. *Молекулярная биология*. 2021;55(6):944–955. https://doi.org/10.31857/S0026898421050062

15. Ramakers C., Ruijter J.M., Deprez R.H., Moorman A.F. Assumption – free analysis of quantitative real-time polymerase chain reaction (PCR) data. *Neurosci. Lett*. 2003;339(1):62–66. https://doi.org/10.1016/s0304-3940(02)01423-4

About the authors

Aleksei S. Epifanov, Laboratory Assistant, Engelhardt Institute of Molecular Biology, Russian Academy of Sciences (32, Vavilova ul., Moscow, 119991, Russia). E-mail: alex.E.797@yandex.ru. https://orcid.org/0009-0005-5604-8171

Valeriy E. Shershov, Researcher, Engelhardt Institute of Molecular Biology, Russian Academy of Sciences (32, Vavilova ul., Moscow, 119991, Russia). E-mail: shershov@list.ru. Scopus Author ID 55581995700, RSCI SPIN-code 9183-7807, https://orcid.org/0000-0003-3308-7133

Sergey A. Surzhikov, Cand. Sci. (Chem.), Senior Researcher, Engelhardt Institute of Molecular Biology, Russian Academy of Sciences (32, Vavilova ul., Moscow, 119991, Russia). E-mail: ssergey77@mail.ru. Scopus Author ID 7006525454, RSCI SPIN-code 5012-0760, https://orcid.org/0000-0002-6043-1182

Alexander V. Chudinov, Cand. Sci. (Chem.), Head of the Laboratory, Engelhardt Institute of Molecular Biology, Russian Academy of Sciences (32, Vavilova ul., Moscow, 119991, Russia). E-mail: chud@eimb.ru. Scopus Author ID 7003833018, RSCI SPIN-code 8357-4576, https://orcid.org/0000-0001-5468-4119

Sergey A. Lapa, Cand. Sci. (Biol.), Senior Researcher, Engelhardt Institute of Molecular Biology, Russian Academy of Sciences (32, Vavilova ul., Moscow, 119991, Russia). E-mail: lapa@biochip.ru. Scopus Author ID 6603461000, RSCI SPIN-code 3809-6735, https://orcid.org/0000-0002-9011-134X

Investigation of the substrate properties of fluorescently labeled pyrimidine triphosphates
in recombinase polymerase amplification

Aleksei S. Epifanov,
et al.

Об авторах

Епифанов Алексей Сергеевич, лаборант, ФГБУН Институт молекулярной биологии им. В.А. Энгельгардта, Российская академия наук (119991, Россия, Москва, ул. Вавилова, д. 32). E-mail: alex.E.797@yandex.ru. https://orcid.org/0009-0005-5604-8171

Шершов Валерий Евгеньевич, научный сотрудник, ФГБУН Институт молекулярной биологии им. В.А. Энгельгардта, Российская академия наук (119991, Россия, Москва, ул. Вавилова, д. 32). E-mail: shershov@list.ru. Scopus Author ID 55581995700, SPIN-код РИНЦ 9183-7807, https://orcid.org/0000-0003-3308-7133

Суржиков Сергей Алексеевич, к.х.н., старший научный сотрудник, ФГБУН Институт молекулярной биологии им. В.А. Энгельгардта, Российская академия наук (119991, Россия, Москва, ул. Вавилова, д. 32). E-mail: ssergey77@mail.ru. Scopus Author ID 7006525454, SPIN-код РИНЦ 5012-0760, https://orcid.org/0000-0002-6043-1182

Чудинов Александр Васильевич, к.х.н., заведующий лабораторией, ФГБУН Институт молекулярной биологии им. В.А. Энгельгардта, Российская академия наук (119991, Россия, Москва, ул. Вавилова, д. 32). E-mail: chud@eimb.ru. Scopus Author ID 7003833018, SPIN-код РИНЦ 8357-4576, https://orcid.org/0000-0001-5468-4119

Лапа Сергей Анатольевич, к.б.н., старший научный сотрудник, ФГБУН Институт молекулярной биологии им. В.А. Энгельгардта, Российская академия наук (119991, Россия, Москва, ул. Вавилова, д. 32). E-mail: lapa@biochip.ru. Scopus Author ID 6603461000, SPIN-код РИНЦ 3809-6735, https://orcid.org/0000-0002-9011-134X

Translated from Russian into English by H. Moshkov
Edited for English language and spelling by Dr. David Mossop

Biochemistry and biotechnology

Биохимия и биотехнология

RESEARCH ARTICLE

Solubilization of *n*-hexadecane by micellar solutions of trehalolipid— surfactants of biological origin

Irina A. Nechaeva[1, ✉], **Anastasia S. Parfenova**[1], **Anastasia S. Filippova**[1], **Andrey E. Filonov**[1, 2]

[1] *Tula State University, Tula, 300012 Russia*

[2] *Pushchino Scientific Center for Biological Research, G.K. Skryabin Institute of Biochemistry and Physiology of Microorganisms, Russian Academy of Sciences, Pushchino, 142290 Russia*

✉ *Corresponding author, e-mail: nechaeva1902@gmail.com*

Abstract

Objectives. To isolate biosurfactants of glycolipid nature produced by oil hydrocarbon degrading bacteria and to establish their ability to solubilize hydrophobic compounds in the case of *n*-hexadecane.

Methods. Trehalolipids were isolated from bacteria *Rhodococcus erythropolis* X5 (VKM Ac-2532 D) and *Rhodococcus erythropolis* S67 (VKM Ac-2533 D) included in the MikroBak biopreparation for the bioremediation of oil-contaminated territories. The genome of *R. erythropolis* X5 is deposited in the National Center for Biotechnology Information database under GenBank accession numbers CP044283 and CP044284, BioSample – SAMN12818508, BioProject – PRJNA573614, and SRA – PRJNA573614. The content of trehalolipid biosurfactants was estimated by the amount of trehalose in aqueous solutions of biosurfactants using the phenol-sulfur method. The surface tension of the obtained aqueous solutions of biosurfactants was determined by the du Noüy ring method using a Kruss K6 tensiometer (*Kruss*, Germany). The critical concentration of micelle formation was determined by the inflection point on the curves of surface tension dependence on the concentration of the biosurfactant solution. In order to establish the solubilizing ability of biosurfactants, the residual concentration of *n*-hexadecane in an aqueous sample of different concentrations was determined using a gas chromatographic method of analysis.

Results. At a constant surface tension of 24.2 mN/m and 25.0 mN/m for *R. erythropolis* X5 and *R. erythropolis* S67, respectively, the critical micelle concentration for both strains was 33 mg/L ($3.8 \cdot 10^{-5}$ mol/L). The solubilizing effect of *Rhodococcus* trehalolipid micellar solutions against hydrophobic *n*-hexadecane was demonstrated by gas chromatographic analysis. The solubilization process was characterized using molar solubilization capacity (S_m), molar solubilization ratio (MSR), micelle–water partition coefficient (K_m), and solubilization energy (ΔG_S^0). It was shown that the solubilization process of *n*-hexadecane proceeds spontaneously ($\Delta G_\mathrm{S}^0 = -35.5$ kJ/mol) and more efficiently ($S_\mathrm{m} = 4.3$ mol/mol, MSR = 4.7 mol/mol) than in comparison with other biosurfactants of glycolipid nature.

Conclusions. Based on the value of the molar solubilization coefficient, it can be concluded that trehalolipids of the *R. erythropolis* X5 strain solubilize *n*-hexadecane in aqueous solutions to a greater extent than compared to other biosurfactants of a glycolipid nature, but are inferior to synthetic surfactants.

НАУЧНАЯ СТАТЬЯ

Солюбилизация *н*-гексадекана мицеллярными растворами трегалолипида — ПАВ биологического происхождения

И.А. Нечаева[1, ✉], А.С. Парфенова[1], А.С. Филиппова[1], А.Е. Филонов[1, 2]

[1] *Тульский государственный университет, Тула, 300012 Россия*

[2] *Институт биохимии и физиологии микроорганизмов им. Г.К. Скрябина, Российская академия наук, Пущинский научный центр биологических исследований Российской академии наук, Пущино, 142290 Россия*

✉ *Автор для переписки, e-mail: nechaeva1902@gmail.com*

Аннотация

Цели. Выделить биосурфактанты гликолипидной природы, продуцируемые бактериями-деструкторами углеводородов нефти, и установить их способность к солюбилизации гидрофобных соединений на примере *н*-гексадекана.

Методы. Трегалолипиды выделяли из бактерий *Rhodococcus erythropolis* Х5 (ВКМ Ас-2532 Д) и *Rhodococcus erythropolis* S67 (ВКМ Ас-2533 Д), входящих в биопрепарат «МикроБак» для биоремедиации нефтезагрязненных территорий. Геном *R. erythropolis* Х5 депонирован в базе данных National Center for Biotechnology Information под номерами доступа GenBankCP044283 и CP044284, BioSample – SAMN12818508, BioProject – PRJNA573614 и SRA – PRJNA573614. Содержание трегалолипидных биосурфактантов оценивали по количеству трегалозы в водных растворах биосурфактантов с помощью фенольно-серного метода. Поверхностное натяжение полученных водных растворов биосурфактантов определяли методом отрыва кольца де Нуи с использованием тензиометра Kruss K6 (*Kruss*, Германия). Критическую концентрацию мицеллообразования определяли по точке перегиба на кривых зависимостей поверхностного натяжения от концентрации раствора биосурфактанта. Для установления солюбилизирующей способности биосурфактантов определяли остаточную концентрацию *н*-гексадекана в водной пробе различной концентрации с помощью газохроматографического метода анализа.

Результаты. При постоянном поверхностном натяжении 24.2 мН/м и 25.0 мН/м для *R. erythropolis* Х5 и *R. erythropolis* S67 соответственно значение критической концентрации мицеллообразования для обоих штаммов составило 33 мг/л ($3.8 \cdot 10^{-5}$ моль/л). С помощью газохроматографического метода анализа показано солюбилизирующее действие мицеллярных растворов трегалолипидов родококков в отношении гидрофобного *н*-гексадекана. Процесс солюбилизации охарактеризовали с помощью молярной солюбилизирующей способности (molar solubilization capacity, S_m), молярного коэффициента солюбилизации (molar solubilization ratio, MSR), коэффициента распределения мицелла–вода (micelle–water partition coefficient, K_m) и энергии солюбилизации (ΔG_S^0). Показано, что процесс солюбилизации *н*-гексадекана протекает самопроизвольно ($\Delta G_S^0 = -35.5$ кДж/моль) и более эффективно ($S_m = 4.3$ моль/моль, MSR = 4.7 моль/моль) по сравнению с другими биосурфактантами гликолипидной природы.

Выводы. На основании величины молярного коэффициента солюбилизации можно сделать вывод, что трегалолипиды штамма *R. erythropolis* Х5 в большей степени солюбилизируют *н*-гексадекан в водных растворах по сравнению с другими биосурфактантами гликолипидной природы, однако уступают синтетическим поверхностно-активным соединениям.

INTRODUCTION

Biosurfactants or surfactants of biological origin have significant advantages over synthetic surfactants due to their physicochemical and biological properties. They are rapidly occupying a significant niche in the production of so-called green products and displacing analogues of chemical origin from the market. Due to their structural diversity and properties, such as reduction of surface and interfacial tension, foaming, emulsification, wetting, stabilization of emulsions and solubilization of hydrophobic substances, biosurfactants can be used in the pharmaceutical and food industries [1], cosmetology [2], to increase oil recovery, in bioremediation of polluted areas [3], in bioelectrochemistry [4], in agriculture [5], and in wastewater treatment technologies. Biosurfactants are produced by microorganisms of various taxonomic groups, such as bacteria of the genera *Pseudomonas*, *Rhodococcus*, *Arthrobacter*, *Mycobacterium*, *Nocardia*, *Corynebacterium* and yeasts of the genera *Candida* and *Rhodotorula* [6].

Among bacteria capable of forming and releasing biosurfactants into the environment, special attention needs to be paid to the bacteria of the *Rhodococcus* genus. The metabolic activity of *Rhodococcus* is due to the presence of a large number of enzyme systems which enable them to degrade many natural and anthropogenic organic compounds, such as alkanes, cycloalkanes, aromatic compounds, phenols, polycyclic aromatic hydrocarbons, halogenated hydrocarbons, and polychlorinated compounds. The list of toxic environmental pollutant compounds which can be mineralized or transformed by *Rhodococci* is quite large. It also includes explosives, pharmaceuticals, plastics and difficult-to-degrade synthetic polymers [7].

Rhodococci are characterized by the formation of surfactants of a glycolipid nature in response to the presence of alkanes in the nutrient medium. Such substances are one or two nonreducing disaccharides of trehalose bound to mycolic acids: long-chain α-branched-α-hydroxylated fatty acids with different carbon chain lengths [8].

Due to their low critical micelle formation concentration (CMC), the ability to reduce surface and interfacial tension, high activity under extreme environmental conditions (temperature, pH), good emulsifying ability combined with high biodegradability, low toxicity and environmental safety, as well as the possibility of being obtained from renewable sources of raw materials [9], these biological surfactants are more promising for the development of environmentally friendly biotechnologies.

In connection with the above properties and the wide application of trehalolipids in a range of industrial fields, the study of the solubilizing ability of their micellar solutions is both topical and in demand.

The aim of the study was to isolate biosurfactants of a glycolipid nature produced by the bacteria-destructors of the *Rhodococcus* genus of petroleum hydrocarbons, and to evaluate their solubilizing ability with respect to hydrophobic compounds on the example of *n*-hexadecane.

MATERIALS AND METHODS

Rhodococcus erythropolis X5 (VKM Ac-2532 D) and *Rhodococcus erythropolis* S67 (VKM Ac-2533 D) strains were obtained from the collection of the Laboratory of Biology and Plasmids of the G.K. Skryabin Institute of Biochemistry and Physiology of Microorganisms of the Russian Academy of Sciences. The MicroBak biopreparation contains these bacteria and is used for bioremediation of oil-contaminated territories [10]. The genome of *R. erythropolis* X5 is deposited in the NCBI database[1] under GenBank accession numbers CP044283 and CP044284, BioSample – SAMN12818508, BioProject – PRJNA573614 and SRA – PRJNA573614 [11].

Microorganisms were cultured in rocking flasks in 200 mL of liquid Evans mineral medium [12] with the addition of *n*-hexadecane (20 g/L) (*ECOS-1*, Russia) as the sole source of carbon and energy at 26°C and aeration at 180 rpm on an Excella 25 orbital rocker (*Eppendorf*, Germany) for 3 days.

Biosurfactants were isolated from culture fluid samples by means of liquid–liquid extraction [13]. Glycolipid components were separated by means of thin-layer chromatography on TLC plates Silica gel 60 F254 (*Merck*, Germany) [14].

The total biosurfactant content was determined by the concentration of carbohydrate in the sample spectrophotometrically using the phenol–sulfur method [15], after previously constructing a graduation relationship for the corresponding carbohydrate—trehalose. In order to calculate the concentration of trehalolipid, the obtained value of sugar concentration was multiplied by a coefficient equal to the ratio of the molecular weight of glycolipid (862) to the molecular weight of trehalose (342). This is respectively equal to 2.5.

---

[1] National Center for Biotechnology. Information https://www.ncbi.nlm.nih.gov. Accessed June 31, 2024.

The surface tension of the aqueous solutions of biosurfactants obtained was determined by means of the method [13] using a Kruss K6 tensiometer (*Kruss*, Germany). An initial aqueous solution with a concentration of 250 mg/L was prepared. A series of samples with biosurfactant concentrations in the range of 0–250 mg/L was obtained by dilution method, and the surface tension of each solution was measured. The CMC was determined by the inflection point on the curves of surface tension dependence on concentration.

In order to establish the solubilizing ability of biosurfactant, we determined the residual concentration of *n*-hexadecane in aqueous samples of biosurfactant of different concentrations according to the method [16] with our modifications. For this purpose, 300 μL of *n*-hexadecane and 10 mL of biosurfactant solution of the corresponding concentration were added to the tubes, which were corked and shaken vigorously for 1 min. Subsequently, the tubes were left at 28°C, and 180 rpm on an Excella 25 orbital rocker (*Eppendorf*, Germany) for 24 h. The contents of the tubes were poured into a separating funnel and left for 2 h for phase separation. Then the *n*-hexadecane layer was withdrawn into a separate tube. 10 mL of hexane was added to the tubes using a graduated pipette, corked and shaken vigorously for 1 min. The gas chromatographic determination of the residual concentration of *n*-hexadecane extracted with hexane was then carried out. The method used to determine oil product content in natural and waste waters was the gas chromatographic method[2] on a Chromatek Crystal 5000.2 gas chromatograph (*Chromatek*, Russia) with Varian Capillary Column CP-Sil 8 CB (50 m) and flame ionization detector. The concentration of hexadecane was calculated by means of the absolute graduation method.

Experiments were performed in triplicate, statistical processing was performed using Microsoft Office Excel 2010 and SigmaPlot® 2011 software. The average value ± confidence interval was calculated.

RESULTS AND DISCUSSION

Representatives of the *Rhodococcus* genus are efficient degraders of oil hydrocarbons. They easily adapt to extreme environmental conditions and are often included in the composition of biopreparations for cleaning from oil pollution[3]. They produce biosurfactants of glycolipid nature, namely trehalolipids. The hydrophobic nature of oil hydrocarbons is the reason for their low bioavailability in the process of biodegradation. However, the formation of micellar solutions of trehalolipids can contribute to its increase. In the present work, the solubilizing ability of *R. erythropolis* X5 and *R. erythropolis* S67 strains was evaluated with respect to a hydrophobic compound, using *n*-hexadecane as an example.

Biosurfactants of a glycolipid nature were isolated from the culture fluid of petroleum hydrocarbon-degrading bacteria *R. erythropolis* X5 and *R. erythropolis* S67 by means of extraction with a system of polar organic solvents. Previously, 2,3,4-succinyl-octanoyl-dodecanoyl-2'-decanoyl-trehalose and 2,3,4-succinyl-dioctanoyl-2'-decanoyl-trehalose had been found to be the main biosurfactants produced by these bacteria grown on *n*-hexadecane, both at 26°C and 10°C [13, 17].

In order to confirm the chemical structure of the isolated substances synthesized by the studied bacteria, the lipid extract obtained was analyzed by thin-layer chromatography. In order also to detect trehalose tetraethers, we used α-naphthol reagent which is a specific developer for sugars. This enabled us to identify glycolipids among other lipid components. When comparing the obtained data with date from the literature (Table 1), it can be noted that *Rhodococcus* biosurfactants appear on chromatograms with a different number of spots and retention values. However, the spot which appears to have the highest intensity with a retention factor of R_f 0.35–0.39 is present in all chromatograms, except for *R. erythropolis* A29-k1 strain and *R. ruber* IEGM 231 strain.

Table 1. Comparative characteristics of the R_f values of trehalolipids of various *Rhodococcus* strains

Microbial strain	R_{f1}	R_{f2}	R_{f3}
R. erythropolis X5	0.38	0.50	0.59
R. erythropolis S67	0.37	0.50	–
R. ruber IEGM 231 [18]	0.18	0.39	0.75
R. erythropolis A29-k1 [19]	0.46	0.54	–
R. sp. 3–2 [15]	0.35	0.53	0.56

---

[2] Methodology for measurement of oil product content in natural and waste waters by gas chromatographic method with flame ionization detector. MVI-05-94. M.: 1994.

[3] Neustroev M.M. *Ecological assessment of oil-contaminated permafrost soils and development of methods of their bioremediation*. Cand. Sci. Thesis. (Biol.). Yakutsk. 2016.

The trehalolipid components thus revealed may have structural differences, but they all contain carbohydrate residues. The results obtained are consistent with the results of earlier studies [20].

The amount of isolated trehalolipids of *R. erythropolis* X5 and *R. erythropolis* S67 bacteria after 3 days of cultivation was determined by means of measuring the trehalose content in the analyzed samples. Strain X5 produced more biosurfactants (0.31 g/L, $36 \cdot 10^{-5}$ mol/L) in contrast to strain S67 (0.25 g/L, $29 \cdot 10^{-5}$ mol/L). The results presented agree with the data of Luong [14], in which the content of trehalolipid biosurfactants was about 0.3 g/L. The same amount of trehalolipids was obtained by White [21] in the cell-free supernatant during cultivation of *Rhodococcus sp.* PLM026 on sunflower oil at 19°C.

One of the important colloidal-chemical properties of surfactants of both chemical and biological origin is the ability to reduce the surface tension (air–water). As a consequence, the effectiveness of biosurfactants can be evaluated by means of measuring the surface tension of their solutions and plotting the graphical dependence of surface tension on the biosurfactant content (Fig. 1). At low contents (up to 25 mg/L), a linear dependence can be observed. There is a sharp decrease in surface tension when the biosurfactant content is increased within the range of 30 to 35 g/L. With a further increase in the biosurfactant content, there is a slowing of the rate of surface tension. This is due to gradual saturation of the surface layer with biosurfactant molecules. When the CMC is reached, biosurfactants in aqueous solution begin to form micelles and the surface tension does not change further. The CMC of isolated trehalolipids of strains X5 and S67 was determined using the inflection point of the graphical dependence of surface tension on the biosurfactant concentration.

At a constant surface tension of 24.2 and 25 mN/m for *R. erythropolis* X5 and *R. erythropolis* S67, respectively, the CMC value for both strains was 33 mg/L ($3.8 \cdot 10^{-5}$ mol/L). Table 2 summarizes the surface tension and CMC values of biosurfactants isolated by other researchers.

The results obtained by us agree with the data of other authors (Table 2). The trehalolipids studied are not inferior to other types of glycolipids in terms of efficiency in reducing the surface tension of water. The advantage of the isolated trehalolipids of *R. erythropolis* X5 and *R. erythropolis* S67 over synthetic surfactants should be noted. For example, sodium dodecyl sulfate (CMC = 2.34 g/L) and Tween-80 (CMC = 0.016 g/L) reduce the surface tension of water from 72 to 37 and 34.8 mN/m, respectively [28], while natural surfactants reduce the surface tension of water to lower values.

An interesting objective was to evaluate the solubilizing ability of the trehalolipids to increase the bioavailability of hydrophobic pollutants to bacterial cells by increasing their hydrophilicity. The solubilization process can be described as colloidal dissolution of various substances in surfactant micelles, therefore, solutions with trehalolipid content multiple of CMC were used to determine the solubilizing ability of trehalolipids.

Solubilization can be quantitatively characterized by using the molar solubilizing capacity (S_m). This is the ratio of the number of moles of *n*-hexadecane to the number of moles of trehalolipid:

$$S_m = \frac{C_1}{C_2}, \tag{1}$$

wherein C_1 is the *n*-hexadecane concentration, mol/L, C_2 is the trehalolipid concentration, mol/L.
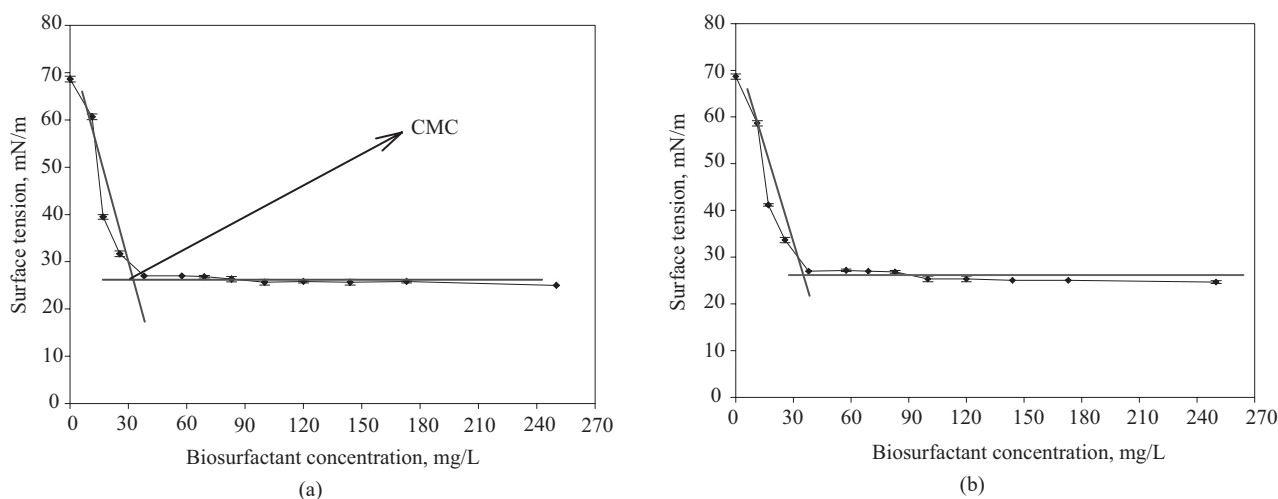
Fig. 1. Dependence of surface tension on biosurfactant content of *R. erythropolis* X5 (a) and *R. erythropolis* S67 strains (b)

Table 2. Characteristics of biosurfactants

Microorganism	Biosurfactant	Surface tension, mN/m	CMC, mg/L
Pseudomonas aeruginosa S6 [22]	Rhamnolipids	33.9	50.0
Staphulococcuss aprophyticus SBPS-15 [23]	Glycolipids (staphylosan)	30.9	24.0
Rhodococcus sp. HL-6 [24]	Glycolipids	30.7	40.0
Rhodococcus ruber IEGM 235 [25]		26.8	54.0
Rhodococcus erythropolis DSM 43215 [25]	Trehalolipids	26.0–32.0	4.0–15.0
Rhodococcus wratislaviensis BN38 [26]		24.4	5.0
Rhodococcus qingshengii FF [27]		–	85.0

With increased concentration of trehalolipid micellar solutions, the amount of solubilized *n*-hexadecane naturally increased in the range of trehalolipid contents above the CMC. This indicates solubilization of the hydrophobic compound in surfactant micelles. After 24 h, the average molar solubilization of *n*-hexadecane in aqueous solution of biosurfactant strain X5 was 4.3 mol of *n*-hexadecane per 1 mol of trehalolipid. The solubilization isotherm has a linear character at the concentration of trehalolipid above the CMC, indicating a constant micelle shape (Fig. 2).
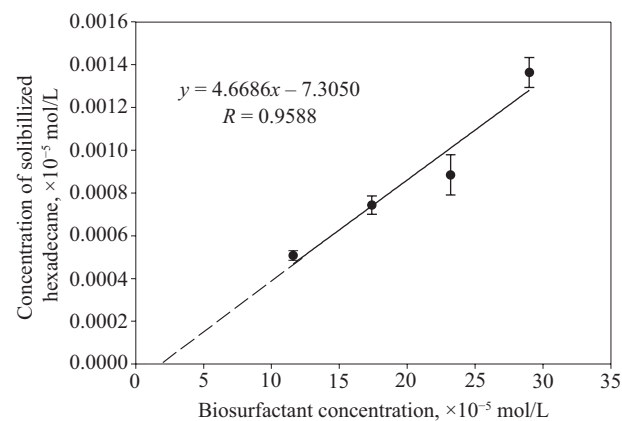
Fig. 2. Solubilization isotherm of *n*-hexadecane by trehalolipid micelles

Solubilization isotherms enable us to determine the values of CMC for which solubilization isotherms should be extrapolated to the concentration axis. Segments cut off on the concentration axis give the desired CMC values [28]. According to Fig. 2, the CMC value of trehalolipid biosurfactant produced by *R. erythropolis* X5 strain is $2.5 \cdot 10^{-5}$ mol/L. This value is slightly different from the value of CMC found from the surface tension isotherm ($3.8 \cdot 10^{-5}$ mol/L). This may be due to an error in the method of determining the solubilizing capacity of biosurfactants.

The solubilization isotherm presented also allows us to determine the molar solubilization ratio (MSR) as the tangent of the slope of this straight line (Fig. 2). MSR is the amount of *n*-hexadecane that can be solubilized by one mole of micellar solution of trehalolipid and characterizes in general the ability of surfactant to solubilize *n*-hexadecane.

We consider the binding constant or molar distribution coefficient as a parameter of interaction between *n*-hexadecane and trehalolipid. This is calculated according to the following formula:

$$K_m = \frac{\mathrm{MSR}}{S_{\mathrm{CMC}} V_w \left(1 + \mathrm{MSR}\right)}, \qquad (2)$$

wherein MSR is the molar solubilization ratio, mol/mol; S_{CMC} is the solubility of *n*-hexadecane at CMC; V_w is the molar volume of water; $V_w = 0.01805$ dm^3/mol at 298 K.

A knowledge of thermodynamic parameters is necessary to achieve a better understanding of the solubilization mechanism. From the thermodynamic point of view, solubilization can be considered as the distribution of *n*-hexadecane between micellar and aqueous phases. The free energy of solubilization is calculated on the basis of the following equation:

$$\Delta G_S^0 = R \cdot T \cdot \left(\ln \frac{CMC}{mol_w} \right), \qquad (3)$$

wherein ΔG_S^0 is solubilization free energy, kJ/mol; R is the gas constant, $R = 8.31$ J/mol·K; T is the temperature, K; mol_w is the solvent (water) molarity, $mol_w = 55.5$.

In order to describe the solubilizing ability of surfactants, MSR and CMC values are primarily established. Determination of the micelle–water distribution coefficient (K_m) and solubilization energy (ΔG_S^0) is less frequently used in research work. Among glycolipid biosurfactants (Table 3), isolated trehalolipids solubilize *n*-hexadecane in aqueous solutions more efficiently. However, they are inferior to synthetic surfactants, namely those surfactants of a nonionic nature (Tween-80 and Triton X-100). In [29–31], the difference in the solubilizing ability of synthetic surfactants of different chemical structure in relation to *n*-hexadecane and chlorine derivatives of hydrocarbons is shown. For nonionogenic surfactants, the solubilizing ability of *n*-hexadecane is higher than that of chlorine derivatives. For sodium dodecyl sulfate, an ionogenic surfactant, a lower solubilization capacity of

n-hexadecane and chlorine derivatives can be observed. Thus, the value of molar solubilizing capacity may differ depending on the chemical structure of the surfactant itself and the solubilized substance. In [31] it is demonstrated that the solubility of naphthalene, phenanthrene and pyrene increased linearly with an increasing concentration of rhamnolipid biosurfactant of bacteria of the *Bacillus* genus. In addition, the values of molar solubilization coefficient decreased in the series: naphthalene > phenanthrene > pyrene.

With regards to the system which we studied, the free energy value has a negative value ($\Delta G_S^0 = -35.5$ kJ/mol), indicating a spontaneous solubilization process. It was shown in [34] that the solubilization processes of nitrogen-containing heterocyclic substances (aniline, indole, quinolone), surfactants of chemical (sodium dodecyl sulfate (Tween-80, Span 20, and TX-100)) and biological (rhamnolipid) origin are spontaneous ($\Delta G_S^0 \leq 0$). The value of solubilization free energy for rhamnolipid is markedly lower than for synthetic surfactants. This proves the better solubilizing ability of rhamnolipid and is consistent with our data.

Table 3. Comparative table of data (obtained and from literature) of the physicochemical characteristics of solubilization of different substances by nature

Surfactant	Solubilizate	MSR, mol/mol	ΔG_S^0, kJ/mol	$\lg K_m$	Reference
Trehalolipids	Hexadecane	4.7	−35.5	1.065	This work
Monorhamnolipids		0.89	–	8.25	[33]
Diramnolipids		3.8	–	–	
Sodiumdodecylsulfate	Hexadecane	0.018	−54.5	–	[29]
	Perchloroethylene	0.16	–	–	[30]
Twin-80	Hexadecane	15.1	−64.4	–	[29]
	Hexachloroethane	0.15	–	–	[31]
Triton X-100	Hexadecane	40	−64.6	–	[29]
	Hexachlorobutadiene	1.22	–	–	[31]

CONCLUSIONS

For *Rhodococcus* trehalolipids, their solubilizing effect on hydrophobic *n*-hexadecane was demonstrated using the following physicochemical values: molar solubilizing capacity; molar solubilization coefficient; micelle–water distribution coefficient; and solubilization energy. Based on the value of the molar solubilization coefficient, it can be concluded that trehalolipids of *R. erythropolis* X5 strain solubilize *n*-hexadecane in aqueous solutions to a greater extent than other biosurfactants of glycolipid nature, while they are inferior to synthetic surfactants.

Authors' contributions

I.A. Nechaeva—formulating the research objectives and methodology, and writing the text of the article.

A.S. Parfenova—planning and conducting experiments, processing experimental data, and discussion of the results.

A.S. Filippova—conducting experiments, processing experimental data.

A.E. Filonov—scientific consulting, editing the article.

The authors declare no conflicts of interest.

REFERENCES

1. Alizadeh-Sani M., Hamishehkar H., Khezerlou A., Azizi-Lalabadi M., Azadi Y., Nattagh-Eshtivani E. Bioemulsifiers Derived from Microorganisms: Applications in the Drug and Food Industry. *Adv. Pharm. Bull*. 2018;8(2):191–199. https://doi.org/10.15171/apb.2018.023

2. Adu S.A., Naughton P.J., Marchant R., Banat I.M. Microbial Biosurfactants in Cosmetic and Personal Skincare Pharmaceutical Formulations. *Pharmaceutics*. 2020;12(11):1099. https://doi.org/10.3390/pharmaceutics12111099

3. Fenibo E.O., Ijoma G.N., Selvarajan R., Chikere C.B. Microbial Surfactants: The Next Generation Multifunctional Biomolecules for Applications in the Petroleum Industry and Its Associated Environmental Remediation. *Microorganisms*. 2019;7(11):581. https://doi.org/10.3390/microorganisms7110581

4. Pasternak G., Askitosari T.D., Rosenbaum M.A. Biosurfactants and Synthetic Surfactants in Bioelectrochemical Systems: A Mini-Review. *Front. Microbiol*. 2020;11:358. https://doi.org/10.3389/fmicb.2020.00358

5. Kumar A., Singh S.K., Kant C., Verma H., Kumar D., Singh P.P., *et al.* Microbial Biosurfactant: A New Frontier for Sustainable Agriculture and Pharmaceutical Industries. *Antioxidants*. 2021;10(9):1472. https://doi.org/10.3390/antiox10091472

6. Gouthami K., Mallikarjunaswamy A.M.M., Bhargava R.N., Ferreira L.F.R., Rahdar A., Saratale G.D., Bankole P.O., Mulla S.I. Microbial Biodegradation and Biotransformation of Petroleum Hydrocarbons: Progress, Prospects, and Challenges. In: *Genomics Approach to Bioremediation. Genomics Approach to Bioremediation: Principles, Tools, and Emerging Technologies*. 2023. P. 229–247. https://doi.org/10.1002/9781119852131.ch13

7. Eras-Muñoz E., Farré A., Sánchez A., Font X., Gea T. Microbial biosurfactants: a review of recent environmental applications. *Bioengineered*. 2022;13(5):12365–12391. https://doi.org/10.1080/21655979.2022.2074621

8. Claus S., Jenkins Sánchez L., Van Bogaert I.N.A. The role of transport proteins in the production of microbial glycolipid biosurfactants. *Appl. Microbiol. Biotechnol*. 2021;105(5):1779–1793. https://doi.org/10.1007/s00253-021-11156-7

9. Sobrinho H.B.S., Luna J.M., Rufino R.D., Porto A.L.F., Sarubbo L.A. Biosurfactants: Classification, properties and environmental applications. In: *Recent Developments in Biotechnology*. 1st ed. Houston, USA: Studium Press LLC; 2013. P. 303–330.

10. Filonov A.E., Kosheleva I.A., Samoilenko V.A., Shkidchenko A.N., *et al*. Biological preparation for cleaning of soils from contaminations with oil and oil products, method of its production and application: RU Pat. 2378060. Publ. 10.01.2010 (in Russ.).

11. Delegan Y., Valentovich L., Petrikov K., Vetrova A., Akhremchuk A., Akimov V. Complete Genome Sequence of *Rhodococcus erythropolis* X5, a Psychrotrophic Hydrocarbon-Degrading Biosurfactant-Producing Bacterium. *Microbiol. Resour. Announc*. 2019;8(48). https://doi.org/10.1128/mra.01234-19

12. Karimova V.T., Dmitrieva E.D., Nechaeva I.A. The effect of humic substances from different origin peats of the Tula region on the growth of microbial degraders of oil *Rhodococcus erythropolis* S67 and *Rhodococcus erythropolis* X5. *Izvestiya Tul'skogo gosudarstvennogo universiteta. Estestvennye nauki = News of the Tula State University. Natural Sciences*. 2017;2:60–68 (in Russ.).

13. Luong T.M., Ponamoreva O.N., Nechaeva I.A., Petrikov K.V., Delegan Ya.A., Surin A.K., Linklater D., Filonov A.E. Characterization of biosurfactants produced by the oil-degrading bacterium *Rhodococcus erythropolis* S67 at low temperature. *World J. Microbiol. Biotechnol*. 2018;34(2):20. https://doi.org/10.1007/s11274-017-2401-8

14. Lyong T.M., Nechaeva I.A., Petrikov K.V., Puntus I.F., Ponamoreva O.N. Oil-degrading microorganisms of genus Rhodococcus – potential producers of biosurfactants. *Izvestiya vuzov. Prikladnaya khimiya i biotekhnologiya = Proceedings of Universities. Applied Chemistry and Biotechnology*. 2016;6(1–16):50–60 (in Russ.).

15. Leonova T.I., Akatova E.V., Puntus I.F. Isolation of glycolipid biosurfactants produced by bacteria Rhodococcus sp. 3-2 by extraction method. *Izvestiya Tul'skogo gosudarstvennogo universiteta. Estestvennye nauki = News of the Tula State University. Natural Sciences*. 2021;(2):33–41 (in Russ.). https://doi.org/10.24412/2071-6176-2021-2-33-41

16. Yang X., Tan F., Zhong H., Liu G., Ahmad Z., Liang Q. Sub-CMC solubilization of *n*-alkanes by rhamnolipid biosurfactant: the Influence of rhamnolipid molecular structure. *Colloids Surf. B: Biointerfaces*. 2020;192:111049. https://doi.org/10.1016/j.colsurfb.2020.111049

17. Lyong T.M., Nechaeva I.A., Petrikov K.V., Filonov A.E., Ponamoreva O.N. Structure and physicochemical properties of glycolipid biosurfactants, produced by oil-degrading bacteria *Rhodococcus* sp. X5. *Izvestiya vuzov. Prikladnaya khimiya i biotekhnologiya = Proceedings of Universities. Applied Chemistry and Biotechnology*. 2017;7(2–21):72–79 (in Russ.). https://doi.org/10.21285/2227-2925-2017-7-2-72-79

18. Kuyukina M.S., Ivshina I.B., Philp J.C., Christofi N., Dunbar S.A., Ritchkova M.I. Recovery of *Rhodococcus* biosurfactants using methyl tertiary-butyl ether extraction. *J. Microbiol. Methods*. 2001;46(2):149–156. https://doi.org/10.1016/S0167-7012(01)00259-7

19. Ratnikava M.S., Charniauskaya M.I., Bukliarevich H.A., Myamin U.Y., Meloni F., Lussu R., Titok M.A. *Rhodococcus erythropolis* strain A29-K1 – an effective producer of surface active compounds. In: *Biotechnology of Microorganisms*: *Proc. International Scientific-Practical Conference*. 2019. P. 163–165.

20. Petrikov K., Delegan Y., Surin A., Ponamoreva O., Puntus I., Filonov A., Boronin A. Glycolipids of *Pseudomonas* and *Rhodococcus* oil-degrading bacteria used in bioremediation preparations: formation and structure. *Process Biochem*. 2013;48(5–6):931–935. https://doi.org/10.1016/j.procbio.2013.04.008

21. White D.A., Hird L.C., Ali S.T. Production and characterization of a trehalolipid biosurfactant produced by the novel marine bacterium *Rhodococcus* sp., strain PML026. *J. Appl. Microbiol*. 2013;115(3):744–755. https://doi.org/10.1111/jam.12287

22. Yin H., Qiang J., Jia Y., Ye J., Peng H., Qin H., Zhang N., He B. Characteristics of biosurfactant produced by *Pseudomonas aeruginosa* S6 isolated from oil-containing wastewater. *Process Biochem*. 2009;44(3):302–308. https://doi.org/10.1016/j.procbio.2008.11.003

23. Balan S.S., Mani P., Kumar C.G., Jayalakshmi S. Structural characterization and biological evaluation of Staphylosan (dimannooleate), a new glycolipid surfactant produced by a marine *Staphylococcus saprophyticus* SBPS-15. *Enzyme Microb. Technol*. 2019;120:1–7. https://doi.org/10.1016/j.enzmictec.2018.09.008

24. Tian Z.J., Chen L.Y., Li D.H., Pang H.Y., Wu S., Liu J.B., Huang L. Characterization of a Biosurfactant-producing Strain *Rhodococcus* sp. HL-6. *Romanian Biotechnol. Lett*. 2016;21(4):11650–11659.

25. Philp J.C.M.S., Kuyukina M., Ivshina I., Dunbar S., Christofi N., Lang S., Wray V. Alkanotrophic *Rhodococcus ruber* as a biosurfactant producer. *Appl. Microbiol. Biotechnol*. 2002;59(2):318–324. https://doi.org/10.1007/s00253-002-1018-4

26. Tuleva B., Cohen R., Stoev G., Stoineva I. Production and structural elucidation of trehalose tetraesters (biosurfactants) from a novel alkanothrophic *Rhodococcus wratislaviensis* strain. *J. Appl. Microbiol*. 2008;104(6):1703–1710. https://doi.org/10.1111/j.1365-2672.2007.03680.x

27. Wang Y., Nie M., Diwu Z., Lei Y., Li H., Bai X. Characterization of trehalose lipids produced by a unique environmental isolate bacterium *Rhodococcus qingshengii* strain FF. *J. Appl. Microbiol*. 2019;127(5):1442–1453. https://doi.org/10.1111/jam.14390

28. Dremuk A.P., Kienskaya K.I., Avramenko G.V., Nazarov V.V., Belova I.A. Features of the solubilization action of the binary and ternary surfactant mixtures based on alkyl glucoside. *Prikladnaya khimiya i biotekhnologiya = Proceedings of Universities. Applied Chemistry and Biotechnology*. 2017;7(1):49–55 (in Russ.). https://doi.org/10.21285/2227-2925-2017-7-1-50-56

29. Zarueva E.S., Nechaeva I.A., Ponamoreva O.N. Solubilization of *n*-hexadecane in a mineral medium with surfactants. *Izvestiya Tul'skogo gosudarstvennogo universiteta. Estestvennye nauki = News of the Tula State University. Natural Sciences*. 2020;(1):3–12 (in Russ.).

30. Harendra S., Vipulanandan C. Effects of surfactants on solubilization of perchloroethylene (PCE) and trichloroethylene (TCE). *Ind. Eng. Chem. Res*. 2011;50(9):5831–5837. https://doi.org/10.1021/ie102589e

31. Rodrigues R., Betelu S., Colombano S., Masselot G., Tzedakis T., Ignatiadis I. Influence of temperature and surfactants on the solubilization of hexachlorobutadiene and hexachloroethane. *J. Chem. Eng. Data*. 2017;62(10):3252–3260. https://doi.org/10.1021/acs.jced.7b00320

32. Li S., Pi Y., Bao M., Zhang C., Zhao D., Li Y., Sun P., Lu J. Effect of rhamnolipid biosurfactant on solubilization of polycyclic aromatic hydrocarbons. *Marine Pollut. Bull*. 2015;101(1):219–225. https://doi.org/10.1016/j.marpolbul.2015.09.059

33. Zhong H., Liu Y., Liu Z., Jiang Y., Tan F., Zeng G., Yuan X., Yan M., Niu Q., Liang Y. Degradation of pseudo-solubilized and mass hexadecane by a *Pseudomonas aeruginosa* with treatment of rhamnolipid biosurfactant. *Int. Biodeterior. Biodegradation*. 2014;94:152–159. https://doi.org/10.1016/j.ibiod.2014.07.012

34. Yang Z., Cui J., Yin B. Solubilization of Nitrogen Heterocyclic Compounds Using Different Surfactants. *Water, Air, Soil Pollut*. 2018;229(9):304. https://doi.org/10.1007/s11270-018-3917-8

About the authors

Irina A. Nechaeva, Cand. Sci. (Biol.), Associate Professor, Biotechnology Department, Institute of Natural Science, Tula State University (92, Lenina pr., Tula, 300012, Russia). E-mail: nechaeva1902@gmail.com. Scopus Author ID 22958438500, ResearcherID ABF-1379-2020, RSCI SPIN-code 5627-7670, https://orcid.org/0000-0003-2736-080X

Anastasia S. Parfenova, Master Student, Biotechnology Department, Institute of Natural Science, Tula State University (92, Lenina pr., Tula, 300012, Russia). E-mail: asya17.parfenova@mail.ru. RSCI SPIN-code 3154-4258, https://orcid.org/0000-0002-4894-4591

Anastasia S. Filippova, Junior Researcher, Laboratory of Environmental and Medical Biotechnology, BioChemTechCenter; Master Student, Biotechnology Department, Institute of Natural Science, Tula State University (92, Lenina pr., Tula, 300012, Russia). E-mail: stasya.filippova.01@gmail.com. RSCI SPIN-code 6966-6230.

Andrey E. Filonov, Dr. Sci. (Biol.), Professor, Biotechnology Department, Institute of Natural Science, Tula State University (92, Lenina pr., Tula, 300012, Russia); Leading Researcher, Laboratory of Plasmid Biology, Pushchino Scientific Center for Biological Research, G.K. Skryabin Institute of Biochemistry and Physiology of Microorganisms, Russian Academy of Sciences (5, Nauki pr., Pushchino, Moscow oblast, 142290, Russia). E-mail: filonov.andrey@rambler.ru. Scopus Author ID 35608598500, ResearcherID E-8335-2014, RSCI SPIN-code 2615-4487, https://orcid.org/0000-0003-4800-7706

Об авторах

Нечаева Ирина Александровна, к.б.н., доцент, доцент кафедры биотехнологии, Естественно-научный институт, ФГБОУ ВО «Тульский государственный университет» (300012, Россия, Тула, пр-т Ленина, д. 92). E-mail: nechaeva1902@gmail.com. Scopus Author ID 22958438500, ResearcherID ABF-1379-2020, SPIN-код РИНЦ 5627-7670, https://orcid.org/0000-0003-2736-080X

Парфенова Анастасия Сергеевна, магистрант кафедры биотехнологии, Естественно-научный институт, ФГБОУ ВО «Тульский государственный университет» (300012, Россия, Тула, пр-т Ленина, д. 92). E-mail: asya17.parfenova@mail.ru. SPIN-код РИНЦ 3154-4258, https://orcid.org/0000-0002-4894-4591

Филиппова Анастасия Сергеевна, младший научный сотрудник, лаборатория экологической и медицинской биотехнологии БиоХимТехЦентра; магистрант кафедры биотехнологии, Естественнонаучный институт, ФГБОУ ВО «Тульский государственный университет» (300012, Россия, Тула, пр-т Ленина, д. 92). E-mail: stasya.filippova.01@gmail.com. SPIN-код РИНЦ 6966-6230, https://orcid.org/0000-0002-4894-4591

Филонов Андрей Евгеньевич, д.б.н., профессор кафедры биотехнологии, Естественно-научный институт, ФГБОУ ВО «Тульский государственный университет» (300012, Россия, Тула, пр-т Ленина, д. 92); ведущий научный сотрудник лаборатории биологии плазмид, Институт биохимии и физиологии микроорганизмов им. Г.К. Скрябина, Российская академия наук (ИБФМ РАН) – обособленное подразделение Федерального государственного бюджетного учреждения науки «Федеральный исследовательский центр «Пущинский научный центр биологических исследований Российской академии наук» (142290, Россия, Пущино, пр-т Науки, д. 5). E-mail: filonov.andrey@rambler.ru. Scopus Author ID 35608598500, ResearcherID E-8335-2014, SPIN-код РИНЦ 2615-4487, https://orcid.org/0000-0003-4800-7706

RESEARCH ARTICLE

Features of the change in the thermal coefficient of electrical resistance upon heating electrically conductive composites of crystallizable polyolefins with carbon black

Anatoly V. Markov✉, Alexander E. Zverev, Vasily A. Markov

MIREA – Russian Technological University (M.V. Lomonosov Institute of Fine Chemical Technologies), Moscow, 119571 Russia

✉ *Corresponding author, e-mail: markovan@bk.ru*

Abstract

Objectives. To investigate electrically conductive polymer composite materials (EPCMs) based on crystallizable polyolefins and electrically conductive carbon black for the production of self-regulating heaters; to study the mechanism of the occurrence of positive and negative temperature coefficients (PTC and NTC) upon heating such composites.

Methods. A comprehensive study of the structure and properties of crystallizable EPCMs with electrically conductive technical carbon was carried out. In order to measure the electrical characteristics of the composites, they were compacted into plates to model polymer heaters. Contact electrodes made of an ungreased brass mesh were embedded in their ends. The temperature dependencies of the electrical characteristics of the samples were investigated in a modified thermal chamber of an FWV 633.10 Vicat softening temperature meter. The change in the degree of crystallinity was analyzed by means of differential scanning calorimetry with a NETZSCH DSC 204 F1 Phoenix calorimeter. The dilatometric and rheological characteristics of the samples were studied using an IIRT-AM melt flow index tester.

Results. It was determined that the self-regulation ability (an abnormally high positive thermal coefficient of electrical resistance) of self-regulating heaters made of composites of crystallizable polyolefins with electrically conductive technical carbon cannot be explained by the thermal expansion of EPCMs alone. It was shown that in crystallizable polyolefin-based EPCMs, the inversion of the thermal coefficients of electrical resistance (transition from PTC to NTC) is associated with a change in the aggregate state of EPCMs and the beginning of its transition to a viscous-flow state. A mechanism involving a sharp increase in the electrical resistance of self-regulating crystallizable polyolefin-based composite with electrically conductive technical carbon was proposed and substantiated. This mechanism takes into account the additional shear deformation effect produced on the crystalline phase of the EPCM by numerous expanding melt microvolumes formed at the early stages of the melting process with a minimum change in the degree of crystallinity.

Features of the change in the thermal coefficient of electrical resistance upon heating electrically conductive composites of crystallizable polyolefins with carbon black

Anatoly V. Markov,
Alexander E. Zverev, Vasily A. Markov

НАУЧНАЯ СТАТЬЯ

Особенности изменения термического коэффициента электрического сопротивления при нагревании электропроводящих композиций кристаллизующихся полиолефинов с техническим углеродом

А.В. Марков✉, **А.Е. Зверев, В.А. Марков**

МИРЭА – Российский технологический университет (Институт тонких химических технологий им. М.В. Ломоносова), Москва, 119571 Россия

✉ *Автор для переписки, e-mail: markovan@bk.ru*

Аннотация

Цели. Исследовать электропроводящие полимерные композиционные материалы (ЭПКМ) на основе кристаллизующихся полиолефинов и электропроводного технического углерода (ЭТУ) для производства саморегулирующихся нагревателей. Изучить механизм возникновения эффектов положительного и отрицательного температурных коэффициентов (ПТК и ОТК) в процессе нагревания композитов.

Методы. Проведено комплексное исследование структуры и свойств кристаллизующихся ЭПКМ с ЭТУ. Для исследования электрических характеристик композиций были отпрессованы пластины с запрессованными на концах контактными электродами из обезжиренной латунной сетки, моделирующие полимерные нагреватели. Исследование зависимостей электрических характеристик образцов от температуры проводили в модифицированной термокамере прибора FWV 633.10 для определения температуры размягчения Вика. Изменение степени кристалличности исследовали методом дифференциальной сканирующей калориметрии на приборе NETZSCH DSC 204F1 Phoenix. Исследование дилатометрических и реологических характеристик образцов проводили на приборе для определения показателя текучести (ИИРТ-АМ).

Результаты. Установлено, что появление у саморегулирующихся нагревателей, изготовленных из кристаллизующихся полиолефиновых композиций с ЭТУ, способности саморегулирования (появления аномально высокого положительного термического коэффициента электрического сопротивления) нельзя объяснить только термическим расширением ЭПКМ. Показано, что в кристаллизующихся полиолефиновых ЭПКМ инверсия термических коэффициентов электрического сопротивления (переход от ПТК к ОТК) связана с изменением агрегатного состояния ЭПКМ и началом его перехода в вязкотекучее состояние. Предложен и обоснован механизм резкого роста электрического сопротивления саморегулирующихся кристаллизующихся полиолефиновых композиций с ЭТУ, учитывающий дополнительное сдвиговое деформационное воздействие на кристаллическую фазу ЭПКМ множества расширяющихся микрообъемов расплава, возникающих на ранних стадиях процесса плавления при минимальном изменении степени кристалличности.

Features of the change in the thermal coefficient of electrical resistance upon heating
electrically conductive composites of crystallizable polyolefins with carbon black

Anatoly V. Markov,
Alexander E. Zverev, Vasily A. Markov

INTRODUCTION

Electrically conductive polymer composite materials (EPCMs) with electrically conductive carbon black (ECB) as a conductive filler have found the following applications: in electrically conductive coatings; electromagnetic shielding for protection against static electricity; fuses against overloads in electrical grid equipment; temperature and pressure sensors [1–7]; and self-regulating heaters [8–12]. The production of self-regulating heaters is important for the safety of household heating appliances. The self-regulation of power of heaters based on EPCMs is due to an abnormally high positive temperature coefficient of electrical resistance (PTC) of crystallizable polymer matrices (e.g., polyolefins) in the temperature range of the onset of their melting [8–13]. This phenomenon is virtually absent in amorphous EPCMs.

An important condition for obtaining EPCMs with high electrical conductivity is believed to be the uniform distribution of ECB particles in the composite [14, 15]. Increased electrical resistance upon heating of self-regulating EPCMs is usually attributed to an increase in the distance between the particles and aggregates of ECB during thermal expansion upon heating [16–19]. However, studies indicate an increase in the electrical conductivity of materials with a nonuniform distribution of ECB in the crystallizable polymer phase, as well as in mixtures of such polymers [20–24]. This nonuniformity of such EPCMs makes the system of conductive channels formed from ECB particles less stable at high temperatures. This instability of EPCMs can lead to reversible disruptions of the conductive channels in the microzones between the melting crystalline formations [6, 10, 11, 13, 24]. With an increase in temperature, the number of such zones increases. The electrical resistance of the heater increases rapidly, and its power drops sharply. The purpose of the work was to confirm the mechanism of the occurrence of abnormally high PTC in polyolefin-based EPCMs.

EXPERIMENTAL

The objects of this study were thermoplastic polyolefins with different melting temperatures: stabilized cable high-density polyethylene (HDPE) 277-73 (GOST 16338-85[1]); low-density polyethylene (LDPE) 10813-020 (GOST 16337-77[2]); and polypropylene (PP) 01050 (TU 2211-074-05766563-2015[3]). The electrically conductive filler was UM-76 finely divided ECB (TU 38-10001-94) intended for use in EPCMs.

Composites were prepared using a VK-6 laboratory-scale two-roll mixing mill (GRANAT, Russia) with electric heating of the rolls at a mixing temperature of 180 ± 10°C. The UM-76 powder was added to a preliminarily prepared polyethylene melt. After homogenization, rolling was continued for 10 min. The ECB content in all the composites was the same and amounted to 20 wt % (11.7 vol %). It was previously shown that this UM-76 content is optimal for self-regulating EPCMs [9].

In order to study the electrical characteristics of the composites, samples were compacted from them at a pressure of 15.0 MPa at 180°C and cooled in a mold to 50°C. The samples consisted of plates with a length of $L = 120 \pm 5$ mm, a width of $b = 10 \pm 0.5$ mm, and a thickness of $\delta = 1.0 \pm 0.05$ mm. Contact electrodes made of an L-80 ungreased brass mesh (GOST 6613-86[4]) were embedded in their ends. Slow cooling guaranteed the stability of the structure of the properties of the samples. The electrical resistance of the samples was measured with a DT9208A ohmmeter (DELTA Battery, China). Tests at elevated temperatures were performed in a modified thermal chamber of an FWV 633.10 Vicat softening temperature (GOST 15088-2014[5]) meter (Zwick Roell, Germany) at a heating rate of ~3°C/min. The temperature coefficient of electrical resistance (TCR, α; K^{-1}) was calculated by the formula:

$$\alpha = \frac{\Delta\rho}{\rho_0 \Delta T}, \qquad (1)$$

wherein $\Delta\rho$ is the change in the volume electrical resistivity at a temperature change ΔT (°C), and ρ_0 is the volume electrical resistivity (Ω·m) under normal conditions.

The change in the degree of crystallinity was studied by differential scanning calorimetry (DSC) with a DSC 204 F1 Phoenix instrument (NETZSCH, Germany) at a heating rate of 3°C/min. The degree of crystallinity α_{cr} was calculated by the formula:

---

[1] GOST 16338-85. Interstate Standard. Low-pressure polyethylene. Specifications. Moscow: Standartinform; 2005.

[2] GOST 16337-77. Interstate Standard. High-pressure polyethylene. Specifications. Moscow: Standartinform; 2005.

[3] TU 2211-074-05766563-2015. Balene (polypropylene and propylene copolymers). Specifications. https://polimermsk.ru/image/catalog/product/passport/TU%202211-074-05766563-2015.pdf. Accessed May 22, 2024.

[4] GOST 6613-86. Interstate Standard. Square meshed woven wire cloths. Specifications. Moscow: Standartinform; 2006.

[5] GOST 15088-2014 (ISO 306:2004). Interstate Standard. Plastics. Method for determination of Vicat softening temperature of thermoplastics. Moscow: Standartinform; 2014.

Features of the change in the thermal coefficient of electrical resistance upon heating
electrically conductive composites of crystallizable polyolefins with carbon black

Anatoly V. Markov,
Alexander E. Zverev, Vasily A. Markov

$$\alpha_{cr} = \frac{\Delta H_{melt}}{\Delta H_{cr}}, \qquad (2)$$

wherein ΔH_{melt} is the enthalpy of melting of the crystalline phase of the sample calculated taking into account the weight fraction of ECB (kJ/mol). ΔH_{cr} is the enthalpy of melting of the crystalline phase of the polymer (kJ/mol).

Dilatometric and rheological studies of the composites were made using an IIRT-AM melt flow index device (*Altavir*, Russia) (GOST 11645-2021[6]) and known methods described earlier [23]. Dilatometric tests were carried out by measuring the change in the height of cylindrical samples (with an accuracy of ±0.01 mm) in the working chamber of the IIRT-AM device. The coefficient of volumetric thermal expansion β (K^{-1}) was calculated by the formula:

$$\beta = \frac{\Delta v}{v_0 \Delta T}, \qquad (3)$$

wherein Δv (cm^3) is the product of the displacement of the rod and the cross-sectional area of the cylindrical working chamber of the device at a change in the temperature in it of ΔT (°C), and v_0 is the volume (cm^3) of the pellet under normal conditions.

RESULTS AND DISCUSSION

The phenomenon of a sharp increase in electrical resistance with increasing temperature is an integral property of polymer self-regulating heating elements. This phenomenon is especially pronounced in crystallizable polyolefins. The dependencies obtained earlier [25] (Fig. 1) confirm this and have a shape characteristic of self-regulating composites with ECB.

All polyolefins presented in Fig. 1 are characterized by extreme changes in ρ/ρ_0 with increasing temperature. The highest value of ρ/ρ_0 upon heating is exhibited by the EPCM based on HDPE which has a degree of crystallinity α_{cr} of 70.8% at normal temperature. For PP and LDPE, the degrees of crystallinity are significantly lower: 48.1 and 41.1%, respectively.

Based on the results of our studies, the TCR α values (K^{-1}) of these EPCMs were calculated over a wide range of temperatures (Fig. 2). As can be seen from Fig. 2, the temperatures of minima of TCR virtually coincide with the temperatures of maxima of ρ/ρ_0 in Fig. 1.

Several temperature regions can be distinguished on the curves of these dependencies. They differ in magnitude and sign of the change in electrical resistance. At low temperatures, the resistance increases proportionally
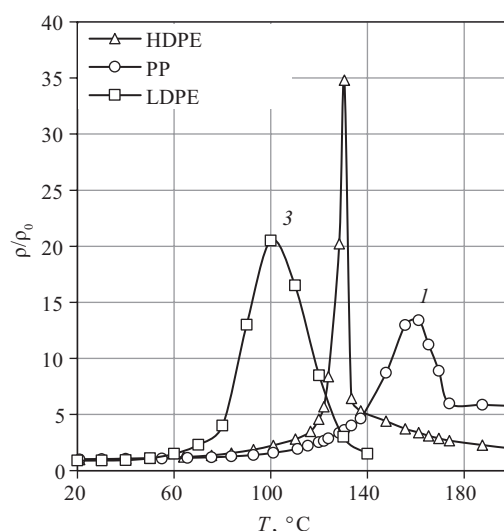
Fig. 1. Effect of temperature T (°C) on the normalized volume electrical resistivity ρ/ρ_0 (Ω·m/Ω·m) of polyolefin composites with ECB:
(*1*) polypropylene (PP), (*2*) high-density polyethylene (HDPE), and (*3*) low-density polyethylene (LDPE)

to the increase in temperature. Such a change is due to the volumetric thermal expansion of the EPCM and is characterized by the size of the temperature zone of TCR. The α values (K^{-1}) in this zone were as follows: LDPE, 0.0033; HDPE, 0.0014; and PP, 0.0024. As the temperature approaches the temperature regions of polymer melting, the increase in resistance accelerates exponentially (the so-called temperature zone of abnormal PTC). In Fig. 2b, for polyethylenes, the beginning of this zone approximately corresponds to a temperature of 60–70°C (for HDPE, this can be better seen in an enlarged figure); also for polypropylene, to 110–120°C. The power of self-regulating EPCMs is regulated at the beginning of the PTC zone. This is due to the intensification of the destruction of conductive channels of ECB in them. A further increase in temperature in the polymer melting region leads to an inversion of the electrical resistance change at its point of maximum and the occurrence of the phenomenon of NTC. The NTC temperature zone ends with the complete melting of the polymer and the transition of the EPCM to the temperature zone of volumetric thermal expansion of the melt. The change in electrical resistance in this zone is proportional to the change in temperature, and is characterized by the value of the melt TCR zone. It follows that the temperature zones of interest, PTC and NTC, are associated with different stages of the melting of the polymer matrix of the EPCM. Gradual melting causes a sharp (extreme) change in electrical

---

[6]   GOST 11645-2021. Interstate Standard. Plastics. Methods for determination of flow index of thermoplastics melt. Moscow: Russian Institute of Standardization; 2021.

Features of the change in the thermal coefficient of electrical resistance upon heating
electrically conductive composites of crystallizable polyolefins with carbon black

Anatoly V. Markov,
Alexander E. Zverev, Vasily A. Markov
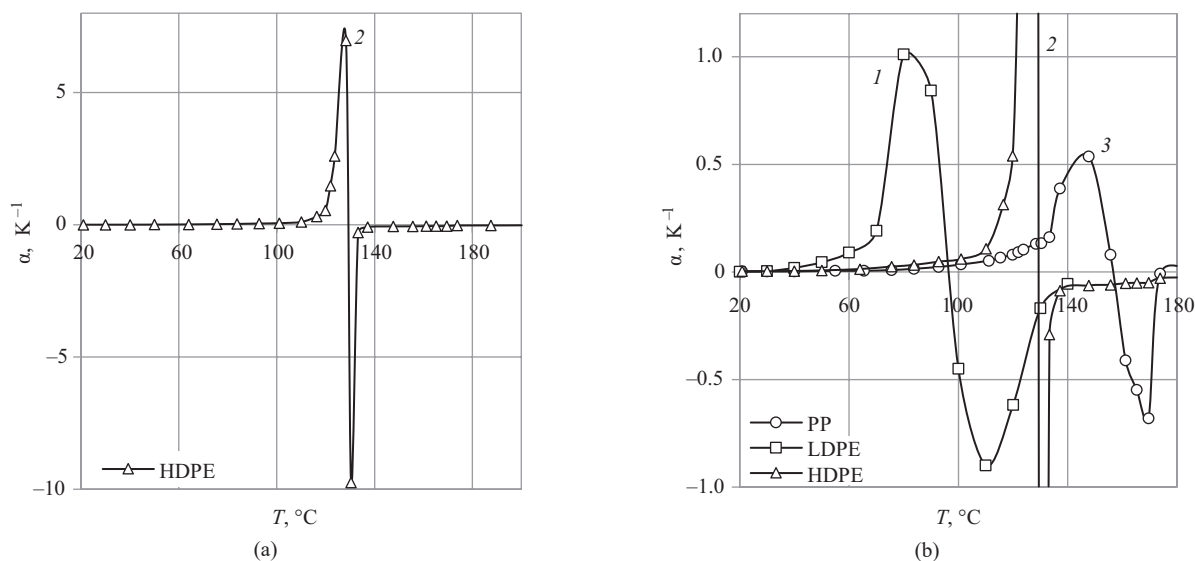
Fig. 2. Effect of temperature T (°C) on the thermal coefficients of electrical resistance α (K^{-1}) of polyolefin composites with ECB: (*1*) PP, (*2*) HDPE, and (*3*) LDPE

resistance. It is important to note that, only in the TCR temperature zones of the melt, can the volumetric thermal expansion be considered the main mechanism of the effect of temperature on the electrical resistance of the EPCM. When transitioning from the PTC temperature zone to the NTC zone, the polymer continues to expand gradually, since the melting of the polyolefin matrix continues, while the fraction of the denser crystalline phase continues to decrease. This is confirmed by the dilatometry and DSC results given below.

In order to refine the mechanism of the occurrence of PTC and NTC, the effect of temperature was studied on the degree of crystallinity of the given EPCMs during

melting. Figure 3 presents the results of these studies. The degrees of crystallinity α_{cr} of EPCMs were estimated at temperatures corresponding to the maximum values of ρ/ρ_0, at which inversion transitions from PTC to NTC were observed. For this purpose, the thermal coefficients of change in α_{cr} (Fig. 3b) were calculated, similar to thermal coefficients α and β.

Unlike electrical coefficients α, these coefficients are positive at all the temperatures studied. The temperatures of the maximum values of ρ/ρ_0 and the temperatures of the maxima of the thermal coefficients of change in α_{cr} in Fig. 3b were found to virtually coincide. In Fig. 3a, their positions are indicated by vertical dashed lines.
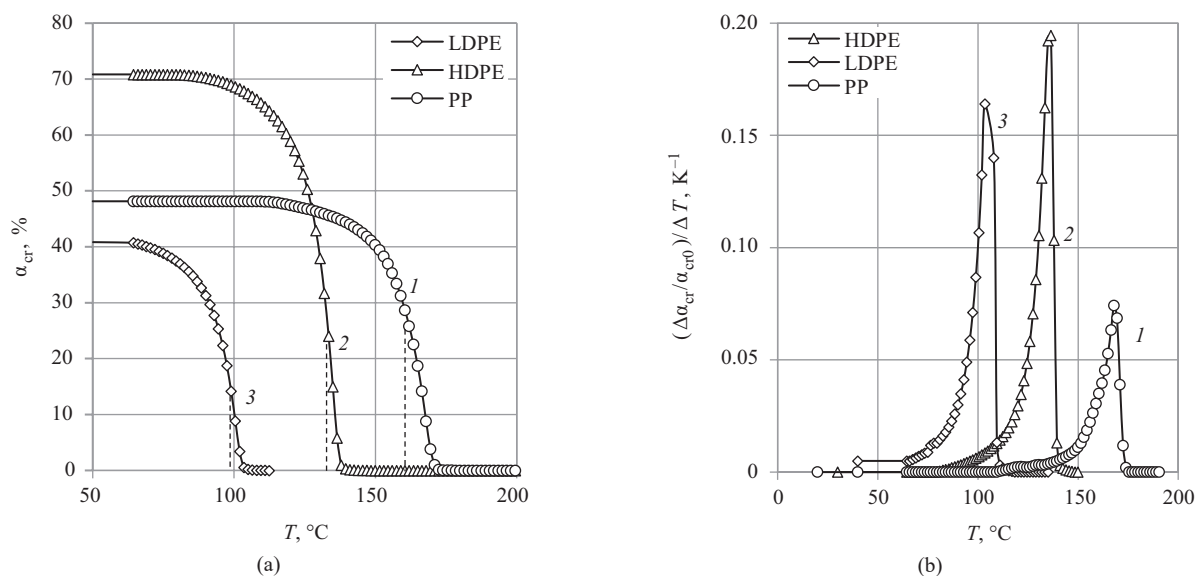
Fig. 3. Effect of temperature T (°C) on (a) the degree of crystallinity α_{cr} (%) and (b) the thermal coefficients of change in α_{cr} (K^{-1}) of polyolefin composites with ECB: (*1*) PP, (*2*) HDPE, and (*3*) LDPE

Features of the change in the thermal coefficient of electrical resistance upon heating
electrically conductive composites of crystallizable polyolefins with carbon black

Anatoly V. Markov,
Alexander E. Zverev, Vasily A. Markov

In crystallizable polyolefin-based EPCMs, the inversion of the change in the thermal coefficients of electrical resistance (the transition from PTC to NTC) occurs when the degree of crystallinity reaches 20–25%. Therefore, at degrees of crystallinity less than 20%, the barrier resistance may not appear, as in the case of amorphous polymers. In addition, this allows us to assume that the transition from PTC to NTC is caused by a sharp change in the aggregate state of the EPCM, and the beginning of its transition to a viscous-flow state. This is a result of fragmentation of the crystalline phase formed at the early stage of the crystallization process at high temperatures. The melt becomes a continuous phase. On the other hand, in the PTC temperature zone, the EPCM continues to contain the continuous crystalline phase with discrete inclusions of the melt formed from low-melting components of the crystalline phase formed at low temperatures at the late stage of the crystallization process at the boundaries of spherulites. Even a small decrease in the degree of crystallinity in the initial PTC temperature zone (at the temperatures of power regulation of the self-regulating heater) leads to significant destruction of conductive channels in ECB and a multiple increase in the resistance of the EPCM. This is due to the fact that self-regulating EPCMs respond with an increase in electrical resistance not only to thermal, but also to deformation effect [8, 9, 26, 27]. Therefore, the cause of the significant increase in resistance at these temperatures can also be the formation of melt microinclusions in the crystalline polymer and the increase in their volume. In this case, the shear deformation effect of many such expanding microvolumes is transferred to the crystalline phase.

This causes additional shear destruction of conductive channels of ECB in the crystalline phase and accelerated increase in the electrical resistance of the EPCM in the PTC temperature zone even at a minimum change in the degree of crystallinity.

This factor ceases to act in the NTC temperature zone (in the continuous phase of the melt), despite the continued volumetric thermal expansion of the EPCM. Such a PTC mechanism confirms the weak manifestation of the phenomenon of PTC in EPCMs based on amorphous polymers [25] and its occurrence in mixtures of amorphous and crystallizable polymers [10, 22]. This can also explain the stabilization of the phenomenon of PTC and the absence of the phenomenon of NTC in self-regulating EPCMs subjected to radiation crosslinking [28–32] or chemical crosslinking [8–11, 33], thus deprived of the possibility of transition to a viscous-flow state.

In order to confirm the proposed mechanism, dilatometric tests of the given EPCMs were carried out. Figure 4a shows the dependencies of the change in their specific volume $\upsilon = V/V_0$ on temperature during thermal expansion of the EPCM. Here V_0 and V_T are the initial value of the sample volume and its current value at temperature T, respectively.

Naturally, the volume of all EPCMs increases in all the temperature zones described above. In the curves in Fig. 4a, the PTC and NTC temperature zones form a common melting zone, characterized by an accelerated smooth increase in the volume of the samples and is separated by two zones with a slow increase in the TCR. In this case, the calculated coefficient of volumetric thermal expansion in Fig. 4b is positive throughout the studied
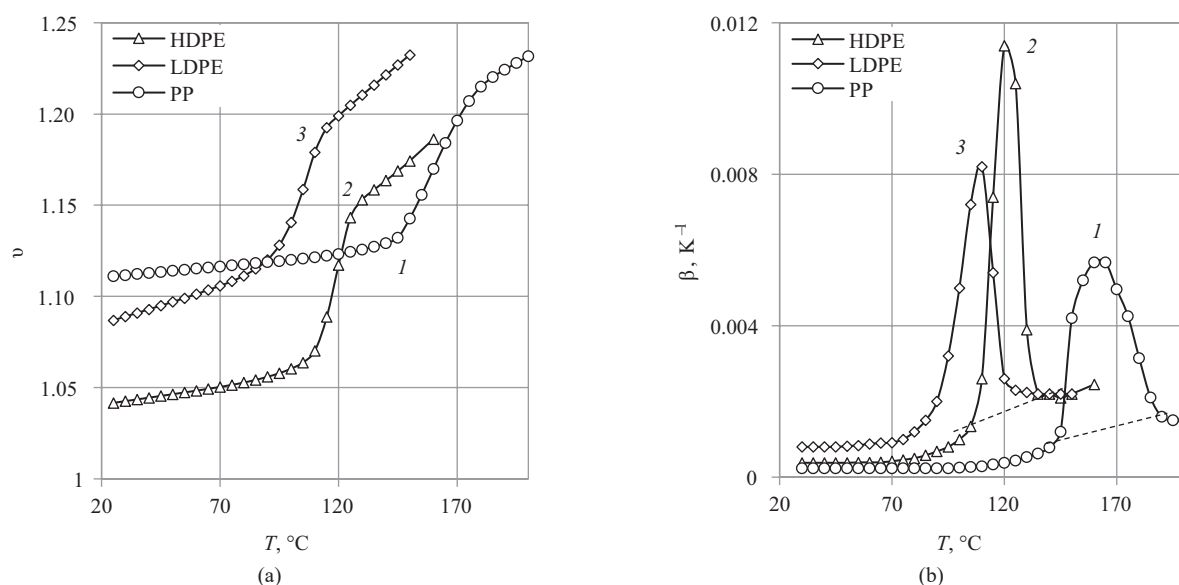
Fig. 4. Effect of temperature T (°C) on the specific volume υ during thermal expansion and (b) the coefficient of volumetric thermal expansion β (K^{-1}) of polyolefin-based composites with ECB: (*1*) PP, (*2*) HDPE, and (*3*) LDPE

Features of the change in the thermal coefficient of electrical resistance upon heating
electrically conductive composites of crystallizable polyolefins with carbon black

Anatoly V. Markov,
Alexander E. Zverev, Vasily A. Markov

temperature range. The temperature zones of the TCR of the melt are a continuation of the TCR zones of solid EPCMs (Fig. 4b, dashed lines). The temperatures of the maximum values of ρ/ρ_0 in Fig. 1 and the temperatures of the maxima in Fig. 4b are very close. However, the coefficients of volumetric thermal expansion β are greater than an order of magnitude lower than the thermal coefficients of electrical resistance α. This also indicates that volumetric expansion is not the only mechanism of the abnormally high PTC of EPCMs (Table 1).

Table 1. Initial thermal coefficients of electrical resistance α and the coefficients of volumetric thermal expansion β of polyolefin-based electrically conductive polymer composite materials (EPCMs)

Polyolefin	LDPE	HDPE	PP
α_0, K^{-1}	0.0033	0.0014	0.0024
β_0, K^{-1}	0.000195	0.00038	0.00011

In order to refine the features and mechanism of the change in the electrical resistance of the studied EPCMs during heating, it is useful to establish the activation energies of destruction of conductive channels formed by ECB particles using the Arrhenius equation [34]. In order to do this, an electrical characteristic needs to be selected. The behavior of this characteristic needs to be symbatic to that of this destruction. Change in electrical resistance is not suitable for this purpose, since it increases with a decrease in the number of conductive channels. However, if electrical resistance is replaced by electrical conductivity ($\sigma/\sigma_0 = \rho_0/\rho$), this problem can be resolved. The electrical conductivity should decrease proportionally to the decrease in these channels. Curve *1* in Fig. 5 illustrates the dependence of the logarithm of the electrical conductivity of the EPCM based on HDPE on the inverse temperature in the Arrhenius coordinates $\ln(\sigma/\sigma_0) = f(1/T, \text{K}^{-1})$.

The activation energies of the processes are proportional to the slopes of the experimentally obtained curves: $\ln(\sigma/\sigma_0) = f(1/T, \text{K}^{-1})$. The activation energy can change in different sections of the curves when the mechanism of the destruction of conductive channels in ECB changes.

The temperature dependence of electrical conductivity (Fig. 5, curve *1*) has several regions with different slopes. These are temperature zones with different activation energies: a low-temperature zone of TCR of solid EKPMs with the lowest slope and a PTC zone with the increasing slope. The NTC temperature zone, which was not used in the calculations, is represented by one point.

The low slope of curve *1* (low values of the activation energy E_{el} of change in electrical conductivity) in the TCR zone indicates that the mechanism of the decrease in the conductivity at these temperatures is the thermal motion of molecules, causing volumetric thermal expansion of the material. The increase in the slope at temperatures above 60°C (the increase in E_{el}) confirms the assumption about a change in the mechanism of the destruction of conductive channels in EKPM at the beginning of the PTC temperature zone. In the NTC zone, the electrical conductivity begins to increase.

For comparison, Fig. 5 also shows the DSC (curve *2*) and dilatometry (curve *3*) results processed in a similar manner. The decrease in the degree of crystallinity (curve *2*), related to the destruction of spherulites upon heating, should lead to the destruction of conductive channels in the EPCM. However, the shape of curve *2* differs significantly from the shape of curve *1*, analyzed above. The degree of crystallinity changes little until 110°C is reached. Curve *2* has virtually no temperature zone corresponding to the PTC zone on curve *1*, and the corresponding activation energy cannot be calculated.

The results of the dilatometric tests are shown in curve *3* of Fig. 5. By analogy with the dependence of σ/σ_0 on $1/T$ (K^{-1}), the inverse of the specific volume υ, the specific density $q/q_0 = 1/\upsilon$, was chosen as a dilatometric characteristic symbatic to σ/σ_0. The low values of the activation energy (the low slope of the line) indicate that the volumetric thermal expansion of the material is not the main cause of the occurrence of the abnormally high PTC of the studied EPCMs.
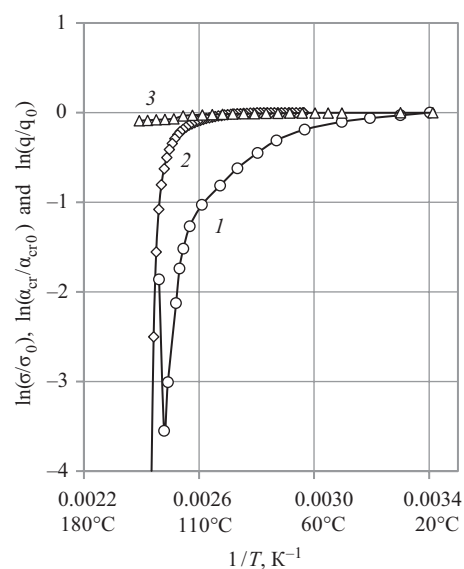
Fig. 5. Comparison of the temperature dependencies of the normalized values of electrical conductivity σ/σ_0, degree of crystallinity α_{cr}/α_{cr0}, and density q/q_0 of HDPE-based composites with ECB:
(*1*) $\ln(\sigma/\sigma_0)$, (*2*) $\ln(\alpha_{cr}/\alpha_{cr0})$, and (*3*) $\ln(q/q_0)$

Features of the change in the thermal coefficient of electrical resistance upon heating
electrically conductive composites of crystallizable polyolefins with carbon black

Anatoly V. Markov,
Alexander E. Zverev, Vasily A. Markov

Figure 6 presents the temperature dependencies of σ/σ_0 on $1/T$ (K^{-1}) for all the studied polyolefin-based EPCMs. The dashed lines in Fig. 6 are tangents to the experimentally obtained curves in the regions of interest at the beginning of the PTC temperature zones. These are responsible for regulating the power of the EPCM heaters with increasing temperature.
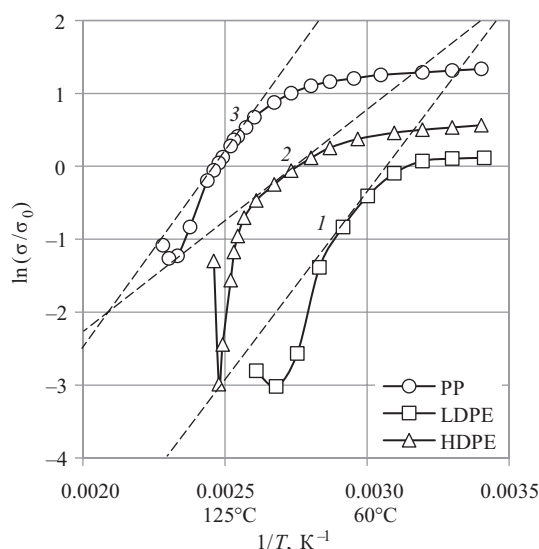
Fig. 6. Effect of temperature ($1/T$, K^{-1}) on the logarithms of the normalized values of electrical conductivity σ/σ_0 of polyolefin-based composites with ECB:
(*1*) PP, (*2*) HDPE, and (*3*) LDPE

Table 2 presents the results of the calculation of the activation energies E_{el} of these processes occurring in these temperature zones of change in electrical conductivity. Table 2 also shows the values of the activation energies E_{vf} of viscous flow of melts, as determined by rheological studies.

Table 2. Calculated activation energies E_{el} and E_{vf} of destruction of conductive channels in the PTC zone and viscous flow of melts of polyolefin-based EPCMs

Polyolefin	LDPE	HDPE	PP
E_{el}, kJ/mol	41.6	29.3	45.1
E_{vf}, kJ/mol	45.5	30.5	45.4

The closeness of the E_{el} and E_{vf} values can be considered as confirmation of the expected influence of shear effect on the crystalline phase of numerous expanding microinclusions of the melt formed at the early stages of melting of polyolefin-based EPCMs.

CONCLUSIONS

A comprehensive study of the structure and properties of crystallizable polyolefin-based EPCMs with ECB was made. It was determined that the self-regulation ability (an abnormally high positive thermal coefficient of electrical resistance) of self-regulating heaters made of composites of crystallizable polyolefins with ECB cannot be explained by the thermal expansion of EPCMs alone. It was shown that in crystallizable polyolefin-based EPCMs, the inversion of the thermal coefficients of electrical resistance (transition from PTC to NTC) is due to a change in the aggregate state of EPCM and the beginning of its transition to a viscous-flow state.

A mechanism of the sharp increase in the electrical resistance of self-regulating crystallizable polyolefin-based composites with ECB was proposed and substantiated. This mechanism takes into account the additional shear deformation effect on the crystalline phase of the EPCM of numerous expanding melt microvolumes formed at the early stages of the melting process with a minimal change in the degree of crystallinity.

Authors' contributions

A.V. Markov—creation of the concept of the study, processing the experimental data.

A.E. Zverev—conducting the experimental studies, processing the experimental data.

V.A. Markov—adjustment of the concept of the study.

The authors declare no conflicts of interest.

Features of the change in the thermal coefficient of electrical resistance upon heating electrically conductive composites of crystallizable polyolefins with carbon black

Anatoly V. Markov, Alexander E. Zverev, Vasily A. Markov

REFERENCES

1. Ragushina M.D., Evseeva K.A., Kalugina E.V., Ushakova O.B. Polymer composite materials with electrically conductive antistatic properties. *Plasticheskie Massy*. 2021;(3–4):6–9 (in Russ.). https://doi.org/10.35164/0554-2901-2021-3-4-6-9

2. Bregman A., Taub A., Michielssen E. Computational design of composite EMI shields through the control of pore morphology. *MRS Communications*. 2018;8(3):1153–1157. https://doi.org/10.1557/mrc.2018.171

3. Chen J., Zhu Y., Huang J., Zhang J., Pan D., Zhou J., Ryu J., Umar A., Guo Z. Advances in Responsively Conductive Polymer Composites and Sensing Applications. *Polym. Rev.* 2021;61(1):157–193. https://doi.org/10.1080/15583724.2020.1734818

4. Chen L., Zhang J. Designs of conductive polymer composites with exceptional reproducibility of positive temperature coefficient effect: A review. *J. Appl. Polym. Sci.* 2021;138(3):49677. https://doi.org/10.1002/app.49677

5. Zhang P., Wang B. Positive temperature coefficient effect and mechanism of compatible LLDPE/HDPE composites doping conductive graphite powders. *J. Appl. Polym. Sci.* 2018;135(27):46453. https://doi.org/10.1002/app.46453

6. Zhang C., Ma C.A., Wang P., Sumita M. Temperature dependence of electrical resistivity for carbon black filled ultra-high molecular weight polyethylene composites prepared by hot compaction. *Carbon*. 2005;43(12):2544–2553. https://doi.org/10.1016/j.carbon.2005.05.006

7. Shen L., Wang F.Q., Yang H., Meng Q.R. The combined effects of carbon black and carbon fiber on the electrical properties of composites based on polyethylene or polyethylene/polypropylene blend. *Polym. Test.* 2011;30(4):442–448. https://doi.org/10.1016/j.polymertesting.2011.03.007

8. Markov V.A., Kandyrin L.B., Markov A.V. The effect of deformation on the electrical resistance of composites based on polyethylene and carbon black. *Konstruktsii iz kompozitsionnykh materialov = Composite Materials Constructions*. 2013;4:40–44 (in Russ.).

9. Markov A.V., Tarasova K.S., Markov V.A. Effect of relaxation processes during deformation on electrical resistivity of carbon black polypropylene composites. *Tonk. Khim. Tekhnol. = Fine Chem. Technol.* 2021;16(4):345–351. https://doi.org/10.32362/2410-6593-2021-16-4-345-351

10. Markov A.V., Gushchin V.A., Markov V.A. Thermoelectric characteristics of electrically conductive composites based on mixtures of crystallizing and amorphous polymers with technical carbon. *Plasticheskie Massy*. 2019;(1–2):44–47 (in Russ.).

11. Markov A.V., Markov V.A., Chizhov A.S. The influence of the characteristics of polyethylene on thermoelectric properties of their composites with black carbon. *Plasticheskie Massy*. 2021;(5–6):18–23 (in Russ.). https://doi.org/10.35164/0554-2901-2021-5-6-18-23

12. Zeng Y., Lu G., Wang H., Du J., Ying Z., Liu C. Positive temperature coefficient thermistors based on carbon nanotube/polymer composites. *Sci. Rep.* 2014;4(1):6684. https://doi.org/10.1038/srep06684

13. Luo S., Wong C.P. Study on effect of carbon black on behavior of conductive polymer composites with positive temperature coefficient. *IEEE Trans. Compon. Packag. Technol.* 2000;23(1):151–156. https://doi.org/10.1109/6144.833054

14. Vigueras-Santiago E., Hernnández-López S., Camacho-Lopez M., Lara-Sanjuan O. Electric anisotropy in high density polyethylene + carbon black composites induced by mechanical deformation. *J. Phys.: Conf. Ser.* 2009;167(1):012039. https://doi.org/10.1088/1742-6596/167/1/012039

СПИСОК ЛИТЕРАТУРЫ

1. Рагушина М.Д., Евсеева К.А., Калугина Е.В., Ушакова О.Б. Полимерные композиционные материалы с антистатическими и электропроводящими свойствами. *Пластические массы*. 2021;(3–4):6–9. https://doi.org/10.35164/0554-2901-2021-3-4-6-9

2. Bregman A., Taub A., Michielssen E. Computational design of composite EMI shields through the control of pore morphology. *MRS Communications*. 2018;8(3):1153–1157. https://doi.org/10.1557/mrc.2018.171

3. Chen J., Zhu Y., Huang J., Zhang J., Pan D., Zhou J., Ryu J., Umar A., Guo Z. Advances in Responsively Conductive Polymer Composites and Sensing Applications. *Polym. Rev.* 2021;61(1):157–193. https://doi.org/10.1080/15583724.2020.1734818

4. Chen L., Zhang J. Designs of conductive polymer composites with exceptional reproducibility of positive temperature coefficient effect: A review. *J. Appl. Polym. Sci.* 2021;138(3):49677. https://doi.org/10.1002/app.49677

5. Zhang P., Wang B. Positive temperature coefficient effect and mechanism of compatible LLDPE/HDPE composites doping conductive graphite powders. *J. Appl. Polym. Sci.* 2018;135(27):46453. https://doi.org/10.1002/app.46453

6. Zhang C., Ma C.A., Wang P., Sumita M. Temperature dependence of electrical resistivity for carbon black filled ultra-high molecular weight polyethylene composites prepared by hot compaction. *Carbon*. 2005;43(12):2544–2553. https://doi.org/10.1016/j.carbon.2005.05.006

7. Shen L., Wang F.Q., Yang H., Meng Q.R. The combined effects of carbon black and carbon fiber on the electrical properties of composites based on polyethylene or polyethylene/polypropylene blend. *Polym. Test.* 2011;30(4):442–448. https://doi.org/10.1016/j.polymertesting.2011.03.007

8. Марков В.А., Кандырин Л.Б., Марков А.В. Влияние деформирования на электрическое сопротивление композитов на основе полиэтилена и технического углерода. *Конструкции из композиционных материалов*. 2013;4:40–44.

9. Марков А.В., Тарасова К.С., Марков В.А. Влияние релаксационных процессов при деформировании на электрическое сопротивление полипропиленовых композитов с техническим углеродом. *Тонкие химические технологии*. 2021;16(4):345–351. https://doi.org/10.32362/2410-6593-2021-16-4-345-351

10. Марков А.В., Гущин В.А., Марков В.А. Термоэлектрические характеристики электропроводящих композитов на основе смесей кристаллизующихся и аморфных полимеров с техническим углеродом. *Пластические массы*. 2019;(1–2):44–47.

11. Марков А.В., Марков В.А., Чижов А.С. Влияние характеристик полиэтилена на термоэлектрические свойства полиэтиленовых композитов с техническим углеродом. *Пластические массы*. 2021;(5–6):18–23. https://doi.org/10.35164/0554-2901-2021-5-6-18-23

12. Zeng Y., Lu G., Wang H., Du J., Ying Z., Liu C. Positive temperature coefficient thermistors based on carbon nanotube/polymer composites. *Sci. Rep.* 2014;4(1):6684. https://doi.org/10.1038/srep06684

13. Luo S., Wong C.P. Study on effect of carbon black on behavior of conductive polymer composites with positive temperature coefficient. *IEEE Trans. Compon. Packag. Technol.* 2000;23(1):151–156. https://doi.org/10.1109/6144.833054

14. Vigueras-Santiago E., Hernnández-López S., Camacho-Lopez M., Lara-Sanjuan O. Electric anisotropy in high density polyethylene + carbon black composites induced by mechanical deformation. *J. Phys.: Conf. Ser.* 2009;167(1):012039. https://doi.org/10.1088/1742-6596/167/1/012039

Features of the change in the thermal coefficient of electrical resistance upon heating electrically conductive composites of crystallizable polyolefins with carbon black

Anatoly V. Markov, Alexander E. Zverev, Vasily A. Markov

15. Chen Y., Song Y., Zhou J., Zheng Q. Effect of uniaxial pressure on conduction behavior of carbon black filled poly(methyl vinyl siloxane) composites. *Chinese Sci. Bull.* 2005;50: 101–107. https://doi.org/10.1007/BF02897510

16. De Focatiis D.S.A., Hull D., Sánchez-Valencia A. Roles of prestrain and hysteresis on piezoresistance in conductive elastomers for strain sensor applications. *Plastics, Rubber and Composites.* 2012;41(7):301–309. https://doi.org/10.1179/174 3289812Y.0000000022

17. Lee G.J., Suh K.D., Im S.S. Study of electrical phenomena in carbon black–filled HDPE composite. *Polym. Eng. Sci.* 1998;38(3):471–477. https://doi.org/10.1002/pen.10209

18. Choi H.J., Kim M.S., Ahn D., Yeo S.Y., Lee S. Electrical percolation threshold of carbon black in a polymer matrix and its application to antistatic fibre. *Sci. Rep.* 2019;9(1):6338. https://doi.org/10.1038/s41598-019-42495-1

19. Tang H., Chen X., Luo Y. Studies on the PTC/NTC effect of carbon black filled low density polyethylene composites. *Eur. Polym. J.* 1997;33(8):1383–1386. https://doi.org/10.1016/S0014-3057(96)00221-2

20. Brigandi P.J., Cogen J.M., Pearson R.A. Electrically conductive multiphase polymer blend carbon-based composites. *Polym. Eng. Sci.* 2014;54(1):1–16. https://doi.org/10.1002/PEN.23530

21. Zaikin A.E., Bikmullin R.S., Zharinova E.A. Specifics of localization of carbon black at the interface between polymeric phases. *Polym. Sci. Ser. A.* 2007;49(3):328–336. https://doi.org/10.1134/S0965545X07030145
[Original Russian Text: Zaikin A.E., Zharinova E.A., Bikmullin R.S. Specifics of localization of carbon black at the interface between polymeric phases. *Vysokomolekulyarnye Soedineniya. Ser. A.* 2007;49(3):499–509 (in Russ.).]

22. Markov A.V., Chizhov A.S. Self-regulating electrically conductive materials based on polyethylene compositions with UHMWPE and carbon black. *Tonk. Khim. Tekhnol. = Fine Chem. Technol.* 2019;14(2):60–69. https://doi.org/10.32362/2410-6593-2019-14-2-60-69

23. Zhou P., Yu W., Zhou C., Liu F., Hou L., Wang J. Morphology and electrical properties of carbon black filled LLDPE/EMA composites. *J. Appl. Polym. Sci.* 2007;103(1):487–492. https://doi.org/10.1002/app.25020

24. Bao Y., Xu L., Pang H., Yan D.X., Chen C., Zhang W.Q., Tang J.H., Li Z.M. Preparation and properties of carbon black/polymer composites with segregated and double-percolated network structures. *J. Mater. Sci.* 2013;48:4892–4898. https://doi.org/10.1007/s10853-013-7269-x

25. Yurkin A.A., Kharlamova K.I., Abramushkina O.I., Surikov P.V. *Tekhnologiya pererabotki plasticheskikh mass (Plastic Processing Technology: educational manual).* Moscow: RTU MIREA; 2023. 95 p. (in Russ.). ISBN 978-5-7339-1995-9

26. Markov V.A., Kandyrin L.B., Markov A.V. The effect of polymer crystallization on the electrical resistance of their compositions with carbon black. *Konstruktsii iz kompozitsionnykh materialov = Composite Materials Constructions.* 2013;3:35–40 (in Russ.).

27. Knite M., Teteris V., Kiploka A., Kaupuzs J. Polyisoprene-carbon black nanocomposites as tensile strain and pressure sensor materials. *Sens. Actuators A: Phys.* 2004;110(1–3): 142–149. https://doi.org/10.1016/j.sna.2003.08.006

28. Starý Z., Krückel J., Schubert D., Münstedt H. Behavior of Conductive Particle Networks in Polymer Melts under Deformation. *AIP Conf. Proc.* 2011;1375:232–239. https://doi.org/10.1063/1.3604483

29. Xie H., Dong L., Sun J. Influence of radiation structures on positive-temperature-coefficient and negative-temperature-coefficient effects of irradiated low-density polyethylene/carbon black composites. *J. Appl. Polym. Sci.* 2005;95(3): 700–704. https://doi.org/10.1002/app.21220

15. Chen Y., Song Y., Zhou J., Zheng Q. Effect of uniaxial pressure on conduction behavior of carbon black filled poly(methyl vinyl siloxane) composites. *Chinese Sci. Bull.* 2005;50: 101–107. https://doi.org/10.1007/BF02897510

16. De Focatiis D.S.A., Hull D., Sánchez-Valencia A. Roles of prestrain and hysteresis on piezoresistance in conductive elastomers for strain sensor applications. *Plastics, Rubber and Composites.* 2012;41(7):301–309. https://doi.org/10.1179/174 3289812Y.0000000022

17. Lee G.J., Suh K.D., Im S.S. Study of electrical phenomena in carbon black–filled HDPE composite. *Polym. Eng. Sci.* 1998;38(3):471–477. https://doi.org/10.1002/pen.10209

18. Choi H.J., Kim M.S., Ahn D., Yeo S.Y., Lee S. Electrical percolation threshold of carbon black in a polymer matrix and its application to antistatic fibre. *Sci. Rep.* 2019;9(1):6338. https://doi.org/10.1038/s41598-019-42495-1

19. Tang H., Chen X., Luo Y. Studies on the PTC/NTC effect of carbon black filled low density polyethylene composites. *Eur. Polym. J.* 1997;33(8):1383–1386. https://doi.org/10.1016/S0014-3057(96)00221-2

20. Brigandi P.J., Cogen J.M., Pearson R.A. Electrically conductive multiphase polymer blend carbon-based composites. *Polym. Eng. Sci.* 2014;54(1):1–16. https://doi.org/10.1002/PEN.23530

21. Заикин А.Е., Жаринова Е.А., Бикмуллин Р.С. Особенности локализации технического углерода на границе раздела полимерных фаз. *Высокомолекулярные соединения. Серия А.* 2007;49(3):499–509.

22. Марков А.В., Чижов Д.С. Электропроводящие саморегулирующиеся материалы на основе полиэтиленовых композиций с СВМПЭ и техническим углеродом. *Тонкие химические технологии.* 2019;14(2):60–69. https://doi.org/10.32362/2410-6593-2019-14-2-60-69

23. Zhou P., Yu W., Zhou C., Liu F., Hou L., Wang J. Morphology and electrical properties of carbon black filled LLDPE/EMA composites. *J. Appl. Polym. Sci.* 2007;103(1):487–492. https://doi.org/10.1002/app.25020

24. Bao Y., Xu L., Pang H., Yan D.X., Chen C., Zhang W.Q., Tang J.H., Li Z.M. Preparation and properties of carbon black/polymer composites with segregated and double-percolated network structures. *J. Mater. Sci.* 2013;48:4892–4898. https://doi.org/10.1007/s10853-013-7269-x

25. Юркин А.А., Харламова К.И., Абрамушкина О.И., Суриков П.В. *Технология переработки пластических масс: учебно-методическое пособие.* М.: РТУ МИРЭА; 2023. 95 с. ISBN 978-5-7339-1995-9

26. Марков В.А., Кандырин Л.Б., Марков А.В. Влияние кристаллизации полимеров на электрическое сопротивление их композиций с техническим углеродом. *Конструкции из композиционных материалов.* 2013;3:35–40.

27. Knite M., Teteris V., Kiploka A., Kaupuzs J. Polyisoprene-carbon black nanocomposites as tensile strain and pressure sensor materials. *Sens. Actuators A: Phys.* 2004;110(1–3): 142–149. https://doi.org/10.1016/j.sna.2003.08.006

28. Starý Z., Krückel J., Schubert D., Münstedt H. Behavior of Conductive Particle Networks in Polymer Melts under Deformation. *AIP Conf. Proc.* 2011;1375:232–239. https://doi.org/10.1063/1.3604483

29. Xie H., Dong L., Sun J. Influence of radiation structures on positive-temperature-coefficient and negative-temperature-coefficient effects of irradiated low-density polyethylene/carbon black composites. *J. Appl. Polym. Sci.* 2005;95(3): 700–704. https://doi.org/10.1002/app.21220

30. Yi X.S., Zhang J.F., Zheng Q., Pan Y. Influence of irradiation conditions on the electrical behavior of polyethylene carbon black conductive composites. *J. Appl. Polym. Sci.* 2000;77(3):494–499. https://doi.org/10.1002/(SICI)1097-4628(20000718)77:3<494::AID-APP4>3.0.CO;2-K

Features of the change in the thermal coefficient of electrical resistance upon heating
electrically conductive composites of crystallizable polyolefins with carbon black

Anatoly V. Markov,
Alexander E. Zverev, Vasily A. Markov

30. Yi X.S., Zhang J.F., Zheng Q., Pan Y. Influence of irradiation conditions on the electrical behavior of polyethylene carbon black conductive composites. *J. Appl. Polym. Sci.* 2000;77(3):494–499. https://doi.org/10.1002/(SICI)1097-4628(20000718)77:3<494::AID-APP4>3.0.CO;2-K

31. Lee G.J., Han M.G., Chung S.Ch., Suh K.D., Im S.S. Effect of crosslinking on the positive temperature coefficient stability of carbon black-filled HDPE/ethylene-ethyalacrylate copolymer blend system. *Polym. Eng. Sci.* 2002;42(8):1740–1747. https://doi.org/10.1002/PEN.11067

32. Xie H., Deng P., Dong L., Sun J. LDPE/Carbon black conductive composites: Influence of radiation crosslinking on PTC and NTC properties. *J. Appl. Polym. Sci.* 2002;85(13):2742–2749. https://doi.org/10.1002/app.10720

33. Seo M.K., Rhee K.Y., Park S.J. Influence of electro-beam irradiation on PTC/NTC behaviors of carbon blacks/HDPE conducting polymer composites. *Curr. Appl. Phys.* 2011;11(3):428–433. https://doi.org/10.1016/j.cap.2010.08.013

34. Markov V.A., Kandyrin L.B., Markov A.V., Sorokina E.A. Effect of silane-crosslinking on electrical properties and heat-resistance of carbon black-filled polyethylene composites. *Plasticheskie Massy.* 2013;(10):21–24 (in Russ.).

31. Lee G.J., Han M.G., Chung S.Ch., Suh K.D., Im S.S. Effect of crosslinking on the positive temperature coefficient stability of carbon black-filled HDPE/ethylene-ethyalacrylate copolymer blend system. *Polym. Eng. Sci.* 2002;42(8):1740–1747. https://doi.org/10.1002/PEN.11067

32. Xie H., Deng P., Dong L., Sun J. LDPE/Carbon black conductive composites: Influence of radiation crosslinking on PTC and NTC properties. *J. Appl. Polym. Sci.* 2002;85(13):2742–2749. https://doi.org/10.1002/app.10720

33. Seo M.K., Rhee K.Y., Park S.J. Influence of electro-beam irradiation on PTC/NTC behaviors of carbon blacks/HDPE conducting polymer composites. *Curr. Appl. Phys.* 2011;11(3):428–433. https://doi.org/10.1016/j.cap.2010.08.013

34. Марков В.А., Кандырин Л.Б., Марков А.В., Сорокина Е.А. Влияние силанольного сшивания на электрические характеристики и теплостойкость ПЭ композитов с техническим углеродом. *Пластические массы.* 2013;(10):21–24.

About the authors

Anatoly V. Markov, Dr. Sci. (Eng.), Professor, Department of Chemistry and Technology of Plastics and Polymer Composites Processing, M.V. Lomonosov Institute of Fine Chemical Technologies, MIREA – Russian Technological University (86, Vernadskogo pr., Moscow, 119571, Russia). E-mail: markovan@bk.ru. Scopus Author ID 57222377754, RSCI SPIN-code 1127-9590, https://orcid.org/0000-0001-7952-7419

Alexander E. Zverev, Postgraduate Student, Department of Chemistry and Technology of Plastics and Polymer Composites Processing, M.V. Lomonosov Institute of Fine Chemical Technologies, MIREA – Russian Technological University (86, Vernadskogo pr., Moscow, 119571, Russia). E-mail: azmonst@gmail.com. RSCI SPIN-code 3609-8535, https://orcid.org/0009-0004-4418-5825

Vasily A. Markov, Cand. Sci. (Eng.), Lead Software Engineer, Bell Integrator Innovations (1, Ramenskii bul., INTTs MGU Vorob'evy Gory, Lomonosov klaster, Moscow, 119192, Russia). E-mail: markov.vasily@mail.ru. Scopus Author ID 57189505018, https://orcid.org/0000-0002-5768-9107

Features of the change in the thermal coefficient of electrical resistance upon heating electrically conductive composites of crystallizable polyolefins with carbon black

Anatoly V. Markov,
Alexander E. Zverev, Vasily A. Markov

Об авторах

Марков Анатолий Викторович, д.т.н., профессор кафедры химии и технологии переработки пластмасс и полимерных композитов, Институт тонких химических технологий им. М.В. Ломоносова, ФГБОУ ВО «МИРЭА – Российский технологический университет» (119571, Россия, Москва, пр-т Вернадского, д. 86). E-mail: markovan@bk.ru. Scopus Author ID 57222377754, SPIN-код РИНЦ 1127-9590, https://orcid.org/0000-0001-7952-7419

Зверев Александр Евгеньевич, аспирант кафедры химии и технологии переработки пластмасс и полимерных композитов, Институт тонких химических технологий им. М.В. Ломоносова, ФГБОУ ВО «МИРЭА – Российский технологический университет» (119571, Россия, Москва, пр-т Вернадского, д. 86). E-mail: azmonst@gmail.com. SPIN-код РИНЦ 3609-8535, https://orcid.org/0009-0004-4418-5825

Марков Василий Анатольевич, к.т.н., ведущий инженер-программист, ООО «Белл Интегратор Инновации» (119192, Россия, Москва, Раменский бульвар, д. 1, ИНТЦ МГУ «Воробьевы горы», кластер «Ломоносов»). E-mail: markov.vasily@mail.ru. Scopus Author ID 57189505018, https://orcid.org/0000-0002-5768-9107

Translated from Russian into English by V. Glyanchenko
Edited for English language and spelling by Dr. David Mossop

RESEARCH ARTICLE

Rheological properties of phosphorus-containing oligoester(meth)acrylate for processing by vacuum infusion

Oleg O. Tuzhikov[1,✉], **Lyubov Yu. Donetskova**[1], **Semyon M. Solomakhin**[1], **Anna V. Nalesnaya**[1],
Ali Al-Hamzawi[2], **Boris A. Buravov**[1], **Sergey V. Borisov**[1], **Oleg I. Tuzhikov**[1]

[1]*Volgograd State Technical University, Volgograd, 400005 Russia*

[2]*Al-Qadisiyah, Al-Diwaniyah, 58002 Iraq*

✉ *Corresponding author, e-mail: tuzhikovoleg@mail.ru*

Abstract

Objectives. To obtain polymer composite materials (PCM) with enhanced physicomechanical properties using the vacuum assisted resin transfer molding (VaRTM) method, binders must have a viscosity of up to 500 mPa·s. In some cases, this leads to restrictions on the use of certain materials or requires the use of temporary diluents. This is closely related to the deterioration of other required composite characteristics, such as increased flammability. Three phosphorus-containing oligoester(meth)acrylates PhOEM-1, PhOEM-2, and PhOEM-3 were synthesized with significant differences in viscosity characteristics in the series PhOEM-1 << PhOEM-2 << PhOEM-3. The polymer based on PhOEM-1 exhibits inferior physicomechanical properties despite having lower viscosity. Hence, the aim of the study was to investigate the viscosity characteristics of mixtures of methacrylate binders of the same nature but different structures and functionalities. This was done by studying the rheological properties of the original oligoester(meth)acrylates and their mixtures taken in various ratios. The method used was to optimize compositions via a simplex lattice (Scheffe's plan), in order to obtain PCM using the VaRTM technology.

Methods. The study of rheological properties of phosphorus-containing oligoester(meth)acrylates and their mixtures was conducted using the method of rotational viscometry on a Brookfield LVDV-II + Pro viscometer with a spindle 27 at different shear rates ranging from 0 to 70 s^{-1} and temperatures from 30 to 70°C. Rheological studies were also conducted on a Lamy Rheology GT300 PLUS (GEL TIMER) viscometer in the same range of shear rates and temperatures.

Results. It was established that the objects under investigation can be characterized by viscosity values ranging from 96 to 2137 mPa·s depending on the temperature. The nature of the viscous flow of phosphorus-containing oligoester(meth)acrylates and their mixtures is similar to that of Newtonian liquids only at certain shear rates. The effective activation energies of the viscous flow of binders and their mixtures were calculated, and the influence of temperature on the viscosity of binders was determined.

Conclusions. The study identified the features and nature of the flow curves of phosphorus-containing oligoester(meth)acrylate binders of the same nature but different structures and functionalities, as well as of their mixtures. The optimal composition ranges of three-component mixtures of phosphorus-containing oligoester(meth)acrylates for use in the VaRTM technological process in producing polymer composite materials within the temperature range of 30 to 70°C were defined. The optimal compositions and temperature conditions for obtaining polymer composite materials using the VaRTM technology were also identified. This enables the production of polymer products with complex geometric shapes and varying sizes.

НАУЧНАЯ СТАТЬЯ

Реологические свойства фосфорсодержащего олигоэфир(мет)акрилата для переработки методом вакуумной инфузии

О.О. Тужиков[1, ✉], Л.Ю. Донецкова[1], С.М. Соломахин[1], А.В. Налесная[1], А. Аль-Хамзави[2], Б.А. Буравов[1], С.В. Борисов[1], О.И. Тужиков[1]

[1]*Волгоградский государственный технический университет, Волгоград, 400005 Россия*

[2]*Университет Аль-Кадисия, Эд-Дивания, 58002 Ирак*

✉ *Автор для переписки, e-mail: tuzhikovoleg@mail.ru*

Аннотация

Цели. Для получения полимерных композиционных материалов (ПКМ) с повышенным уровнем физико-механических свойств методом безавтоклавной технологии (vacuum assisted resin transfer molding, VaRTM) связующие должны обладать вязкостью до 500 мПа·с. В ряде случаев это приводит к ограничению по применению тех или иных материалов, либо требует использования временных разбавителей, что неразрывно связано с ухудшением других требуемых характеристик композита, например, увеличением горючести. Нами были синтезированы три фосфорсодержащих олигоэфир(мет)акрилата PhOEM-1, PhOEM-2, PhOEM-3, обладающих значительными отличиями по характеристикам вязкости в ряду PhOEM-1 << PhOEM-2 << PhOEM-3, при этом полимер на основе PhOEM-1, обладая меньшей вязкостью, характеризуется худшими физико-механическими свойствами. В связи с этим, целью исследования явилось изучение вязкостных характеристик смесей метакрилатных связующих одинаковой природы, разного строения и функциональности путем изучения реологических свойств исходных олигоэфир(мет)акрилатов и их смесей, взятых в различных соотношениях, с применением метода оптимизации составов по симплекс-решетке (плану Шеффе) для получения ПКМ по безавтоклавной (VaRTM) технологии.

Методы. Исследование реологических свойств фосфорсодержащих олигоэфир(мет)акрилатов и их смесей проводили методом ротационной вискозиметрии на вискозиметре Brookfield LVDV-II + Pro с использованием шпинделя 27 при скоростях сдвига в диапазоне от 0 до 70 с$^{-1}$ и температурах от 30 до 70°С. Параллельно проводили реологические исследования на вискозиметре Lamy Rheology GT300 PLUS (GEL TIMER) в том же диапазоне скоростей сдвига и температур.

Результаты. Установлено, что исследуемые объекты, в зависимости от температуры, характеризуются значениями вязкости от 96 до 2137 мПа·с. По характеру вязкого течения фосфорсодержащие олигоэфир(мет)акрилаты и их смеси ведут себя аналогично ньютоновским жидкостям только при определенных скоростях сдвига. Рассчитаны эффективные энергии активации вязкого течения связующих и их смесей, установлено влияние температуры на вязкость связующих.

Выводы. Определены особенности и характер кривых течения фосфорсодержащих олигоэфир(мет)акрилатных связующих одинаковой природы, разного строения и функциональности, а также их смесей. Установлены области оптимальных составов трехкомпонентных смесей фосфорсодержащих олигоэфир(мет)акрилатов для использования их в технологическом процессе VaRTM при получении ПКМ в диапазоне температур от 30 до 70°С. Определены оптимальные составы и температурные условия для получения ПКМ методом VaRTM, что позволяет получать полимерные изделия сложной геометрической формы и разного размера.

INTRODUCTION

Over the past decade, the market for polymer composite materials (PCM) based on thermosets has been growing rapidly. This is due to the unique properties of the polymers obtained: resistance to wear and chemicals, including in a wide temperature range, and the ability to process material using modern energy-saving and environmentally friendly methods, such as vacuum assisted resin transfer molding (VaRTM) [1–3].

In addition to a wide range of choice of binders for obtaining PCM, methods for their processing are also being developed. Examples include manual laying out, spraying, injection and autoclave molding. As a rule, the above methods for obtaining PCM are relatively expensive processes requiring simultaneously increased manufacturability and reduced production cost[1] [4, 5].

One promising technology in terms of cost and manufacturability is a relatively new non-autoclave technology: the vacuum infusion method VaRTM [6, 7]. However, when producing composites in this way, one of the most important technological characteristics limiting the use of the binder is its viscosity. The authors [8–11] found that the optimal viscosity of the binder for vacuum infusion should not exceed 500 mPa·s.

Colleagues previously synthesized and patented a phosphorus-containing trifunctional oligoester(meth)- acrylate (PhOEM-1) [12]. Later, we obtained and patented tetrafunctional oligoester(meth)acrylates containing spacers (PhOEM-2, PhOEM-3) [13, 14]. All of the oligoester(meth)acrylates under consideration are capable of curing in the presence of a peroxide initiator, while possessing different levels of initial viscosity and physical and mechanical properties. Synthesized tetrafunctional ester(meth)acrylates, unlike trifunctional ones, are characterized by relatively high viscosity values at temperatures up to 40°C. These temperatures limit their use under standard production conditions. We selected the above compounds, in order to study the rheological properties of their mixtures in the temperature range of 30–70°C.

Taking the above into account, the aim of this work is to study the features of the flow curves of phosphorus- containing oligoester(meth)acrylates and their mixtures at temperatures of 30–70°C, in order to determine the optimal compositions of three-component mixtures that satisfy the processes of obtaining PCMs by the VaRTM method.

EXPERIMENTAL

The objects of the study were phosphorus-containing polymerizable oligoester(meth)acrylates (PhOEM) with different molecular weights and relative unsaturation, with and without a spacer in the structure.

The compounds were synthesized according to the method described in [15].

The rheological properties of the binders and their mixtures were studied using rotational viscometry. For this purpose, a Brookfield LVDV-II + Pro spindle 27 viscometer (*Brookfield*, USA) and a Lamy Rheology GT300 PLUS (GEL TIMER) viscometer (*Lamy Rheology*, France) were used. The results obtained on the Lamy Rheology GT300 PLUS (GEL TIMER) viscometer showed similar trends in the change in the properties of the binders.

In order to determine the region of optimal compositions of oligoester(meth)acrylates, the STATISTICA program (*StatSoft*, Russia) was used. It implements a graphically oriented approach to the analysis of experimental data [16].

RESULTS AND DISCUSSION

Figures 1–3 presents the structures of the compounds studied and synthesized in accordance with work [15].

Generalized structural formulas are presented in Fig. 4.

Figure 4 shows the difference in the structure of the compounds: different numbers of unsaturated groups; and the presence or absence of a spacer (the fragment of the structure contains an insert between the reactive centers in one molecule) [15].
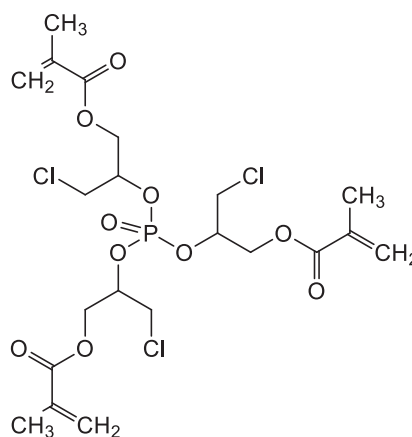
Fig. 1. Structure of PhOEM-1

---

[1] Veshkin EA. *Technologies of non-autoclave molding of low-porous polymer composite materials and large-sized structures made from them.* Diss. Cand. Sci. (Eng.). Moscow: VIAM; 2016. 146 p. (in Russ.).
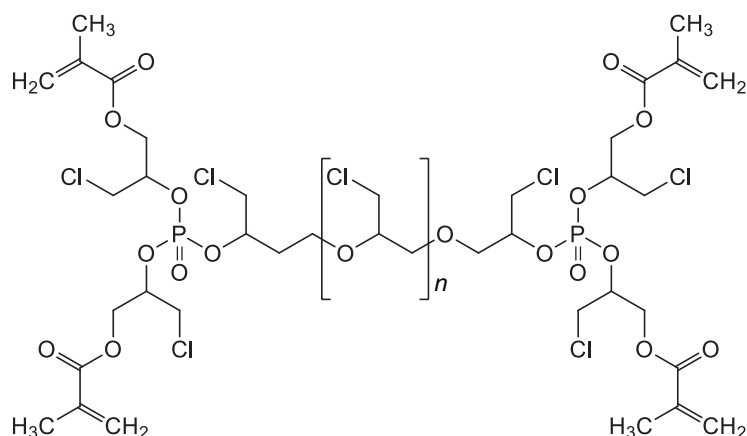
Fig. 2. Structure of PhOEM-2
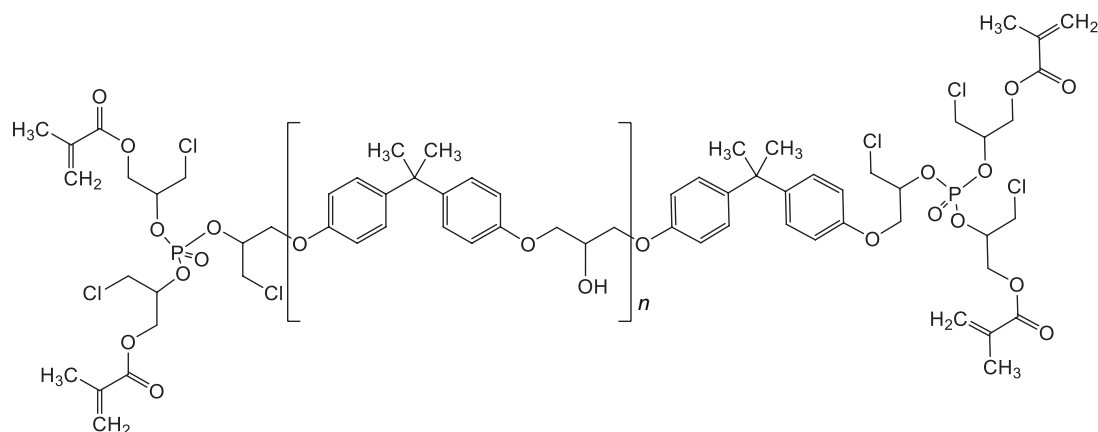
Fig. 3. Structure of PhOEM-3
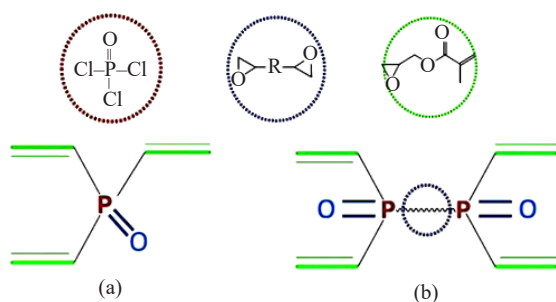
Fig. 4. Generalized structural chemical formulas of PhOEMs and of the starting reagents for their production:
(a) PhOEM-1 (without spacer);
(b) PhOEM-2 and PhOEM-3, with the different spacer structure

Fig. 5. Share rate versus shear stress for PhOEM-1 depending on temperature: τ is shear stress, Pa; γ is shear rate, s^{-1}

The viscosity of the synthesized compounds was studied at different shear rates and temperatures. The results of the studies of the rheological properties in the form of flow curves are presented in Figs. 5–7.
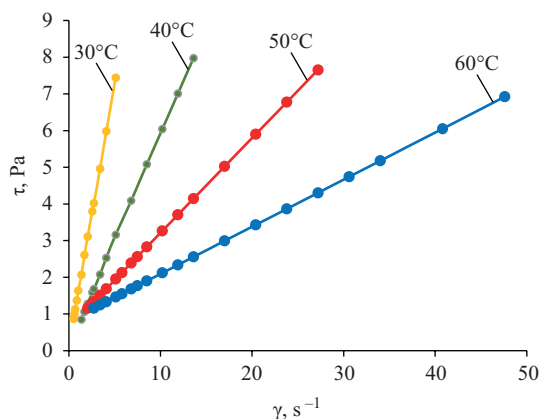
Fig. 6. Share rate versus shear stress for PhOEM-2 depending on temperature: τ is shear stress, Pa, γ is shear rate, s^{-1}
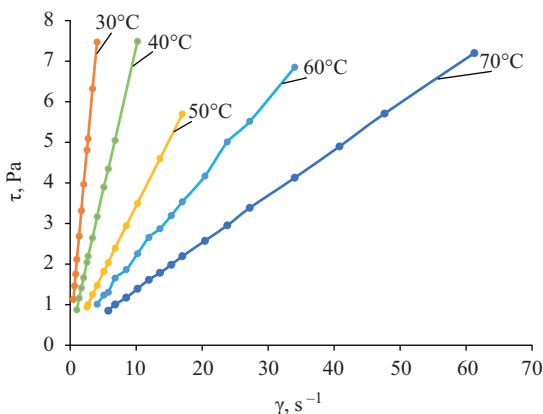
Fig. 7. Share rate versus shear stress for PhOEM-3 depending on temperature: τ is shear stress, Pa, γ is shear rate, s^{-1}

The study of the rheological properties of PhOEM-1 is limited to the temperature range of 30–50°C. This is due to the insufficient sensitivity of the device and the low viscosity of the oligomer at these temperatures. In this case, the developer of the device recommended using a spindle of a different size. However, measurements of liquid viscosity using different geometric spindle sizes are not recommended for comparative studies.

In order to compare the viscosity properties of the oligomers under study, we used a range of shear rates at which the liquids behaved similarly to Newtonian ones. As temperature increased, the study was continued at higher shear rates to ensure the specified conditions.

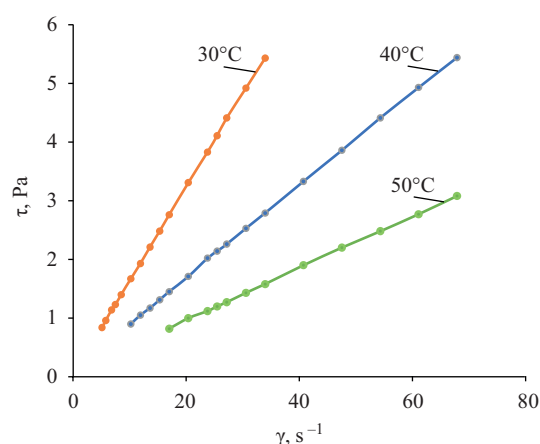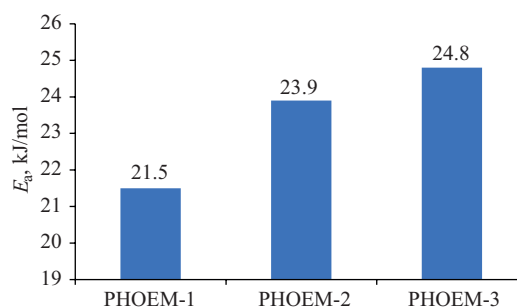Based on the results obtained, the effective activation energies of the viscous flow of the objects under study were calculated using Eq. (1) [17].

$$E_a = \frac{R \cdot T_1 \cdot T_2}{T_1 - T_2} \lg \frac{\eta_2}{\eta_1}, \tag{1}$$

wherein E_a is the effective activation energy of viscous flow, J/mol; R is the gas constant, J/(K·mol); T_i is the test temperature, K; η_i is the viscosity, mPa·s.

The results obtained are presented in Fig. 8.

Fig. 8. Flow activation energy in PhOEM-1, PhOEM-2, PhOEM-3

The data presented shows that the effective activation energy of viscous flow depends on the compound structure (Fig. 4) and the presence of spacers of various structures in it. This must be taken into account when developing the process for obtaining PCM using VaRTM technology.

Studies were carried out using the mathematical planning method of an experiment using a simplex lattice (Scheffe's plan) with the construction of a fourth-order polynomial model [18]. The objective was to select the optimal compositions of oligoester(meth)acrylate mixtures which provide the necessary conditions for the technological criteria for vacuum infusion. The essence of the method consists in constructing a regression dependence of the mixture properties on the content of components. The use of this method makes it possible to establish the dependence of the properties of binders on their composition [19, 20].

The study area of the PhOEM-1, PhOEM-2, PhOEM-3 system includes mass fractions from 0 to 1. This study area is presented in the form of an equilateral Gibbs concentration triangle. Figure 9 shows the position of the experimental points of the compositions, i.e., the points of quantitative ratios of the dosages of the given compounds which form the basis of the experimental planning matrix table.
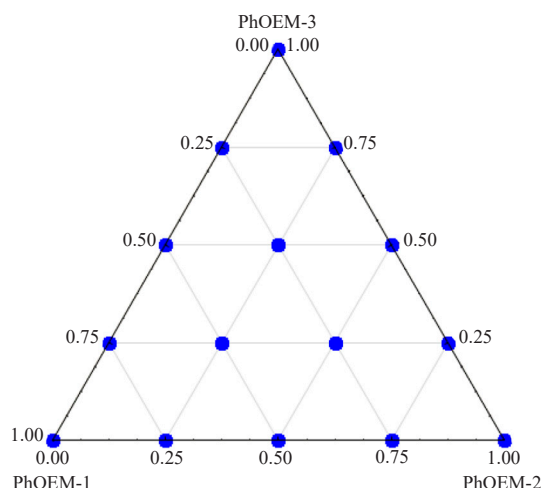
Fig. 9. Gibbs triangle showing concentration
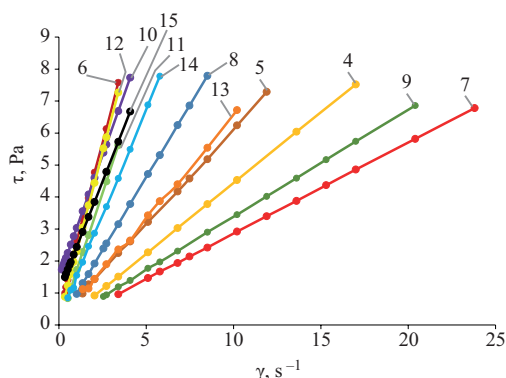
Fig. 10. Share rate versus shear stress for mixtures
at a temperature of 30°C: τ is shear stress, Pa; γ is shear rate, s^{-1}

Figure 10 presents the results of the studies of the rheological properties of the binder mixtures in accordance with mathematical planning using Scheffe's plan (see Table) in the form of flow curves. As in the above study, regions of viscous flow were selected where the mixtures behaved similarly to Newtonian fluids.

The rheological dependencies presented in Fig. 10 show that the mixtures behave similarly to Newtonian fluids [21] and are satisfactorily described by Eq. (2):

$$\tau = \eta \cdot \gamma, \tag{2}$$

wherein η is the dynamic viscosity, Pa·s; τ is the shear stress, Pa; γ is the shear rate, s^{-1}.

Using the results obtained, we then calculated the values of the effective activation energy of viscous flow for the oligomer mixtures.

The ratio of components, viscosity values at temperatures of 30–70°C and the values of the effective activation energy of viscous flow for the mixtures studied are presented in the table.

In order to determine the region of optimal compositions of oligoester(meth)acrylates using a graphical method, the STATISTICA program was used. This program implements a graphical-oriented approach to the analysis of experimental data. Diagrams of the nature of the change in properties from the composition of phosphorus-containing binders are presented in Fig. 11.

Figure 11 shows that there are ranges of viscosity values at temperatures of 30 and 40°C, below which

Table. Planning matrix and corresponding viscosities and activation energy of viscous flow (10 rpm)

Composition number	PhOEM			Viscosity, mPa·s					E_a, kJ/mol
	1	2	3	30°C	40°C	50°C	60°C	70°C	
1	1	0	0	162	89	48	–	–	21.5
2	0	1	0	1460	612	434	401	373	23.9
3	0	0	1	1856	776	368	248	155	24.4
4	0.5	0.5	0	445	232	127	66	–	23.2
5	0.5	0	0.5	661	408	220	124	94	20.3
6	0	0.5	0.5	2231	1035	530	304	178	24.2
7	0.75	0.25	0	284	150	96	56	34	19.7
8	0.25	0.75	0	926	436	239	124	71	24.4
9	0.75	0	0.25	349	202	131	89	67	16.6
10	0.25	0	0.75	1987	984	661	506	363	16.6
11	0	0.75	0.25	1652	764	361	195	129	25.9
12	0	0.25	0.75	2137	932	438	255	148	25.8
13	0.5	0.25	0.25	694	347	195	114	74	21.9
14	0.25	0.5	0.25	1347	668	328	192	102	23.7
15	0.25	0.25	0.5	1699	905	530	312	227	20.6
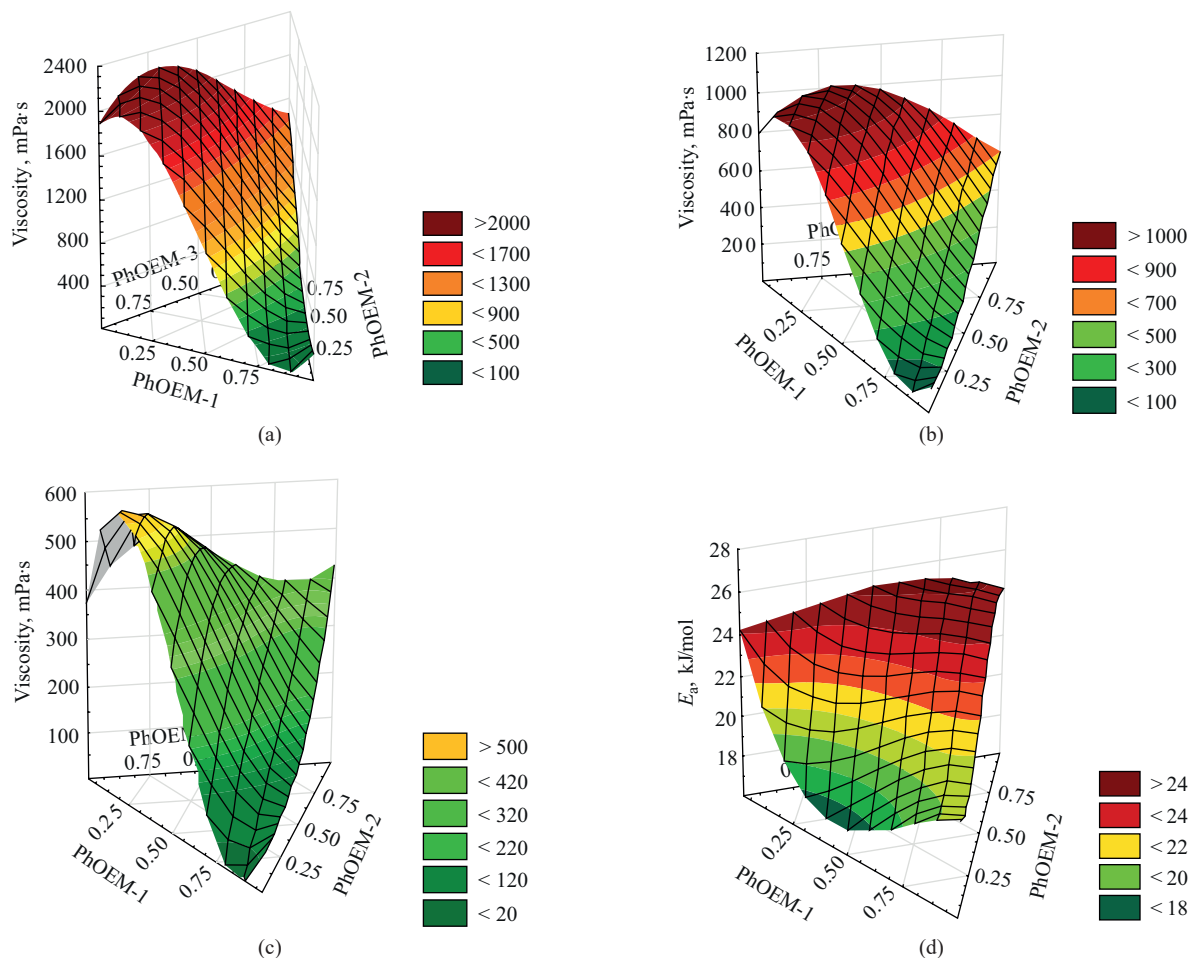
Fig. 11. Composition–property diagrams of mixtures at temperatures:
(a) 30°C, (b) 40°C, (c) 50°C, (d) effective E_a, kJ/mol

the ratio of mixture components is optimal. Note that at temperatures above 50°C, the initial binders and their mixtures meet the requirements for processing polymer materials using the VaRTM technology, since their viscosity values do not exceed 500 mPa·s.

The mixture PhOEM-1 : PhOEM-3 = 1 : 1 has the minimum value of the effective activation energy of viscous flow. The introduction of PhOEM-2 into this mixture leads to an increase in the effective activation energy of viscous flow. This is probably due to the intermolecular interaction of the oligomers and their thermodynamic compatibility.

CONCLUSIONS

The paper studies the features of flow curves of phosphorus-containing oligoester(meth)acrylates and their mixtures. The areas of optimal compositions of three-component mixtures for their use in the VaRTM process for producing PCMs at temperatures from 30 to 70°C were determined.

The difference in the obtained flow curves of methacrylates was determined by the molecular weight of the compounds and their structure, as well as the presence of a spacer in the structure. The flow curves become linear at certain shear rates, above which, within the studied range of rates, the behavior of the studied liquids is similar to a Newtonian fluid.

Compounds with a spacer (PhOEM-2, PhOEM-3) can be characterized by significantly higher viscosity values of 1460 and 1856 mPa·s at 30°C, which is two or more times higher than the viscosity of PhOEM-1 (162 mPa·s). The same tendency remains at high temperatures.

It was established that at temperatures above 50°C, the viscosity of both the initial components and their mixtures in any ratio meets the conditions of the VaRTM technology for obtaining PCM with improved physical and mechanical properties.

By using the composition–viscosity and composition–activation energy diagrams together, the region of optimal technological conditions (temperature, pressure

difference) for obtaining PCM by the vacuum infusion method can be determined.

Authors' contributions

O.O. Tuzhikov—research idea, consultation on experimental procedures, writing the article.

L.Yu. Donetskova—experiment execution, data analysis, data processing.

S.M. Solomakhin—experiment execution, data analysis, data processing.

A.V. Nalesnaya—literature analysis, formalization of the reference list.

A. Al-Hamzawi—consultation on experimental procedures.

B.A. Buravov—experimental data processing, writing the article.

S.V. Borisov—consultation on rheological properties of binders.

O.I. Tuzhikov—consultation on chemistry of phosphorus-containing compounds, as well as on planning, methodology, and implementation of research.

The authors declare no conflicts of interest.

REFERENCES

1. Tkachuk A.I., Donetskii K.I., Terekhov I.V., Karavaev R.Yu. The use of thermosetting matrices for the manufacture of polymer composite materials by the non-autoclave molding methods. *Aviatsionnye materialy i tekhnologii = Aviation Materials and Technologies*. 2021;1(62):22–33 (in Russ.). https://doi.org/10.18577/2713-0193-2021-0-1-22-33

2. Kablov E.N. Innovative developments of FSUE "VIAM" SSC RF on realization of "Strategic directions for the development of materials and technologies for their processing for the period until 2030." *Aviatsionnye materialy i tekhnologii = Aviation Materials and Technologies*. 2015;1(34):3–33 (in Russ.). http://doi.org/10.18577/2071-9140-2015-0-1-3-33

3. Kogan D.I., Chursova L.V., Panina N.N., *et al*. Advanced polymer materials with energy-efficient molding mode for structural composite products. *Plasticheskie Massy*. 2020;3–4:52–54 (in Russ.). https://doi.org/10.35164/0554-2901-2020-3-4-52-54

4. Postnova M.V., Postnov V.I. Development experience out-of-autoclave methods of formation PCM. *Trudy VIAM = Proceedings of VIAM*. 2014;4:6 (in Russ.). https://doi.org/10.18577/2307-6046-2014-0-4-6-6

5. Michels J., Widmann R., Czaderski C., Allahvirdizadeh R., Motavalli M. Glass transition evaluation of commercially available epoxy resins used for civil engineering applications. *Compos. Part B: Eng.* 2015;77:484–493. https://doi.org/10.1016/j.compositesb.2015.03.053

6. Merkulova Yu.I., Mukhametov R.R. Development of a low-viscosity epoxy binder for processing by vacuum infusion. *Aviatsionnye materialy i tekhnologii = Aviation Materials and Technologies*. 2014;1(30):39–41 (in Russ.). https://doi.org/10.18577/2071-9140-2014-0-1-39-41

СПИСОК ЛИТЕРАТУРЫ

1. Ткачук А.И., Донецкий К.И., Терехов И.В., Караваев Р.Ю. Применение термореактивных связующих для изготовления полимерных композиционных материалов методами безавтоклавного формования. *Авиационные материалы и технологии*. 2021;1(62):22–33. https://doi.org/10.18577/2713-0193-2021-0-1-22-33

2. Каблов Е.Н. Инновационные разработки ФГУП «ВИАМ» ГНЦ РФ по реализации «Стратегических направлений развития материалов и технологий их переработки на период до 2030 года». *Авиационные материалы и технологии*. 2015;1(34):3–33. http://doi.org/10.18577/2071-9140-2015-0-1-3-33

3. Коган Д.И., Чурсова Л.В., Панина Н.Н., Гребенева Т.А., Голиков Е.И., Шарова И.А., Баторова Ю.А. Перспективные полимерные материалы для конструкционных композиционных изделий с энергоэффективным режимом формования. *Пластические массы*. 2020;3–4:52–54. https://doi.org/10.35164/0554-2901-2020-3-4-52-54

4. Постнова М.В., Постнов В.И. Опыт развития безавтоклавных методов формирования ПКМ. *Труды ВИАМ*. 2014;4:6. https://doi.org/10.18577/2307-6046-2014-0-4-6-6

5. Michels J., Widmann R., Czaderski C., Allahvirdizadeh R., Motavalli M. Glass transition evaluation of commercially available epoxy resins used for civil engineering applications. *Compos. Part B: Eng.* 2015;77:484–493. https://doi.org/10.1016/j.compositesb.2015.03.053

6. Меркулова Ю.И., Мухаметов Р.Р. Низковязкое эпоксидное связующее для переработки методом вакуумной инфузии. *Авиационные материалы и технологии*. 2014;1(30):39–41. https://doi.org/10.18577/2071-9140-2014-0-1-39-41

7. Sakoshev Z.G., Blaznov A.N., Sakoshev E.G., Zadvornykh G.S. Investigation of rheological properties of binders based on epoxy resin and hardeners HT-152B, IMTHFA, and Etal-450. In: *Technologies and Equipment of the Chemical, Biotechnological, and Food Industries: Materials of the 15th All-Russian Scientific and Practical Conference of Students, Graduate Students, and Young Scientists with International Participation*. Biisk: Altai State Technical University; 2022. P. 234–237 (in Russ).

8. Mukhametov R.R., Akhmadieva K.R., Chursova L.V., Kogan D.I. New polymer binders for promising methods for the production of structural fibrous PCM. *Aviatsionnye materialy i tekhnologii = Aviation Materials and Technologies*. 2011;2(19):38–42 (in Russ.).

9. Sayapin S.N. New Approach to the Manufacturing Technology of Long Hollow Products Made of Fibrous Polymer Composite Materials. *Izvestiya vysshikh uchebnykh zavedenii. Mashinostroenie = BMSTU Journal of Mechanical Engineering*. 2022;11(752):38–46 (in Russ.). https://doi.org/10.18698/0536-1044-2022-11-38-46

10. Donetskiy K.I., Usacheva M.N., Khrulkov A.V. Infusion methods for the manufacture of polymer composite materials (Review). Part 1. *Trudy VIAM = Proceedings of VIAM*. 2022;6(112):58–67 (in Russ.). https://doi.org/10.18577/2307-6046-2022-0-6-58-67

11. Khrulkov A.V., Donetskiy K.I., Usacheva M.N., Goryansky A.N. Infusion methods for the manufacture of polymer composite materials (Review). Part 2. *Trudy VIAM = Proceedings of VIAM*. 2022;7(113):50–62 (in Russ.). https://doi.org/10.18577/2307-2022-0-7-50-62

12. Novakov I.A, Bakhtina G.D., Kochnov A.B., Kostryukova Yu.V. *Method of Producing Phosphorus-and-Chlorine-Containing Methacrylates*: RF Pat. 2447079 C1. Publ. 10.04.2012 (in Russ.).

13. Tuzhikov O.I., Tuzhikov O.O., Buravov B.A., *et al. Use of Oligoether Acrylate of (((((4-((1-(2-((bis((1-Chloro-3-(Methacryloyloxy)propan-2-yl)oxy)phosphine)-oxy)-3-Chlorophenoxy)-3-Chloropropan-2-yl)oxy)-1-Chlorobutan-2-yl)oxy)phosphindiyl)bis(oxy)bis(3-chloropropan-2,1-diyl)-bis(2-methacrylate) as a Monomer for Producing Thermo- and Heat-Resistant Polymers with Low Inflammability*: RF Pat. 2712107. Publ. 24.01.2020 (in Russ.).

14. Tuzhikov O.I., Tuzhikov O.O., Buravov B.A., *et al. Use of Oligoether Acrylate of (((((((((2-hydroxypropane-1,3-diyl)bis(oxy))bis(4,1-phenylene))bis(propan-2,2-diyl))-bis(4.1-phenylene))bis(hydroxy))-bis(1-chloropropane-3,2-diyl))bis(oxy))-bis(phosphintriyl)) tetrakis(oxy))-tetrakis(3-chloropropane-2,1-diyl)tetrakis(2-methyl acrylate) as a Monomer for Obtaining Thermo- and Heat-Resistant Polymers with Low Inflammability*: RF Pat. 2712116. Publ. 24.01.2020.

15. Buravov B.A., Al-Khamzawi A., Bochkarev E.S., Grichishkina N.Kh., Borisov S.V., Sidorenko N.V., Tuzhikov O.I., Tuzhikov O.O. Synthesis of new photo-cured phosphorus-containing oligoestermethacrylates with a spacer in the structure. *Tonk. Khim. Tekhnol. = Fine Chem. Technol.* 2022;17(5):410–426. https://doi.org/10.32362/2410-6593-2022-17-5-410-426

16. Kochetygov A.A. *Analiz dannykh s ispol'zovaniem sistemy STATISTICA (Data Analysis using the STATISTICA System)*: a textbook. Tula: TulGU; 2023. 324 p. (in Russ.). ISBN 975-5-7679-5255-7

17. Polezhaeva N.I. Development of organic binder for solder pastes with strictly specified rheological characteristics. *Reshetnevskie chteniya*. 2018;1:619–620 (in Russ.).

7. Сакошев З.Г., Блазнов А.Н., Сакошев Е.Г., Задворных Г.С. Исследование реологических свойств связующих на основе эпоксидной смолы и отвердителей ХТ-152Б, ИМТГФА и Этал-450. В сб.: *Технологии и оборудование химической, биотехнологической и пищевой промышленности*: *Материалы XV Всероссийской научно-практической конференции студентов, аспирантов и молодых ученых с международным участием*. Бийск: Алтайский государственный технический университет им. И.И. Ползунова; 2022. P. 234–237.

8. Мухаметов Р.Р., Ахмадиева К.Р., Чурсова Л.В., Коган Д.И. Новые полимерные связующие для перспективных методов изготовления конструкционных волокнистых ПКМ. *Авиационные материалы и технологии*. 2011;2(19):38–42.

9. Саяпин С.Н. Новый подход к технологии изготовления длинномерных полых изделий из волокнистых полимерных композиционных материалов. *Известия высших учебных заведений. Машиностроение*. 2022;11(752):38–46. https://doi.org/10.18698/0536-1044-2022-11-38-46

10. Донецкий К.И., Усачева М.Н., Хрульков А.В. Методы инфузии для изготовления полимерных композиционных материалов (обзор). Часть 1. *Труды ВИАМ*. 2022;6(112):58–67. https://doi.org/10.18577/2307-6046-2022-0-6-58-67

11. Хрульков А.В., Донецкий К.И., Усачева М.Н., Горянский А.Н. Методы инфузии для изготовления полимерных композиционных материалов (обзор). Часть 2. *Труды ВИАМ*. 2022;7(113):50–62. https://doi.org/10.18577/2307-2022-0-7-50-62

12. Новаков И.А, Бахтина Г.Д., Кочнов А.Б., Кострюкова Ю.В. *Способ получения фосфорхлорсодержащих метакрилатов*: пат. 2447079 РФ. Заявка № 2011100594/04; заявл. 11.01.2011; опубл. 10.04.2012.

13. Тужиков О.И., Тужиков О.О., Буравов Б.А., Бочкарев Е.С., Солодовникова К.В., Хохлова Т.В., Сидоренко Н.В., Аль-Хамзави А.Х.Д. *Применение олигоэфиракрилата ((((4-((1-(2-((бис((1-галоген-3-(мет-акрилоилокси)-пропан-2-ил)окси)фосфин)окси)-3-галогенпропокси)3-хлорпропан-2-ил)окси)-1-галоген-бутан-2-ил)окси)фосфиндиил)бис(окси))бис(3-галоген-пропан-2,1-диил)бис(2-метакрилата) в качестве мономера для получения термо- и теплостойких полимеров с пониженной горючестью*: пат. 2712107 РФ. Заявка № 2019125870; заявл. 16.08.2019; опубл. 24.01.2020.

14. Тужиков О.И., Тужиков О.О., Буравов Б.А., Бочкарев Е.С., Солодовникова К.В., Хохлова Т.В., Сидоренко Н.В., Аль-Хамзави А.Х.Д. *Применение олигоэфиракрилата (((((((((2-гидрокси-пропан-1,3-диил) бис (окси)) бис (4,1-фенилен)) бис (пропан-2,2-диил) бис (4,1-фенилен)) бис(окси)) бис (1-галогенпропан-3,2-диил)) бис (окси)) бис(фосфинтриил))тетракис (окси)) тетракис (3-галогенпропан-2,1-диил)тетракис (2-метилакрилата) в качестве мономера для получения термо- и теплостойких полимеров с пониженной горючестью*: пат. 2712116 РФ. Заявка № 2019126186; заявл. 20.08.2019; опубл. 24.01.2020.

15. Буравов Б.А., Аль-Хамзави А., Бочкарев Е.С., Гричишкина Н.Х., Борисов С.В., Сидоренко Н.В., Тужиков О.И., Тужиков О.О. Синтез новых фотоотверждаемых фосфорсодержащих олигоэфирметакрилатов со спейсером в структуре. *Тонкие химические технологии*. 2022;17(5):410–426. https://doi.org/10.32362/2410-6593-2022-17-5-410-426

16. Кочетыгов А.А. *Анализ данных с использованием системы STATISTICA*: учебное пособие. Тула: ТулГУ; 2023. 324 с. ISBN 975-5-7679-5255-7

17. Полежаева Н.И. Разработка органического связующего для паяльных паст со строго заданными реологическими характеристиками. *Решетневские чтения*. 2018,1:619–620.

18. Korotkova E.I. *Optimizatsiya mnogofaktornogo eksperimenta v khimii* (*Optimization of a Multifactorial Experiment in Chemistry*): a textbook. Tomsk: TPU; 2021. 85 p. (in Russ.). ISBN 978-5-4387-1055-4

19. Vershinin V.I., Pertsev V.I. *Planirovanie i matematicheskaya obrabotka rezul'tatov khimicheskogo eksperimenta* (*Planning and Mathematical Processing of the Results of a Chemical Experiment*). St. Petersburg: Lan; 2022. 236 p. (in Russ.). ISBN 978-5-8114-9167-4

20. Chetverikova D.K., Brezhnev A.M. Features of planning a multifactorial experiment. In: *Theory and Practice of Innovative Research in the Field of Natural Sciences: Materials of the All-Russian Scientific and Practical Conference with International Participation*. Orenburg: Orenburg State University; 2022. P. 221–225 (in Russ.).

21. Chepurnenko A.S., Kondrat'eva T.N. Prediction of Rheological Parameters of Polymers by Machine Learning Methods. *Advanced Engineering Research* (*Rostov-on-Don*). 2024;24(1):36–47 (in Russ.). https://doi.org/10.23947/2687-1653-2024-24-1-36-47

18. Короткова Е.И. *Оптимизация многофакторного эксперимента в химии*: учебное пособие. Томск: ТПУ; 2021. 85 с. ISBN 978-5-4387-1055-4

19. Вершинин В.И., Перцев В.И. *Планирование и математическая обработка результатов химического эксперимента*. Санкт-Петербург: Лань; 2022. 236 с. ISBN 978-5-8114-9167-4

20. Четверикова Д.К., Брежнев А.М. Особенности планирования многофакторного эксперимента. В сб.: *Теория и практика инновационных исследований в области естественных наук: Материалы Всероссийской научно-практической конференции с международным участием*. Оренбург: Оренбургский государственный университет; 2022. С. 221–225.

21. Чепурненко А.С., Кондратьева Т.Н. Прогнозирование реологических параметров полимеров методами машинного обучения. *Advanced Engineering Research* (*Rostov-on-Don*). 2024;24(1):36–47. https://doi.org/10.23947/2687-1653-2024-24-1-36-47

About the authors

Oleg O. Tuzhikov, Dr. Sci. (Eng.), Associate Professor, Head of the Department of General and Inorganic Chemistry, Volgograd State Technical University (28, pr. im. V.I. Lenina, Volgograd, 400005, Russia). E-mail: tuzhikovoleg@mail.ru. Scopus Author ID 12645529200, RSCI SPIN-code 8142-5915, https://orcid.org/0000-0001-6316-8896

Lyubov Yu. Donetskova, Master Degree, Engineer, Department of General and Inorganic Chemistry, Volgograd State Technical University (28, pr. im. V.I. Lenina, Volgograd, 400005, Russia). E-mail: lovedonetskova@mail.ru. RSCI SPIN-code 8843-1727, https://orcid.org/0009-0008-8085-5071

Semyon M. Solomakhin, Master Degree, Engineer, Department of General and Inorganic Chemistry, Volgograd State Technical University (28, pr. im. V.I. Lenina, Volgograd, 400005, Russia). E-mail: solomakhin-sim@mail.ru. https://orcid.org/0009-0007-5040-3683

Anna V. Nalesnaya, Cand. Sci. (Chem.), Associate Professor, Department of General and Inorganic Chemistry, Volgograd State Technical University (28, pr. im. V.I. Lenina, Volgograd, 400005, Russia). E-mail: nalesnaya@yandex.ru. RSCI SPIN-code 1669-1722, https://orcid.org/0009-0006-4083-129X

Ali Al-Khamzawi, Lecturer, Department of Chemical Engineering, College of Engineering, Al-Qadisiyah University (Al-Qadisiyah, Al-Diwaniyah, 58002, Iraq). E-mail: ali.alhamzawi80@gmail.com. RSCI SPIN-code 2551-0018, https://orcid.org/0000-0003-4491-494X

Boris A. Buravov, Cand. Sci. (Chem.), Associate Professor, Department of General and Inorganic Chemistry; Senior Researcher, Laboratory of Polymer, Composite and Hybrid Functional Materials, Volgograd State Technical University (28, pr. im. V.I. Lenina, Volgograd, 400005, Russia). E-mail: byravov@ya.ru. Scopus Author ID 57972246000, RSCI SPIN-code 6730-5763, https://orcid.org/0000-0001-9039-571X

Sergey V. Borisov, Cand. Sci. (Eng.), Associate Professor, Department of Chemistry and Processing Technology of Elastomers; Senior Researcher, Laboratory of Polymer, Composite and Hybrid Functional Materials, Volgograd State Technical University (28, pr. im. V.I. Lenina, Volgograd, 400005, Russia). E-mail: borisov.volgograd@yandex.ru. Scopus Author ID 57193435253, RSCI SPIN-code 4774-4238, https://orcid.org/0000-0003-4400-0822

Oleg I. Tuzhikov, Dr. Sci. (Chem.), Professor, Department of Technology of Macromolecular and Fibrous Materials, Volgograd State Technical University (28, pr. im. V.I. Lenina, Volgograd, 400005, Russia). E-mail: tuzhikov_oi@vstu.ru. Scopus Author ID 6507272270, RSCI SPIN-code 7255-0330, https://orcid.org/0000-0003-1893-2861

Об авторах

Тужиков Олег Олегович, д.т.н., доцент, заведующий кафедрой общей и неорганической химии, ФГБОУ ВО «Волгоградский государственный технический университет» (400005, Россия, Волгоград, пр-т им. В.И. Ленина, д. 28). E-mail: tuzhikovoleg@mail.ru. Scopus Author ID 12645529200, SPIN-код РИНЦ 8142-5915, https://orcid.org/0000-0001-6316-8896

Донецкова Любовь Юрьевна, магистр, инженер кафедры общей и неорганической химии, ФГБОУ ВО «Волгоградский государственный технический университет» (400005, Россия, Волгоград, пр-т им. В.И. Ленина, д. 28). E-mail: lovedonetskova@mail.ru. SPIN-код РИНЦ 8843-1727, https://orcid.org/0009-0008-8085-5071

Соломахин Семён Михайлович, магистр, инженер кафедры общей и неорганической химии, ФГБОУ ВО «Волгоградский государственный технический университет» (400005, Россия, Волгоград, пр-т им. В.И. Ленина, д. 28). E-mail: solomakhin-sim@mail.ru. https://orcid.org/0009-0007-5040-3683

Налесная Анна Владимировна, к.х.н., доцент кафедры общей и неорганической химии, ФГБОУ ВО «Волгоградский государственный технический университет» (400005, Россия, Волгоград, пр-т им. В.И. Ленина, д. 28). E-mail: nalesnaya@yandex.ru. SPIN-код РИНЦ 1669-1722, https://orcid.org/0009-0006-4083-129X

Аль-Хамзави Али, преподаватель кафедры химической технологии, технический факультет, Университет Аль-Кадисия (58002, Ирак, Эд-Дивания, Аль-Джамаа, Сунния ул.). E-mail: ali.alhamzawi80@gmail.com. SPIN-код РИНЦ 2551-0018, https://orcid.org/0000-0003-4491-494X

Буравов Борис Андреевич, к.х.н., доцент кафедры общей и неорганической химии; старший научный сотрудник лаборатории полимерных, композитных и гибридных функциональных материалов, ФГБОУ ВО «Волгоградский государственный технический университет» (400005, Россия, Волгоград, пр-т им. В.И. Ленина, д. 28). E-mail: byravov@ya.ru. Scopus Author ID 57972246000, SPIN-код РИНЦ 6730-5763, https://orcid.org/0000-0001-9039-571X

Борисов Сергей Владимирович, к.т.н., доцент кафедры химии и технологии переработки эластомеров; старший научный сотрудник лаборатории полимерных, композитных и гибридных функциональных материалов, ФГБОУ ВО «Волгоградский государственный технический университет» (400005, Россия, Волгоград, пр-т им. В.И. Ленина, д. 28). E-mail: borisov.volgograd@yandex.ru. Scopus Author ID 57193435253, SPIN-код РИНЦ 4774-4238, https://orcid.org/0000-0003-4400-0822

Тужиков Олег Иванович, д.х.н., профессор кафедры технологии высокомолекулярных и волокнистых материалов, ФГБОУ ВО «Волгоградский государственный технический университет» (400005, Россия, Волгоград, пр-т им. В.И. Ленина, д. 28). E-mail: tuzhikov_oi@vstu.ru. Scopus Author ID 6507272270, SPIN-код РИНЦ 7255-0330, https://orcid.org/0000-0003-1893-2861

Translated from Russian into English by M. Povorin
Edited for English language and spelling by Dr. David Mossop

Chemistry and technology of inorganic materials
Химия и технология неорганических материалов

RESEARCH ARTICLE

Optical and surface properties of Schiff base ligands and Cu(II) and Co(II) complexes

Alaa Adnan Rashad[1, ✉], **Dina A. Najeeb**[1], **Shaymaa M. Mahmoud**[2], **Evon Akram**[3], **Khalid Zainulabdeen**[1], **Salam Dulaimi**[4], **Rahimi M. Yusop**[5]

[1] *Department of Chemistry, College of Science, Al-Nahrain University, Jadriya, Baghdad, Iraq*

[2] *Department of Chemical Engineering, College of Engineering, Al-Nahrain University, Jadriya, Baghdad, Iraq*

[3] *Forensic DNA Research and Training Center, Al-Nahrain University, Jadriya, Baghdad, Iraq*

[4] *Department of Medical Physics, College of Science, Al-Nahrain University, Jadriya, Baghdad, Iraq*

[5] *School of Chemical Science and Food Technology, Faculty of Science and Technology, University Kebangsaan Malaysia 43600 Bangi, Selangor, Malaysia*

✉ *Corresponding author, e-mail: alaa.adnan@nahrainuniv.edu.iq*

Abstract

Objectives. To study the transition of electrons in 1,2-phenyl(4'-carboxy)benzylidene Schiff base ligand and transition metal ions, optical properties, as well as the surface chemistry of supported transition metals using diffuse reflectance spectroscopy (DRS); to study the roughness and morphology of the Schiff base ligand and its complexes using atomic force microscopy (AFM).

Methods. DRS, AFM, and Fourier-transform infrared spectroscopy instruments were used to identify electron transitions, optical properties, and surface morphology in Schiff base ligands and their complexes.

Results. The DRS revealed the d–d transitions and charge transfer shifts of all compounds, and helped identify the structure of the ligand. One of the optical properties studied was the energy gap calculation of the ligand and its complexes. The copper complex exhibited more semiconducting behavior with surface morphology properties such as surface roughness parameters lower than those of the ligand and the cobalt complex. This can be attributed to the smaller size of the copper atom, as well as lower electron transitions compared to the cobalt complex and the square planar bonding shape.

Conclusions. In Schiff base ligands, the reflectance spectrum bands reveal three electron transitions: $n{\rightarrow}\pi^*$, $\pi{\rightarrow}\pi^*$, and $\sigma{\rightarrow}\sigma^*$ transitions. In cobalt complexes, four transitions are indicated: $4A_2(F){\rightarrow}4T_1(F)$, $4A_2(F){\rightarrow}4T_1(P)$, charge transfer bands, and tetrahedral geometry. Copper complexes exhibit three transitions: $2B_1g{\rightarrow}2A_1g$, $2B_1g{\rightarrow}2Eg$, and charge transfer bands, with a square planar geometry for their structure. The energy gap calculations were 2.42, 2.29, and 2.30 eV, respectively. In the case of the SH ligands, copper complexes, and cobalt complexes, all compounds exhibited semiconductor properties. However, the complexes displayed increased conductivity due to the influence of the metal and coordination structure.

For citation

Rashad A.A., Najeeb D.A., Mahmoud Sh.M., Akram E., Zainulabdeen Kh., Dulaimi S., Yusop R.M. Optical and surface properties of Schiff base ligands and Cu(II) and Co(II) complexes. *Tonk. Khim. Tekhnol. = Fine Chem. Technol.* 2024;19(5):452–461. https://doi.org/10.32362/2410-6593-2024-19-5-452-461

НАУЧНАЯ СТАТЬЯ

Оптические и поверхностные свойства лигандов на базе оснований Шиффа и комплексов Cu(II) и Co(II)

Ала Аднан Рашид[1, ✉], Дина А. Наджиб[1], Шаймаа М. Махмуд[2], Эвон Акрам[3], Халид Зайн уль Абдин[1], Салам Дулайми[4], Рахими М. Юсоп[5]

[1] *Кафедра химии, Научный колледж, Университет Аль-Нахрейн, Джадрия, Багдад, Ирак*

[2] *Кафедра химии, Инженерный колледж, Университет Аль-Нахрейн, Джадрия, Багдад, Ирак*

[3] *Научно-исследовательский и учебный центр судебной экспертизы ДНК, Университет Аль-Нахрейн, Джадрия, Багдад, Ирак*

[4] *Кафедра медицинской физики, Научный колледж, Университет Аль-Нахрейн, Джадрия, Багдад, Ирак*

[5] *Школа химических наук и пищевых технологий, факультет науки и технологий, Университет Кебангсаан, Малайзия 43600 Банги, Селангор, Малайзия*

✉ *Автор для переписки, e-mail: alaa.adnan@nahrainuniv.edu.iq*

Аннотация

Цели. Изучить переход электронов в 1,2-фенил(4'-карбокси)бензилиденовом лиганде основания Шиффа и в ионах переходных металлов, оптические свойства, а также химический состав поверхности нанесенных переходных металлов с помощью спектроскопии диффузного отражения (СДО); изучить шероховатость и морфологию лиганда на базе основания Шиффа и комплексов на его основе с использованием атомно-силовой микроскопии (АСМ).

Методы. Для идентификации электронных переходов, анализа оптических свойств и морфологии поверхности лигандов на базе оснований Шиффа и их комплексов были использованы СДО, АСМ и инфракрасная спектроскопия с преобразованием Фурье.

Результаты. СДО выявила d–d переходы и сдвиги в переносе заряда во всех соединениях и помогла идентифицировать структуру лиганда. Одним из изученных оптических свойств был расчет энергетической щели лиганда и его комплексов. Комплекс меди показал более ярко выраженные полупроводниковые свойства, в то время как морфологические свойства поверхности, такие как шероховатость, у комплекса меди были ниже, чем у лиганда и комплекса кобальта. Это можно объяснить меньшим размером атома меди, более низкими электронными переходами по сравнению с комплексом кобальта, а также плоскоквадратной геометрией.

Выводы. В лигандах на базе оснований Шиффа полосы спектра отражения обнаруживают три электронных перехода: $n{\rightarrow}\pi^*$, $\pi{\rightarrow}\pi^*$ и $\sigma{\rightarrow}\sigma^*$. В комплексах кобальта выявлены переходы 4A2(F)→4T1(F), 4A2(F)→4T1(P), полосы переноса заряда и тетраэдрическая геометрия. Комплексы меди демонстрируют переходы 2B1g→2A1g, 2B1g→2Eg и полосы переноса заряда, при этом структура комплексов меди имеет плоскоквадратную геометрию. Расчеты энергетического зазора составили 2.42, 2.29 и 2.30 эВ соответственно. В случае лигандов SH, комплексов меди и кобальта все соединения проявляли полупроводниковые свойства. Однако комплексы меди и кобальта проявляли повышенную проводимость из-за наличия металла и координационной структуры.

Для цитирования

INTRODUCTION

Understanding the chemical complexes of transition metal ions is crucial in identifying and quantifying their coordination. Diffuse reflectance spectroscopy (DRS) is the technique used to measure the light reflection of powdered samples in various regions of the ultraviolet, visible, and near-infrared (NIR) spectra. DRS is used to gather information about the outer-shell electrons of atoms and can be applied to detect both d–d and charge transfer transitions. DRS technology is suitable for on-site conditions. However, a disadvantage of DRS is the potential for band overlap, which can make the technique technically challenging. In a DRS spectrum, light scattered from the surface of a thick layer is measured as a function of wavelength [1].

Schiff base compounds, first developed by Hugo Schiff, are organic compounds. The functional group of these compounds is the imine group which forms through the condensation reaction of primary aromatic or aliphatic amines with carbonyl compounds (ketones or aldehydes) through nucleophilic addition [2]. Schiff bases have applications in a variety of fields, including biology, where they serve as ligands in inorganic and analytical chemistry [3]. They are an important class of coordination chemistry, involving the coordination between metal ions and azomethine nitrogen bonds [4].

Due to their wide range of applications and unique electronic properties, Schiff base ligands are extensively studied in coordination chemistry. They have garnered significant attention for their roles in organic synthesis, metal refining, metallurgy, analytical chemistry, photography, and electroplating [5]. Moreover, they are extensively employed in materials science, playing roles in supramolecular chemistry, catalysts, photocatalysts, antioxidants, anticancer agents, antimicrobial agents, DNA binding, electrochemistry, and energy materials [6–20].

In this study, we investigated the surface morphology properties, including roughness and 3D surface images, of the Schiff base ligand and its complexes (copper and cobalt complexes). We also studied their optical properties, such as energy band gaps, indicating semiconductor properties, and their reflectance of light through DRS. The DRS data revealed d–d and charge transfer transitions of the metal ions.

EXPERIMENTAL

1,2-phenyl(4'-carboxy)benzylidene Schiff base ligand and its cobalt complexes were prepared as previously reported, and their structures were confirmed [21]. The copper complex was also synthesized in a 1 : 1 molar ratio (metal : ligand) by adding 12.98 g (0.01 mol) of copper chloride anhydrous salt to a solution of 0.46 g (0.01 mol) of Schiff base ligand in 15 mL of absolute ethanol (Scheme 1). The mixture was then refluxed for 4 h. A dark brown precipitate of the Cu complex formed. It was then filtered, recrystallized with ethanol, and dried in an oven at 60°C. Attenuated total reflection infrared (ATR-IR) spectroscopy was performed, in order to identify the complex (Scheme 2).

The following instruments of diffuse reflectance spectroscopy (DRS) were used for identifying electron transitions, optical properties, and surface morphology in Schiff base ligands and their complexes: (AvaLight-DH-S-BAL-2048 UV–Vis, *Avantes*, Netherlands) in a wavelength range of 230–1100 nm, atomic force microscope (AFM) (AA2000, *Angstrom Advanced Inc*., USA, contact mode, atmospheric conditions), and Fourier-transform infrared spectrometer (FTIR) (*Bruker ALPHA*, USA) in the transmission range 400 to 4000 cm^{-1}.
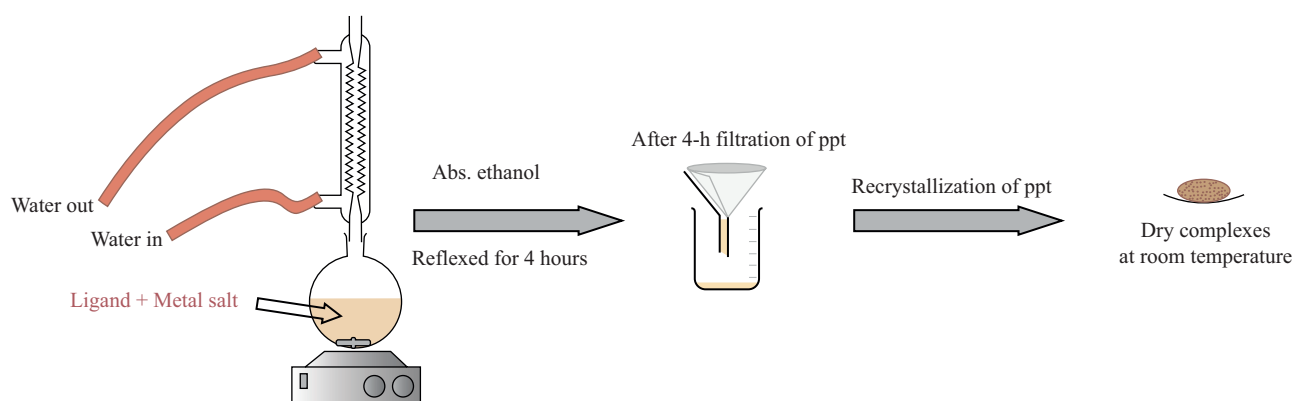
Scheme 1. Steps of copper complex preparation
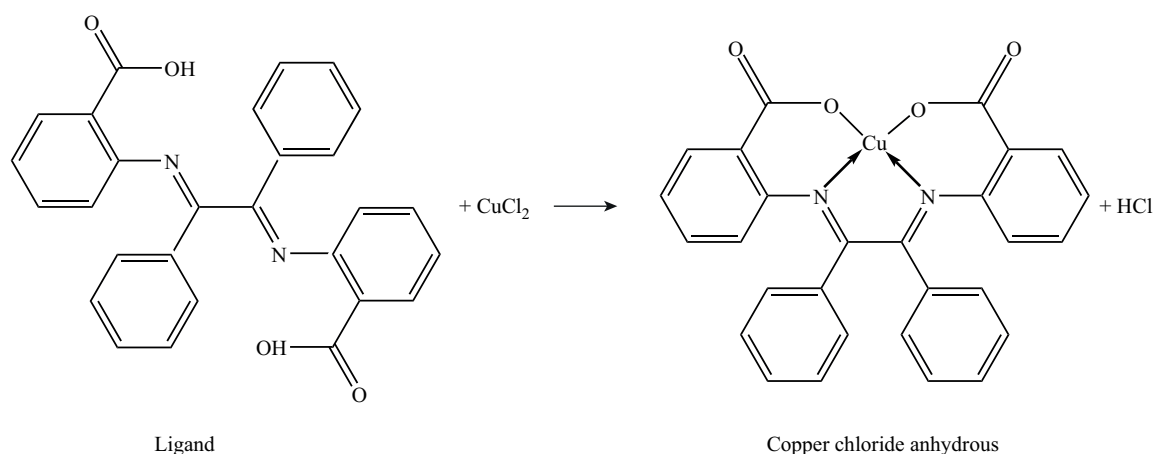
Scheme 2. Structure of copper complex

RESULT AND DISCUSSION

IR analysis

The ATR-IR spectra of both the ligand and the cobalt complex were identified as previously reported [21]. In the case of the copper complex, it was observed that the complex formed with the following linkage: Cu (ligand) [22–25]. Complications arose between the copper metal and the nitrogen atom in the imine, as well as the oxygen atom in the hydroxyl group. This resulted in the disappearance of certain bands and shifts in others. Specifically, the imine band shifted from 1583 cm^{-1} in the ligands to 1533 cm^{-1} in the Cu complexes. Additionally, there was a shift in the carbonyl band from 1661 cm^{-1} in the ligand to 1799 cm^{-1} in the Cu complexes. Table 1 displays some important IR spectra bands of the SH ligand and CuL$_2$ complex, affected and shifted as a result of the complex formation.

Table 1. IR spectra bands (cm^{-1}) of SH ligand and CuL$_2$ complex

Functional groups	SH ligand bands, cm^{-1}	CuL$_2$ complexes bands, cm^{-1}
ν O–H	3320	–
ν C–H Ar	3066	3063
ν C=O	1661	1799
ν C=N	1583	1533
ν C–O	1451	1433

Optical properties

The photophysical properties of the SH ligand, copper complexes, and cobalt complexes were measured using DRS (AvaLight-DH-S-BAL-2048 UV–Vis) in the wavelength range of 238–1000 nm, covering the ultraviolet, visible, and NIR regions. DRS spectroscopy is a valuable analytical tool for obtaining information about outer-shell electrons. It is particularly useful in determining d–d transition and charge transfer spectra in inorganic complexes [1]. Figure 1 depicts the reflectance of light from the surface, while Table 2 presents the DRS data for the ligand, copper complex, and cobalt complex in terms of wavelength and wavenumber. In the Schiff base ligand, the reflectance spectrum shows absorption wave numbers at 11682.24, 13986.01, 20449.90, and 26455.03 cm^{-1}, respectively. These wave numbers may be assigned to $n{\to}\pi^*$, $\pi{\to}\pi^*$, and $\sigma{\to}\sigma^*$ transitions. The positions of these bands can be utilized, in order to calculate shifts in the corresponding positions in the spectra of the metal complexes [26, 27].

The reflectance spectrum of the cobalt complexes displays absorption wave numbers at 10810.81, 17574.69, 26455.03, and 37593.98 cm^{-1}, respectively. They can be attributed to transitions $4A_2(F){\to}4T_1(F)$, $4A_2(F){\to}4T_1(P)$, and charge transfer bands. Active 1: Researchers have assigned several transitions in the cobalt(II) complexes to the tetrahedral geometry of cobalt complexes, with a coordination number of four [28–30].

Absorption wave numbers at 37735.85, 26455.03, and 14771.05 cm^{-1} were observed in the reflectance spectrum of the copper complexes. The various transitions in the copper(II) complexes indicate a square planar structure geometry with a coordination number of four [31–34].

In addition, reflectance describes the amount of light reflected from a surface. As shown in Fig. 2, the surface morphology and structure of the compound affect the reflectance. The ligand reflects more light compared to its complexes, indicating higher reflectance and some absorption. The reflectance of the ligand is higher when compared to its complexes, indicating that more light is

reflected and some is absorbed. In the cobalt complex, a higher percentage of light is absorbed in the visible range, while more light is reflected in the NIR range, possibly due to the transition $4A_2(F) \rightarrow 4T_1(F)$.
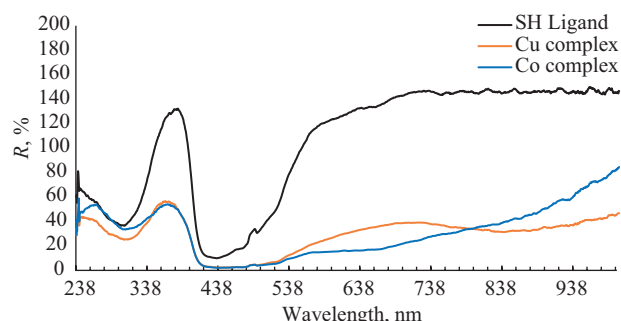
Fig. 1. DRS spectra of SH ligand, copper complex, and cobalt complex

Another optical property which was studied involved determining the energy gap. This was calculated using the DRS data through the application of the Kubelka–Munk theory [35, 36].

$$F(R_\infty) = (1 - R_\infty)^2/2R_\infty, \tag{1}$$

$$\alpha h\nu = C_1(h\nu - E_g)^{1/2},$$

$$\alpha = F(R_\infty),$$

$$[F(R_\infty)\, h\nu]^2 = C_2(h\nu - E_g), \tag{2}$$

where F is the Kubelka–Munk function; R_∞ is the sample reflection coefficient; α is the absorption coefficient; E_g is the energy gap; $h\nu$ (photon energy) = $1240/\lambda$; h is the Plank constant; λ is the absorption wavelength; C_1 is a frequency-independent proportionality constant that includes a matrix element of transition from the valence band to the conduction band; $C_2 = C_1^2$.

Figure 2 shows the plots of $[F(R_\infty) \cdot h\nu]^2$ against photon energy ($h\nu$) for the SH ligand, copper complexes, and cobalt complexes. The intersection point on these plots corresponds to the band gap values. The energy

gap calculations were 2.42, 2.29, and 2.30 eV for the SH ligand, copper complexes, and cobalt complexes, respectively. All of these compounds exhibited semiconductor properties, but the complexes displayed higher conductivity due to the influence of the metal and coordination structure.
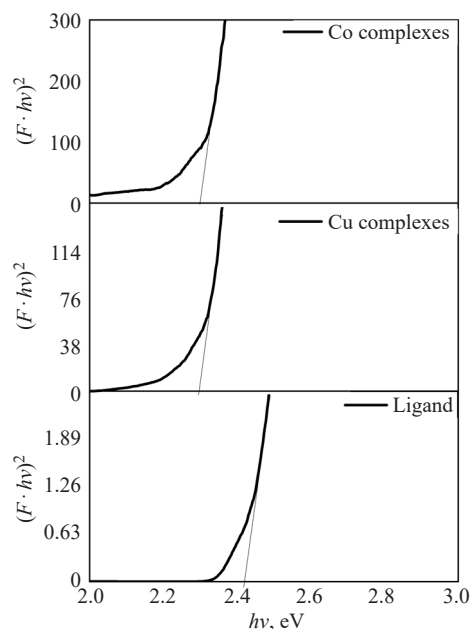
Fig. 2. Energy gap of compounds

Surface morphology study

Surface morphology properties were assessed using AFM. The surface morphology of the Schiff base ligand and its complexes (copper and cobalt) was examined by analyzing 2D and 3D AFM images, changes in surface roughness, cross-sectional profiles, and particle diameters.

Figure 3 presents both 2D and 3D AFM images. The ligand exhibited a rough surface, likely due to its inherent structural features and length, which manifested as contiguous clusters on the surface. In the copper complex, the surface distribution appeared nonuniform.

Table 2. DRS data of ligand, copper complex, and cobalt complex

Ligand		Copper complex		Cobalt complex	
Wavelength, nm	Wavenumber, cm^{-1}	Wavelength, nm	Wavenumber, cm^{-1}	Wavelength, nm	Wavenumber, cm^{-1}
378	26455.03	265	37735.85	266	37593.98
489	20449.90	378	26455.03	378	26455.03
715	13986.01	677	14771.05	569	17574.69
856	11682.24	–	–	925	10810.81

This was possibly due to the stereochemistry of the structure and structural rotations of the complex, as a result of which certain areas appeared as simple particle assemblies. Conversely, in the cobalt complex, the surface was rougher and exhibited heterogeneous distribution, which can likely be attributed to the larger size of cobalt atoms when compared to copper.

Figure 4 indicates the grain distribution on the surface and the histogram of particle diameters. The average diameter was 87.91, 93.87, and 86.02 nm for the ligand, Cu complex, and Co complex, respectively.

Figure 5 also presents cross-sections which reveal both smooth and rough surfaces. In the ligand, the rough surface is evident as a wider peak on the chart, whereas
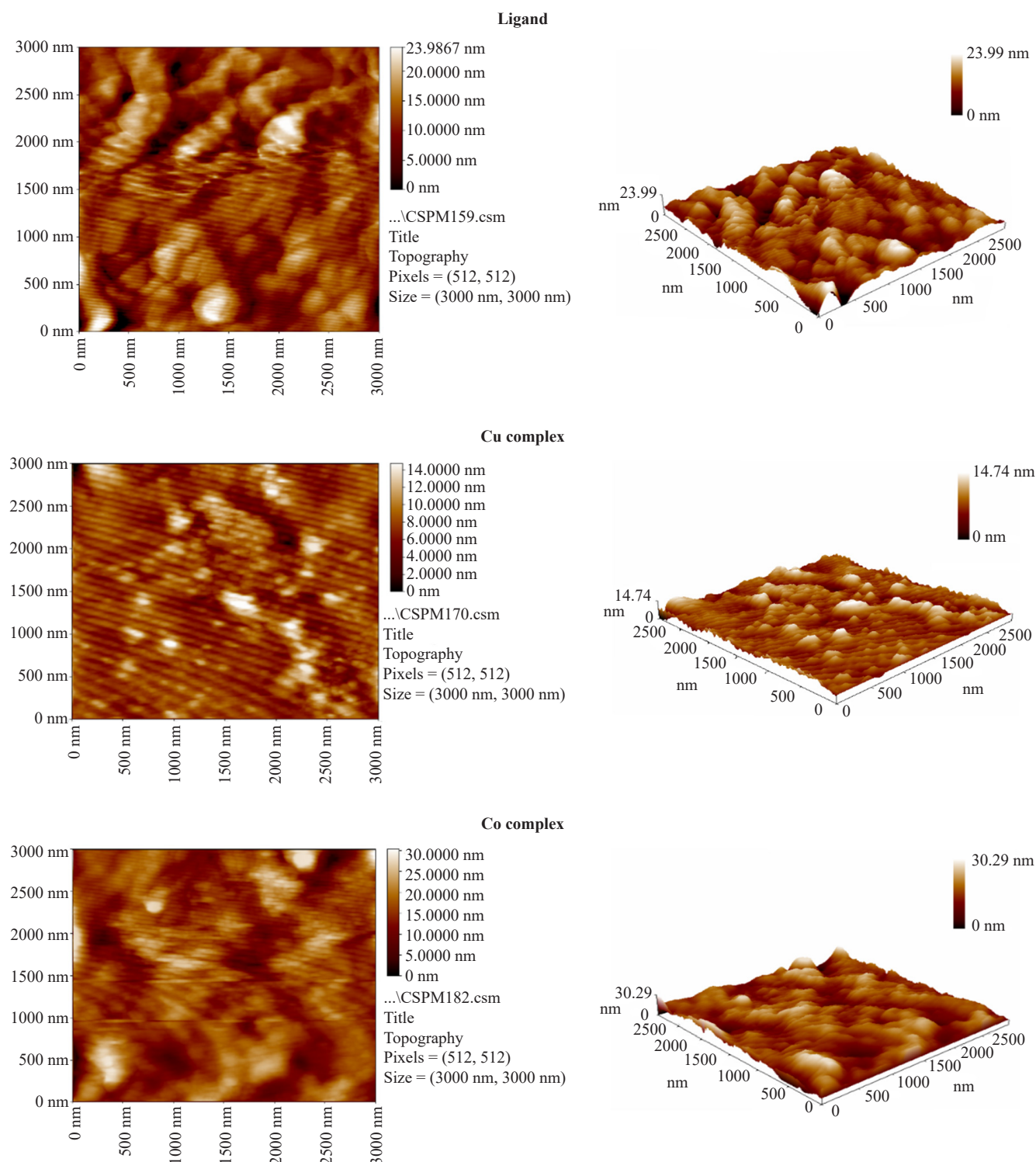
Fig. 3. 2D and 3D AFM image

in copper, the surface is less rough, resembling a sharper peak. In contrast, the cobalt complex exhibits a rougher surface when compared to the ligand, resulting in a wider peak width. This can be attributed to the tetrahedral coordination of the cobalt complex, affecting the surface characteristics.

Values for the surface roughness are provided in Table 2. Here it can be seen that the Cu complex has lower roughness compared to both the ligand and the Co complex.
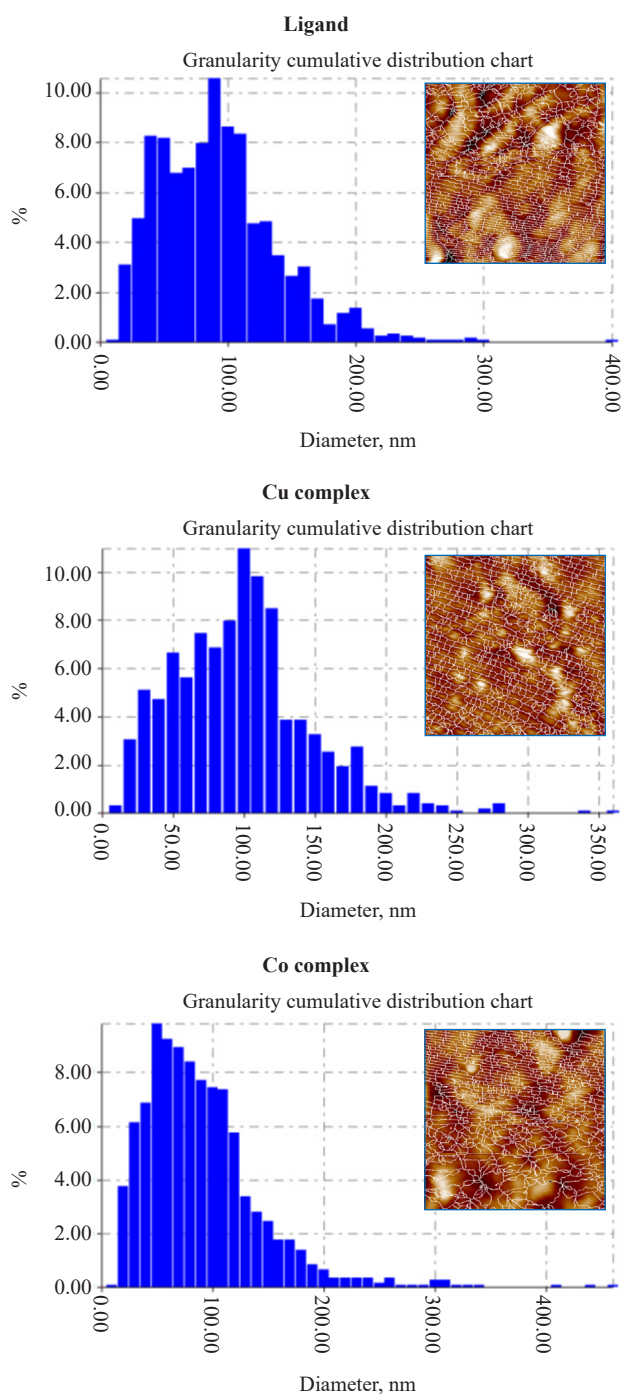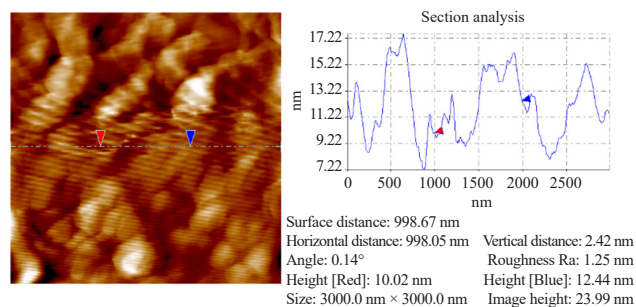
Ligand

Surface distance: 998.67 nm
Horizontal distance: 998.05 nm   Vertical distance: 2.42 nm
Angle: 0.14°   Roughness Ra: 1.25 nm
Height [Red]: 10.02 nm   Height [Blue]: 12.44 nm
Size: 3000.0 nm × 3000.0 nm   Image height: 23.99 nm

Cu complex

Surface distance: 916.79 nm
Horizontal distance: 915.95 nm   Vertical distance: 2.13 nm
Angle: 0.13°   Roughness Ra: 1.75 nm
Height [Red]: 10.65 nm   Height [Blue]: 12.78 nm
Size: 3000.0 nm × 3000.0 nm   Image height: 14.74 nm

Co complex

Surface distance: 1357.21 nm
Horizontal distance: 1356.34 nm   Vertical distance: 2.00 nm
Angle: –0.08°   Roughness Ra: 2.25 nm
Height [Red]: 21.17 nm   Height [Blue]: 19.17 nm
Size: 3000.0 nm × 3000.0 nm   Image height: 30.29 nm

Fig. 5. Cross section of surface

Ligand

Cu complex

Co complex

Fig. 4. Grain and histogram distribution of particle surface

Table 3. Roughness parameter data

Roughness parameter	Ligand	Cu complex	Co complex
Average rough	3.07	1.43	3.31
RMS	3.92	1.92	4.24
Peak peaking	24	14.7	30.1

CONCLUSIONS

The optical and surface properties of the Schiff base ligand complex are influenced by the choice of metal. Cobalt is more significantly affected due to its

tetrahedral coordination structure. This results in four transition electrons shifting from the ground state to the excited state. In contrast, the copper complex forms a square planar coordination structure with only three transition electrons, impacting the energy gap and making copper more semiconductor-like than the cobalt complex.

Furthermore, the surface of the copper complex exhibits lower roughness parameters when compared to the cobalt complex, which due to its tetrahedral structure and the larger size of cobalt atoms has higher values.

Authors' contributions

Alaa Adnan Rashad, **Dina A. Najeeb**—experimental work, writing original draft, and editing.

Shaymaa M. Mahmoud—correction of the research concept.

Evon Akram—research concept, processing experimental data.

Khalid Zainulabdeen, **S. Dulaimi,** and **Rahimi M. Yuso**—processing experimental data and checking English language.

The authors declare no conflicts of interest.

REFERENCES

1. Weckhuysen B.M., Schoonheydt R.A**.** Recent progress in diffuse reflectance spectroscopy of supported metal oxide catalysts. *Catal. Today*. 1999;49:441–451. https://doi.org/10.1016/S0920-5861(98)00458-1

2. Schiff H. Mittheilungen aus dem Universitätslaboratorium in Pisa: Eine neue Reihe organischer Basen. *Justus Liebigs Ann. Chem*. 1864;131(1):118–119. http://dx.doi.org/10.1002/jlac.18641310113

3. Kajal A., Bala S., Kamboj S., Sharma N., Saini V. Schiff bases: A versatile pharmacophore. *J. Catal*. 2013;2013:893512. https://doi.org/10.1155/2013/893512

4. Vigato P.A., Tamburini S. The Challenge of Cyclic and Acyclic Schiff Bases and Related Derivatives. *Coord. Chem. Rev*. 2004;248(17–20):1717–2128. https://doi.org/10.1016/j.cct.2003.09.003

5. More M.S., Joshi P.G., Mishra Y.K., Khanna P.K. Metal complexes driven from Schiff bases and semicarbazones for biomedical and allied applications: a review. *Materials Today Chem*. 2019;14:100195. https://doi.org/10.1016/j.mtchem.2019.100195

6. Vieira A.P., Wegermann C.A., Ferreira A.M. da C. Comparative studies of Schiff base-copper(II) and zinc(II) complexes regarding their DNA binding ability and cytotoxicity against sarcoma cells. *New J. Chem*. 2018;42:13169–13179. https://doi.org/10.1039/C7NJ04799A

7. Zhang J., Xu L., Wong W.Y. Energy materials based on metal Schiff base complexes. *Coord. Chem. Rev*. 2018;355:180–198. https://doi.org/10.1016/j.ccr.2017.08.007

8. Rana S., Biswas J.P., Sen A., Clemancey M., Blondin G., Latou J.M., Rajaraman G., Maiti D. Selective C−H halogenation over hydroxylation by non-heme iron(iv)-oxo. *Chem. Sci*. 2018;9:7843–7858. https://doi.org/10.1039/C8SC02053A

9. Kaczmarek M.T., Zabiszak M., Nowak M., Jastrzab R. Lanthanides: Schiff base complexes, applications in cancer diagnosis, therapy, and antibacterial activity. *Coord. Chem. Rev*. 2018;370:42–54. https://doi.org/10.1016/j.ccr.2018.05.012

10. Silva P.P., Guerra W., Silveira J.N., Ferreira A.M. da C., Bortolotto T., Fischer F.L., Terenzi H., Neves A., Pereira-Maia E.C. Two new ternary complexes of copper(II) with tetracycline or doxycycline and 1,10-phenanthroline and their potential as antitumoral: cytotoxicity and DNA cleavage. *Inorg. Chem*. 2011;50(14):6414–6424. https://doi.org/10.1021/ic101791r

11. Al Zoubi W., Ko Y.G. Organometallic complexes of Schiff bases: Recent progress in oxidation catalysis. *J. Organomet. Chem*. 2016;822:173–188. https://doi.org/10.1016/j.jorganchem.2016.08.023

12. Matsunaga S., Shibasaki M. Multimetallic schiff base complexes as cooperative asymmetric catalysts. *Synthesis*. 2013;45(4):421–437. https://doi.org/10.1055/s-0032-1316846

13. Silva P.P., Guerra W., dos Santos G.C., Fernandes N.G., Silveira J.N., Ferreira A.M. da C., Bortolotto T., Terenzi H., Bortoluzzi A.J., Neves A., Pereira-Maia E.C. Correlation between DNA interactions and cytotoxic activity of four new ternary compounds of copper(II) with N-donor heterocyclic ligands. *J. Inorg. Biochem*. 2014;132:67–76. https://doi.org/10.1016/j.jinorgbio.2013.09.014

14. Cozzi P.G. Metal−Salen Schiff base complexes in catalysis: practical aspects. *Chem. Soc. Rev*. 2004;33(7):410–421. https://doi.org/10.1039/B307853C

15. Gupta K.C., Sutar A.K. Catalytic activities of Schiff base transition metal complexes. *Coord. Chem. Rev*. 2008;252(12–14):1420–1450. https://doi.org/10.1016/j.ccr.2007.09.005

16. Matsunaga S., Shibasaki M. Recent advances in cooperative bimetallic asymmetric catalysis: dinuclear Schiff base complexes. *Chem. Commun*. 2014;50(9):1044–1057. https://doi.org/10.1039/C3CC47587E

17. Yang J., Shi R., Zhou P., Qiu Q., Li H. Asymmetric Schiff bases derived from diaminomaleonitrile and their metal complexes. *J. Mol. Struct*. 2016;1106:242−258. https://doi.org/10.1016/j.molstruc.2015.10.092

18. Kostova I., Saso L. Advances in research of Schiff-base metal complexes as potent antioxidants. *Curr. Med. Chem*. 2013;20(36):4609–4632. http://dx.doi.org/10.2174/09298673113209990149

19. Erxleben A. Transition metal salen complexes in bioinorganic and medicinal chemistry. *Inorg. Chim. Acta*. 2018;472:40–57. https://doi.org/10.1016/j.ica.2017.06.060

20. Lee S.J., Lee S.W. Cd(II), Ni(II), and Co(II) complexes based on a pyridyl−amine Schiff-base ligand: $[M(L)_2(NO_3)]\cdot(NO_3)$ (M = Cd, Ni, Co), cis-$[CoL_2Cl_2]\cdot(C_6H_6)$, and $[Co(L_{33})\cdot(ClO_4)_2$ $(CH_3CN)_2(H_2O)$ (L = *N*-(2-pyridylmethylene)benzene-1,4-diamine, (2-py)–CH=N–C_6H_4–NH_2). *Polyhedron*. 2019;159:259–264. https://doi.org/10.1016/j.poly.2018.12.003

21. Ibrahim F.M., Najeeb D.A. Synthesis, Characterization and Thermal Studies of Cr(III), Co(II) and Ni(II) Complexes with Schiff Base. *Int. J. Res. Pharm. Sci*. 2020;11(4):8026–8033.

22. Bartyzel A. Synthesis, thermal study and some properties of N_2O_4—donor Schiff base and its Mn(III), Co(II), Ni(II), Cu(II) and Zn(II) complexes. *J. Therm. Anal. Calorim*. 2017;127:2133–2147. https://doi.org/10.1007/s10973-016-5804-0

23. Marks J.M., Ward T.B., Duncan M.A. Infrared spectroscopy of coordination and solvation in $Cu^+(C_2H_4)_n$ (n = 1–9) complexes. *Int. J. Mass Spectrometry*. 2019;435:107–113. https://doi.org/10.1016/j.ijms.2018.10.008

24. Munshi M.U., Martens J., Berden G., Oomens J. Gas-Phase Infrared Ion Spectroscopy Characterization of Cu(II/I)Cyclam and Cu(II/I)2,2′-Bipyridine Redox Pairs. *J. Phys. Chem. A*. 2019;123(19):4149–4157. https://doi.org/10.1021/acs.jpca.9b00793

25. Shaalan N., Akram E., Adil D., Ali A.A. Synthesis and Spectroscopic Studies of Metal Complexes with Schiff Bases Derived from 2-[5-(Pyridin-2-Ylmethylene)-Amino]1,3,4-Thiadiazol-2-Yl-Phenol. *Journal of Al-Nahrain University-Science* (*ANJS*). 2018;1(1):37–42. https://anjs.edu.iq/index.php/anjs/article/view/2011

26. Devkota L., SantaLucia D.J., Wheaton A.M., Pienkos A.J., Lindeman S.V., Krzystek J., Ozerov M., Berry J.F., Telser J., Fiedler A.T. Spectroscopic and Magnetic Studies of Co(II) Scorpionate Complexes: Is There a Halide Effect on Magnetic Anisotropy? *Inorg. Chem*. 2023;62(15):5984–6002. https://doi.org/10.1021/acs.inorgchem.2c04468

27. More P.S., Mehta B.H. Structural Elucidation of Transition Metal Complexes of the Schiff Base of 5-Nitro Salicylaldehyde and Anthranalic Acid Using ^{1}H NMR, Thermal Analysis, Diffused Reflectance and ESR Data. *Int. Lett. Chem. Phys. Astron*. 2015;48:1–13. https://doi.org/10.18052/www.scipress.com/ILCPA.48.1

28. Najeeb D.A. Synthesis, Characterization and Theoretical Studies of Transition Metal Complexes of 1,2Phenyl(4-Carboxy)Benzylidene. *Int. J. Pharm. Sci. Rev. Res*. 2016;38(1):223–226.

29. Tafazzoli A., Keypour H., Farida S.H.M., Ahmadvand Z., Gable R.W. Synthesis, biological activities and theoretical studies of a new macrocyclic Schiff base ligand and its related Co(II), Ni(II), and Cu(II) complexes: The X-ray crystal structure of the Co(II) complex. *J. Mol. Struct*. 2023;1276:134770. https://doi.org/10.1016/j.molstruc.2022.134770

30. Lian R., Ou M., Guan H., Cui J., Zhao Z., Liu L., Chen X., Jiao Ch. Cu(II) and Co(II) complexes decorated ammonium polyphosphate as co-curing agents on improving fire safety and mechanical properties of epoxy-based building coatings. *Constr. Build. Mater*. 2023;389:131786. https://doi.org/10.1016/j.conbuildmat.2023.131786

31. Rashad A., Ibrahim F., Ahmed A., Salman E., Akram E. Synthesis and photophysical study of divalent complexes of chelating Schiff base. *Baghdad J. Biochem. Appl. Biol. Sci*. 2020;1(01):5–17. https://bjbabs.org/index.php/bjbabs/article/view/27

32. More P.S., Mehta B.H. ^{1}H NMR, Diffused Reflectance, Thermal Studies, ESR and Anti-Microbial Activities of Schiff Base Derived from 5-Nitro Salicylaldehyde and *p*-Anisidine. *Int. Lett. Chem. Phys. Astron*. 2015;48:14–26. http://dx.doi.org/10.18052/www.scipress.com/ILCPA.48.14

33. Uddin E., Bitu N.A., Asraf A., *et al*. An Updated Perspective of Nano Schiff Base Complexes: Synthesis, Catalytic, Electrochemical, Optical, Crystalline Features and Pharmacological Activities. *Rev. Adv. Chem*. 2022;12:57–95. https://doi.org/10.1134/S2634827622010056

34. Kanwal A., Parveen B., Ashraf R., Haider N., Ali K.G. A review on synthesis and applications of some selected Schiff bases with their transition metal complexes. *J. Coord. Chem*. 2022; 75(19–24):942. https://doi.org/10.1080/00958972.2022.2138364

35. Ravindra N.M., Ganapathy P., Choi J. Energy gap–refractive index relations in semiconductors – An overview. *Infrared Phys. Technol*. 2007;50(1):21–29. https://doi.org/10.1016/j.infrared.2006.04.001

36. Myrick M.L., Simcock M.N., Baranowski M., Brooke H., Morgan S.L., McCutcheon J.N. The Kubelka-Munk diffuse reflectance formula revisited. *Appl. Spectrosc. Rev*. 2011;46(2):140–165. https://doi.org/10.1080/05704928.2010.537004

About the authors

Alaa Adnan Rashad—Assistant Teacher, Master Degree, Department of Chemistry, College of Science, Al-Nahrain University, Jadriya, Baghdad, Iraq. E-mail: alaa.adnan@nahrainuniv.edu.iq. Scopus Author ID 57209788535, https://orcid.org/0000-0002-2600-2448

Dina A. Najeeb—Associate Professor, Master Degree, Department of Chemistry, College of Science, Al-Nahrain University, Jadriya, Baghdad, Iraq. E-mail: dina.najeeb@nahrainuniv.edu.iq. Scopus Author ID 57189488023, https://orcid.org/0000-0002-7903-7599

Shaymaa M. Mahmoud—Assistant Teacher, Master Degree, Department of Chemical Engineering, College of Engineering, Al-Nahrain University, Jadriya, Baghdad, Iraq. E-mail: shaymaa.ali@nahrainuniv.edu.iq. Scopus Author ID 58062049600, https://orcid.org/0000-0002-2890-5448

Evon Akram Abd-Aljabar—Teacher, Master Degree, Forensic DNA Research and Training Center, Al-Nahrain University, Jadriya, Baghdad, Iraq. E-mail: evon.akram@nahrainuniv.edu.iq. Scopus Author ID 57191172531, https://orcid.org/0000-0002-0150-6543

Khalid Zainulabdeen—Teacher, PhD, Department of Chemistry, College of Science, Al-Nahrain University, Jadriya, Baghdad, Iraq. E-mail: khalid_1chem1@yahoo.com. Scopus Author ID 57223028460, https://orcid.org/0000-0003-3829-5783

Salam Dulaimi—Teacher, PhD, Department of Medical Physics, College of Science, Al-Nahrain University, Jadriya, Baghdad, Iraq. E-mail: Salamdulaimi82@gmail.com. Scopus Author ID 57220069401, https://orcid.org/0000-0003-2936-9373

Rahimi M. Yusop—Professor Ts., PhD, School of Chemical Science and Food Technology, Faculty of Science and Technology, University Kebangsaan, Malaysia 43600 Bangi, Selangor, Malaysia. E-mail: drmc@ukm.edu.my. Scopus Author ID 36994895800, https://orcid.org/0000-0002-8843-8677

Об авторах

Alaa Adnan Rashad, ассистент преподавателя, кафедра химии, Научный колледж, Университет Аль-Нахрейн (Джадрия, Багдад, Ирак). E-mail: alaa.adnan@nahrainuniv.edu.iq. Scopus Author ID 57209788535, https://orcid.org/0000-0002-2600-2448

Dina A. Najeeb, доцент, кафедра химии, Научный колледж, Университет Аль-Нахрейн (Джадрия, Багдад, Ирак). E-mail: dina.najeeb@nahrainuniv.edu.iq. Scopus Author ID 57189488023, https://orcid.org/0000-0002-7903-7599

Shaymaa M. Mahmoud, ассистент преподавателя, Кафедра химической технологии, Инженерный колледж, Университет Аль-Нахрейн (Джадрия, Багдад, Ирак). E-mail: shaymaa.ali@nahrainuniv.edu.iq. Scopus Author ID 58062049600, https://orcid.org/0000-0002-2890-5448

Evon Akram Abd-Aljabar, преподаватель, Научно-исследовательский и учебный центр судебной экспертизы ДНК, Университет Аль-Нахрейн (Джадрия, Багдад, Ирак). E-mail: evon.akram@nahrainuniv.edu.iq. Scopus Author ID 7191172531, https://orcid.org/0000-0002-0150-6543

Khalid Zainulabdeen, PhD, преподаватель, Кафедра химии, Научный колледж, Университет Аль-Нахрейн (Джадрия, Багдад, Ирак). E-mail: khalid_1chem1@yahoo.com. Scopus Author ID 57223028460, https://orcid.org/0000-0003-3829-5783

Salam Dulaimi, PhD, преподаватель, Кафедра медицинской физики, Научный колледж, Университет Аль-Нахрейн (Джадрия, Багдад, Ирак). E-mail: Salamdulaimi82@gmail.com. Scopus Author ID 57220069401, https://orcid.org/0000-0003-2936-9373

Rahimi M. Yusop, PhD, доцент, Школа химии наук и пищевых технологий, Факультет науки и технологий, Университет Кебангсаан, Малайзия (43600 Банги, Селангор, Малайзия). E-mail: drmc@ukm.edu.my. Scopus Author ID 36994895800, https://orcid.org/0000-0002-8843-8677

*The text was submitted by the authors in English and
edited for English language and spelling by Dr. David Mossop*

Analytical methods in chemistry
and chemical technology

Аналитические методы в химии
и химической технологии

RESEARCH ARTICLE

Analysis of the ion mobility spectra of chloroacetophenone, tris(2-chloroethyl)amine, and methanethiol

Daria A. Aleksandrova[1, 3, ✉], **Tatiana B. Melamed**[1], **Elena P. Baberkina**[1],
Ekaterina S. Osinova[1], **Lidiya A. Luzenina**[1], **Artem A. Kaplin**[1], **Roman V. Yakushin**[1],
Aleksey E. Kovalenko[1], **Grigory V. Tsaplin**[1], **Yuri B. Sinkevich**[1], **Anatoliy A. Fenin**[1],
Julia R. Shaltaeva[2], **Vladimir V. Belyakov**[2], **Aleksey O. Shablya**[3], **Andrey G. Sazonov**[3]

[1] *Mendeleev University of Chemical Technology of Russia, Moscow, 125047 Russia*

[2] *National Research Nuclear University "MEPHI," Moscow, 115230 Russia*

[3] *Modus, Moscow, 117638 Russia*

✉ *Corresponding author, e-mail: dasha-25.2012@yandex.ru*

Abstract

Objectives. To determine the ion mobilities of chloroacetophenone, tris(2-chloroethyl)amine, and methanethiol; the structure of ions corresponding to characteristic signals; the detection limits of chloroacetophenone, tris(2-chloroethyl)amine, and methanethiol with the Kerber-T ion drift detector and the Segment automatic stationary gas detector.

Methods. Ion mobility spectrometry was used in order to determine the ion mobilities and detect analytes. The enthalpies of reactions of ion formation were calculated using the ORCA 4.1.1 software by means of the B3LYP density functional method with the 6-31G(d,p) basis set.

Results. The ion mobilities of chloroacetophenone, tris(2-chloroethyl)amine, and methanethiol were determined. A method for recording ion mobility spectra and their mathematical processing was developed. The dependencies of the change in ion mobility spectra on the analyte concentration were also studied. Possible mechanisms were proposed for the formation of the ion mobility spectra observed, in accordance with the ionization features of chloroacetophenone, tris(2-chloroethyl)amine, and methanethiol. The enthalpies of ion formation were calculated. The ionization schemes of the compounds were shown. The generalized results of experimental studies were presented, as were the features of compound identification taking into account the structure of the spectra, the concentrations of substances, and the detection conditions.

Conclusions. Characteristic signals of chloroacetophenone, tris(2-chloroethyl)amine, and methanethiol were identified. All studied hazardous substances can be detected with an ion mobility spectrometer at concentrations at the ppm level. The following detection limits of the substances were determined with the Segment gas detector: chloroacetophenone, 245 mg/m^3; tris(2-chloroethyl)amine, 0.01 mg/m^3; and methanethiol, 0.8 mg/m^3.

НАУЧНАЯ СТАТЬЯ

Анализ спектров ионной подвижности хлорацетофенона, трис(2-хлорэтил)амина и метилмеркаптана

Д.А. Александрова[1, 3, ✉], Т.Б. Меламед[1], Е.П. Баберкина[1], Е.С. Осинова[1], Л.А. Лузенина[1], А.А. Каплин[1], Р.В. Якушин[1], А.Е. Коваленко[1], Г.В. Цаплин[1], Ю.Б. Синькевич[1], А.А. Фенин[1], Ю.Р. Шалтаева[2], В.В. Беляков[2], А.О. Шабля[1,3], А.Г. Сазонов[3]

[1] *Российский химико-технологический университет им. Д.И. Менделеева, Москва, 125047 Россия*

[2] *Национальный исследовательский ядерный университет «МИФИ», Москва, 115230 Россия*

[3] *Модус, Москва, 117638 Россия*

✉ *Автор для переписки, e-mail: dasha-25.2012@yandex.ru*

Аннотация

Цели. Определить значения ионной подвижности хлорацетофенона, трис(2-хлорэтил)амин и метилмеркаптана; установить строение ионов, соответствующих характерным сигналам; определить предел обнаружения хлорацетофенона, метилмеркаптана и трис-(2-хлорэтил)амина на ионно-дрейфовом детекторе «Кербер-Т» и автоматическом стационарном газосигнализаторе «Сегмент».

Методы. Метод спектрометрии ионной подвижности использован для определения значений ионной подвижности и детектирования аналитов. Энтальпии реакций образующихся ионов расчитаны в программе ORCA 4.1.1 методом функционала плотности B3LYP с набором базисных функций 6-31G(d,p).

Результаты. Определены значения ионной подвижности хлорацетофенона, трис(2-хлорэтил)амина и метилмеркаптана. Разработана методика получения спектров ионной подвижности и их математической обработки. Изучены зависимости изменения спектров ионной подвижности от концентрации аналита. Предложены возможные механизмы формирования наблюдаемых спектров ионной подвижности в соответствии с особенностями ионизации хлорацетофенона, метилмеркаптана и трис(2-хлорэтил)амина. Рассчитаны энтальпии образования ионов. Показаны схемы ионизации соединений. Приведены обобщенные результаты экспериментальных исследований, особенности идентификации соединений с учетом структуры спектров, концентраций веществ и условий детектирования.

Выводы. Выявлены характеристические сигналы хлорацетофенона, трис(2-хлорэтил)амина и метилмеркаптана. Все исследованные вещества группы аварийно-химически опасных веществ могут быть детектированы спектрометром ионной подвижности при аналитически значимых концентрациях на уровне 10^{-2} мг/м^3. Определены пределы обнаружения исследуемых веществ на газосигнализаторе «Сегмент». Предел обнаружения хлорацетофенона – 245 мг/м^3, трис(2-хлорэтил)амина – 0.01 мг/м^3 и метилмеркаптана – 0.8 мг/м^3.

INTRODUCTION

Ion mobility devices currently use worldwide for the main purpose of detecting chemical warfare agents, drugs, and explosives [1, 2]. In addition, detectors based on ion mobility spectrometry have been successfully adapted for industrial, technological, and environmental studies, including food quality analysis and air composition monitoring [3–7].

The main advantage of devices based on ion mobility spectrometry, in comparison with those based on chromatography and mass spectrometry, is the speed of analysis. The average time to record a reliable profile of the ion mobility spectrum of the compound under study is from 3 to 10 s. The Kerber-T ion drift detector[1] (Kerber-T IDD) and the Segment automatic stationary gas detector[2] (Segment ASGD) (*Modus*, Russia) are portable, operate at atmospheric pressure, and do not incorporate large-sized systems for creating a vacuum.

This aim of this work is not to study the influence of interfering factors, including the presence of mechanical and other impurities in the air being analyzed. An important and practical matter is to optimize the design of the Segment ASGD enabling the use of the ion mobility spectrometer in a wide range of temperatures, including in winter at subzero temperatures. In order to remove dust and dirt particles, additional protection of the gas channel is provided, preventing air from blowing in with a coarse filter in the inlet sampling channel.

Currently, *Modus* is successfully working to achieve import substitution and develop devices for the rapid control of hazardous chemical substances, in order to prevent their use in terrorist activities. Also, increased requirements have recently been imposed on safety at industrial facilities, in the aims of monitoring air composition in the working area and in crowded places, thus requiring detection of a wider range of compounds.

The available literature describes the detection of a number of hazardous chemical substances. However, but the main attention of researchers is focused on organophosphorus compounds and mustard agents [8]. Expanding the database is the reason for carrying out this study.

All the objects under study are highly toxic and relatively available. Methanethiol is widely used in the organic synthesis of pesticides and herbicides and is used as an odorizing additive to natural gas. Tris-(2-chloroethyl)amine is a blister agent and is currently the only nitrogen mustard to retain its significance in chemical warfare. Chloroacetophenone is used in gas canisters as a riot control agent. Departments of the Ministry of Internal Affairs of the Russian Federation have at their disposal various types of aerosol sprays containing chloroacetophenone. These compounds need to be studied for the timely detection and elimination of the consequences of spraying these substances into the air and mixing them with water.

EXPERIMENTAL

The studies were carried out with the Kerber-T IDD and the Segment ASGD (*Modus*, Russia). Table 1 presents the specifications of the devices.

Kerber-T IDD is already widely used in the inspection equipment market. Segment ASGD is also intensively implemented by the Ministry of Internal Affairs, the Federal Security Service, and the Ministry of Defense of the Russian Federation, in order to detect hazardous chemical substances. Therefore, in order to expand the equipment database, comparative studies of the substances need to be performed on both devices.

The ion mobility spectra were recorded at atmospheric pressure with ambient air as a drift gas. The ability to record measurement results was provided by the device software. The result was a text file containing data on the target substances detected and drift time. These were used to construct an ion mobility spectrum.

For the purposes of this study, methanethiol with liquefied gas from a canister (*Merck*, Germany) and ethanethiol diluted in dry air from a cylinder (*GAZ-ANALITIK*, Russia) were used. Hydrogen sulfide was obtained by extracting aluminum sulfide from a freezer and decomposing it to hydrogen sulfide at a humidity of 20 to 55%. Tris(2-chloroethyl)amine was synthesized especially for the study. The purity of the reagent obtained was controlled by gas chromatography–mass spectrometry: a compound with a sample content of at least 99% was obtained. Chloroacetophenone, bromoacetophenone, and acetophenone (*Sigma-Aldrich*, USA) with a purity of at least 98% were also used in the study.

Samples for the preparation of solutions were weighed on an AND GR-120 scales (*A&D*, Japan) with a resolution of 0.0001 g.

A Lenpipet Light dispenser (*Thermo Scientific*, Russia) was used to prepare solutions and apply 1–10 μL of solutions of the required concentrations to a sampling cloth. The sampling cloth was made of a foil 11–15 μm thick, pre-annealed in the Kerber-T IDD furnace at 180°C.

---

[1]   Kerber-T portable ion drift detector. URL: http://www.analizator.ru/production/ims/kerber-t/. Accessed January 27, 2023.

[2]   Segment automatic stationary gas detector. URL: https://www.analizator.ru/production/ims/segment/. Accessed January 27, 2023.

Table 1. Specifications of the Kerber-T IDD and Segment ASGD

Characteristic	Kerber-T IDD	Segment ASGD
Detection range of low-volatile organic substances for 2,4,6-trinitrotoluene (TNT), g	From $1.0 \cdot 10^{-11}$ to $2.0 \cdot 10^{-7}$	–
Detection limit of low-volatile organic substances for TNT – for solid particles, g – for vapor, g/cm^3	No more than $1.0 \cdot 10^{-10}$ No more than $5.0 \cdot 10^{-13}$	–
Alarm threshold for controlled substances under normal climatic conditions, mg/m^3 – for sarin – for soman – for VX-type substance – for chlorine – for hydrogen sulfide	–	$1.0 \cdot 10^{-2} \pm 30\%$ $1.0 \cdot 10^{-2} \pm 30\%$ $3.0 \cdot 10^{-3} \pm 30\%$ $1.0 \pm 30\%$ $10.0 \pm 30\%$
Ionization method	Pulsed corona discharge	Pulsed corona discharge
Drift tube temperature, °C	100	100
Time of detection and identification for all detectable substances, s	No more than 5	No more than 5
Probability of false alarm, %	No more than 1	No more than 1
Detector cleaning time in the event of contamination with target substances within detection range, min	No more than 3	No more than 3

The enthalpies of reactions were calculated using the ORCA 4.1.1 software (*FAccTs GmbH*, Germany) by the B3LYP[3] density functional method with the 6-31G(d,p) basis set.

Specifics of ion mobility spectrometry

The ion mobility spectrometry method is based on the ionization of molecules of the substance being studied at atmospheric pressure. First, reactant ions are formed in the discharge chamber, the concentration of which significantly exceeds the concentration of the substances to be determined. When the target substances enter the device, the reactant ions transfer a charge to the molecules by the mechanism of chemical ionization at atmospheric pressure [9].

Formation of ions in the ionization region

The formation of reactant ions in negative polarity under the influence of a corona discharge occurs as a result of resonant electron capture by neutral molecules, e.g., oxygen molecules. Ion–molecular reactions with sample molecules to form product ions can take place in accordance with the following scheme:

$$M + O_2^-(H_2O)_n \rightarrow MO_2^-(H_2O)_{n-x} + xH_2O,$$

wherein M is the sample, $O_2^-(H_2O)_n$ is the reactant ion, $MO_2^-(H_2O)_{n-x}$ is the product ion, and xH_2O is water.

This product ion may live long enough for the signal of its spectrum to manifest itself in the ion mobility spectrum, or it may undergo further transformations leading, e.g., to the ion M^-.

---

[3]   B3LYP is the Becke–3-parameter–Lee–Yang–Parr exchange–correlation functional.

When colliding with reactant ions in positive polarity, molecules of the substance being studied form cluster ions. These are transformed into more stable hydrated cluster ions by the elimination of water molecules:

$$M^+ + H^+(H_2O)_n \rightarrow MH^+(H_2O)_n \rightarrow$$
$$\rightarrow MH^+(H_2O)_{n-x} + xH_2O,$$
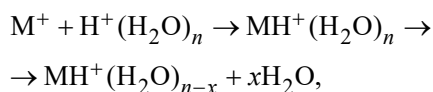
wherein M is the molecule of the substance being studied, $H^+(H_2O)_n$ is the reactant ion, $MH^+(H_2O)_n$ is the cluster ion, and $MH^+(H_2O)_{n-x}$ is the ion of the substance being studied.

The product ion formed in this process is called *protonated monomer*. The formation of a protonated dimer $M_2H^+(H_2O)_n$ and other molecular ions is possible. The number of water molecules in the cluster ranges from 1 to 3 depending on the nature of the compound [10, 11].

Ionized molecules of differing substances move in the drift chamber at different velocities depending on their charge, weight, and the effective cross-section of the formed ion. Molecular ions of differing compounds vary in drift time τ_d to the collector, enabling their nature to be determined. This time is proportional to the length L (cm) of the drift chamber, inversely proportional to the electric field gradient E, and calculated as:

$$\tau_d = \frac{1}{K} \cdot \frac{L}{E}, \tag{1}$$

wherein K is the ion mobility coefficient, $cm^2/(V·s)$.

The ion mobility depends on temperature and pressure. In order to compare ion mobility values obtained under different conditions, the K values are converted to normal conditions:

$$K_0 = \frac{KP}{760} \cdot \frac{273}{T}, \tag{2}$$

wherein T and P are the temperature (K) and pressure (mm·Hg), respectively, in the gas atmosphere in which the ions move; and K_0 is called the reduced mobility

(or reduced mobility coefficient). Reduced ion mobility is used in this work. The results are presented in the form of an ion mobility spectrum with the background spectrum subtracted.

Experimental procedure

In the course of work using Kerber-T IDD and Segment ASGD, a procedure for recording and determining the characteristic values of ion mobility was developed. A method for mathematical processing of the spectra was previously described in detail [12, 13].

Ion mobility spectra were recorded at atmospheric pressure with ambient air as a drift gas.

Tris(2-chloroethyl)amine was studied in various modifications: pure substance, hydrochloride, and a solution of the hydrochloride in water.

Using an Agilent microsyringe (*Agilent Technologies*, USA), 1, 2, 5, 8, and 12 µL of saturated vapor of pure tris(2-chloroethyl)amine were collected into 25-mL flasks.

Chloroacetophenone was detected by collecting saturated vapor and diluting it with ambient air. Using a two-component syringe, 2 to 10 mL of the saturated vapor of chloroacetophenone were collected into 35-mL flasks. The saturated vapor concentration in the gas phase was calculated using the ideal gas law:

$$pV = \frac{m}{M} \cdot RT, \tag{3}$$

wherein p is the saturated vapor pressure, V is the volume, m is the weight of the substance, M is the molecular weight, R is the universal gas constant, and T is room temperature in K.

Table 2 presents the concentrations of the analytes that were calculated using formula (3).

The sensitivity for the hydrochloride is lower than for the pure substance. Therefore, the hydrochloride was measured by heating the sampling cloth with

Table 2. Concentrations of tris(2-chloroethyl)amine in the gas phase

No.	Saturated vapor volume, µL	Flask volume, mL	Concentration, mg/m^3
1	1	25	0.005
2	2	25	0.01
3	5	25	0.025
4	8	25	0.04
5	12	25	0.06

the substance in the Kerber-T IDD. The analyte concentration C was calculated as:

$$C = \frac{C_{sv} \cdot V_{sv}}{V_f}, \quad (4)$$

wherein C_{sv} is the saturated vapor concentration, V_{sv} is the saturated vapor volume, and V_f is the flask volume.

Table 3 presents the calculated concentrations of analytes for the Segment ASGD.

Kerber-T IDD monitored the sorption of the substance with passive sampling from the flask. Therefore, the sample was injected from a syringe, the substance then passed through the gas channel under pressure, and the peak of the substance was detected. The concentration was calculated under the assumption that the sample was diluted with an inlet air flow at a rate of $F = 500$ mL/min by the formula (5):

$$C = \frac{C_{sv} \cdot V_{sv}}{F \cdot t}, \quad (5)$$

wherein C is the concentration, C_{sv} is the saturated vapor concentration, V_{sv} is the saturated vapor volume, F is the inlet flow rate of the device, and t is the sample injection time.

Table 4 presents the concentrations of analytes for the Kerber-T IDD, calculated by formula (5).

Methanethiol measurements were performed as follows. The saturated methanethiol vapor was collected from a gas cylinder in 50-mL flask 1. The saturated vapor concentration was calculated using the ideal gas law. A 1-mL sample of the saturated vapor was collected in 500-mL flask 2; thus, the saturated vapor was diluted 500 times. The vapor from flask 2 was used to obtain the final concentrations.

Then 5 and 10 μL of the saturated vapor were taken with an Agilent microsyringe, and 0.1, 0.25, 0.5, and 1 mL of the saturated vapor were collected in 25-mL flasks using an insulin syringe.

Table 5 presents the concentrations of analytes, calculated using formula (5).

Table 3. Chloroacetophenone concentrations measured with the Segment ASGD in the gas phase

No.	Saturated vapor volume, μL	Flask volume, mL	Concentration, mg/m³
1	4	35	485
2	5	35	600
3	6	35	725
4	8	35	970
5	10	35	1200

Table 4. Chloroacetophenone concentrations measured with the Kerber-T IDD in the gas phase

No.	Saturated vapor volume, μL	Sample injection time, s	Concentration, mg/m³
1	3	5	300
2	4	5	400
3	5	5	500

Table 5. Methanethiol concentrations in the gas phase

No.	Saturated vapor volume in flask 2, μL	Flask volume, mL	Concentration, mg/m³
1	5	25	0.8
2	10	25	1.6
3	100	25	16
4	250	25	40
5	500	25	80
6	1000	25	160

A glass flask containing an air mixture with a given concentration of the analyte was placed at the sampling channel of the ion mobility spectrometer for 5 s. The device automatically sampled the contents of the flask in the gas phase analysis mode.

Measurements were made after changing analyte concentration from 0.01 mg/m³ to the concentration corresponding to the saturated vapor pressure of the analyte at a temperature of 20–25°C. The work presents spectra in the optimal range of detection concentrations.

RESULTS AND DISCUSSION

Study of chloroacetophenone

A series of chloroacetophenone spectra was recorded with the Kerber-T IDD at various concentrations, then mathematically processed to give an approximate estimation of the relative numbers of ions (Fig. 1). In negative polarity, the amplitude of one main peak of 2.709 cm²/(V·s) increased with increasing concentration of the sample. In positive polarity, with increasing concentration, the amplitudes of all observed signals increase. However, the amplitude of the signal with a mobility of 1.475 cm²/(V·s) is more stable, possible indicating the cluster nature of the ion structure.

Figure 2 shows a series of spectra of chloroacetophenone that were recorded with Segment ASGD.

According to these procedures and measurement conditions, the lower detection limit of chloroacetophenone for the Kerber-T IDD is 300 mg/m³. For Segment ASGD it is 245 mg/m³. Several peaks can be used to identify both polarities simultaneously: 1.708 and 1.475 cm²/(V·s) with a deviation of 0.7% in positive polarity; and 2.650 cm²/(V·s) with a deviation of 2.5% in negative polarity.

The ion mobility spectra of chloroacetophenone, acetophenone, and bromoacetophenone recorded with the Kerber-T IDD were compared, in order to determine the structures of the ions (Fig. 3).

In negative polarity, one peak can be observed for each of the halogen-containing compounds. The mobilities of the peaks of chloroacetophenone and bromoacetophenone correspond to the chloride ion (2.650 cm²/(V·s)) and the bromide ion (2.485 cm²/(V·s)), respectively. In positive polarity, there are three peaks for acetophenone: at 1.706, 1.578, and 1.300 cm²/(V·s). These correspond in mobility to the peaks of chloro- and bromoacetophenone, indicating the same nature of protonation and, possibly, that the substances are ionized after the elimination of halogens. However, in the case of chloroacetophenone, two more peaks can be observed: at 1.776 and 1.478 cm²/(V·s), probably related to protonated chlorine derivatives of ions. For bromoacetophenone, a peak at 1.397 cm²/(V·s) is also detected, characterizing the protonated bromine derivative ion. The enthalpies of reactions of the resulting ions were calculated using the ORCA 4.1.1 program by means of the B3LYP

(a)

(b)
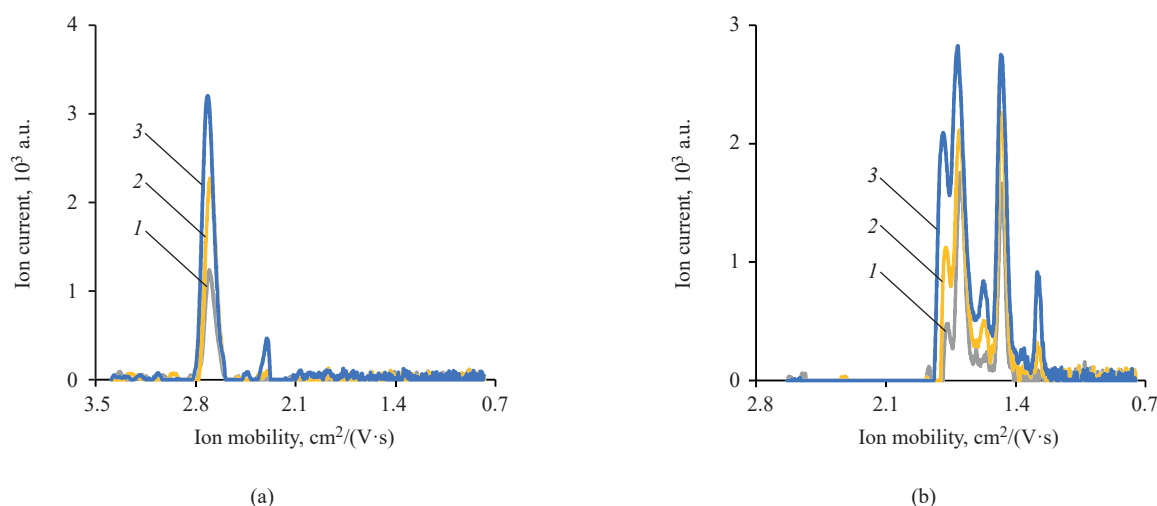
Fig. 1. Ion mobility spectra of chloroacetophenone recorded with Kerber-T IDD in
(a) negative and
(b) positive polarity
at concentrations of
(*1*) 300 mg/m³ (grey line),
(*2*) 400 mg/m³ (yellow line), and
(*3*) 500 mg/m³ (dark blue line)
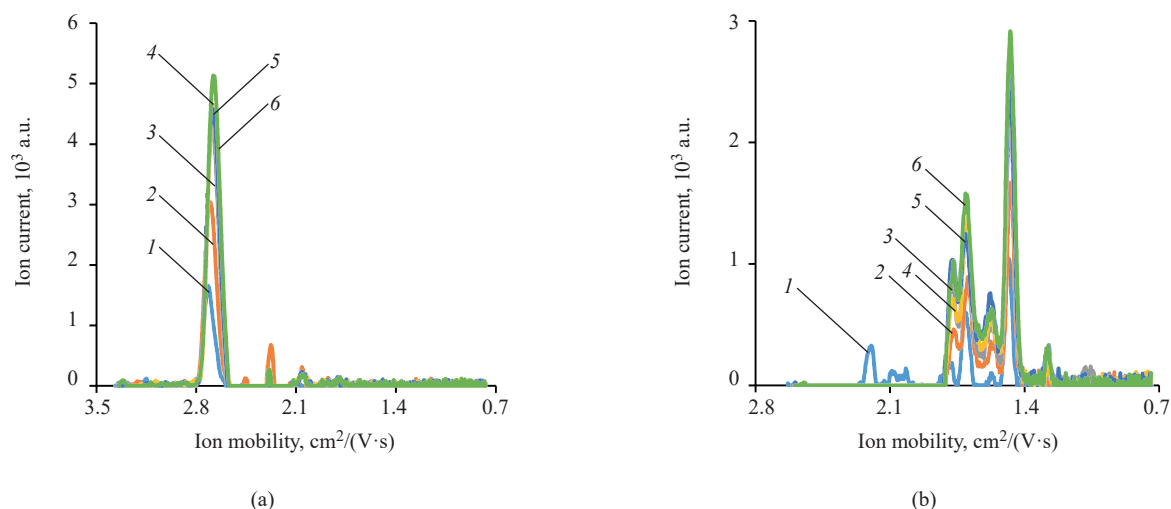
Fig. 2. Ion mobility spectra of chloroacetophenone recorded with the Segment ASGD in
(a) negative and
(b) positive polarity
at concentrations of
(*1*) 245 mg/m^3 (blue line),
(*2*) 485 mg/m^3 (orange line),
(*3*) 600 mg/m^3 (gray line),
(*4*) 725 mg/m^3 (yellow line),
(*5*) 970 mg/m^3 (dark blue line), and
(*6*) 1200 mg/m^3 (green line)

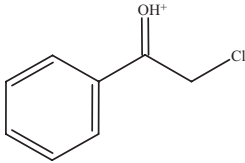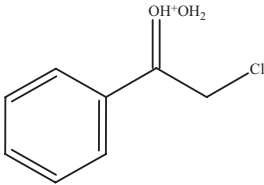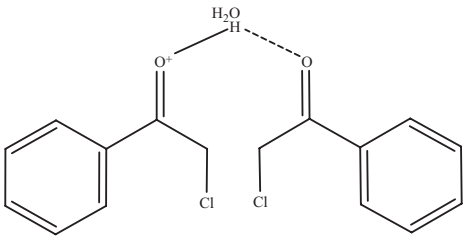density functional method with the 6-31G(d,p) basis set (Table 6).

The most energetically favorable is the formation of a monomer ion with the elimination of a water molecule. However, the formation of an ion with a water molecule is also possible. The dimer of chloroacetophenone is easily formed. Trimers have a chain structure. According to calculations, they are unstable and easily dissociate into a dimer and a monomer upon collision with any molecule [12, 13]. Thus, the presence of signals of monomer and dimer ions in the ion mobility spectrum is most likely.
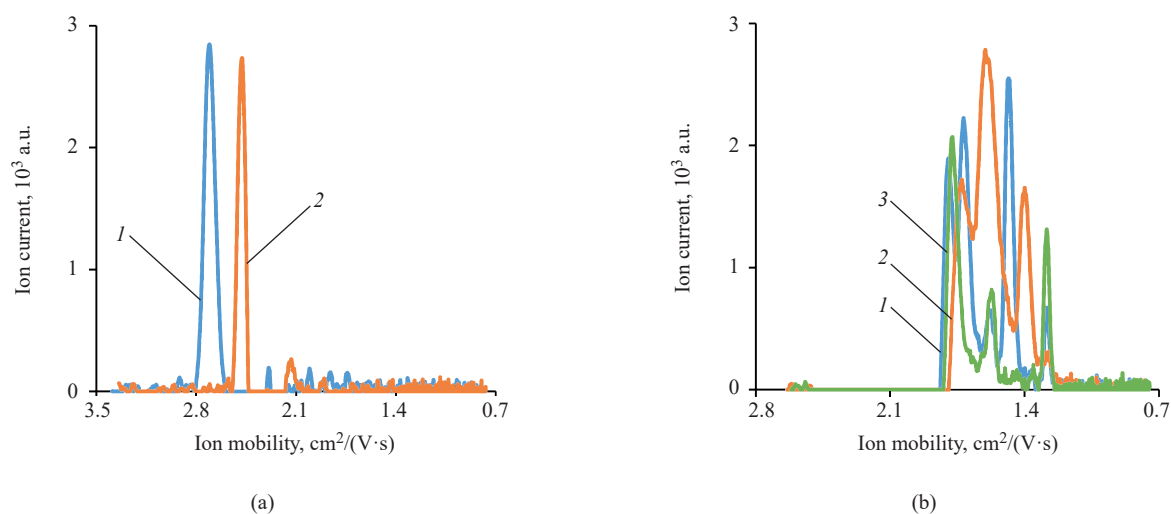
Fig. 3. Comparison of the ion mobility spectra of
(*1*) chloroacetophenone (blue line),
(*2*) bromoacetophenone (orange line), and
(*3*) acetophenone (green line) in (a) negative and (b) positive polarity

**Table 6.** Enthalpies of formation of chloroacetophenone ions

Structure of molecular ion	Enthalpy of formation, kJ/mol
	−148.9
	−85.2
	−88.3

Study of tris(2-chloroethyl)amine

Figure 4 shows the spectra of tris(2-chloroethyl)amine that were recorded with Kerber-T IDD.

In negative polarity, instability of signals of the chloride ion can be observed. In positive polarity, there is a pronounced characteristic signal at a mobility of 1.512 cm^2/(V·s) which is assigned to protonation at the nitrogen atom. As a result of the measurements, the optimal detection concentration was determined to be 0.04 mg/m^3.

(a)   (b)
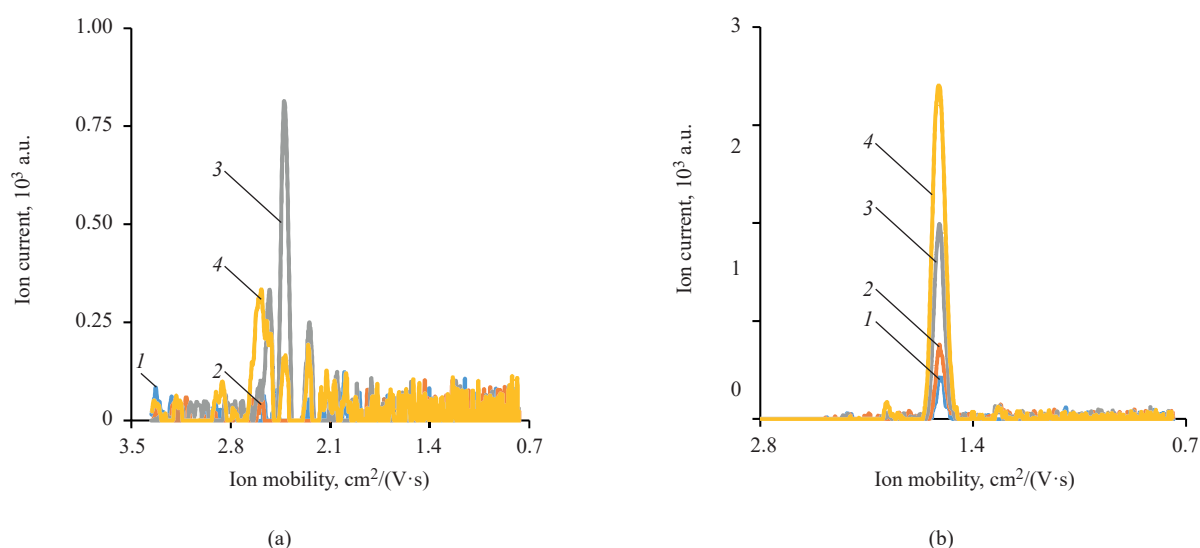
Fig. 4. Ion mobility spectra of tris(2-chloroethyl)amine recorded with Kerber-T IDD in
(a) negative and
(b) positive polarity at concentrations of
(*1*) 0.01 mg/m^3 (blue line),
(*2*) 0.025 mg/m^3 (orange line),
(*3*) 0.04 mg/m^3 (gray line), and
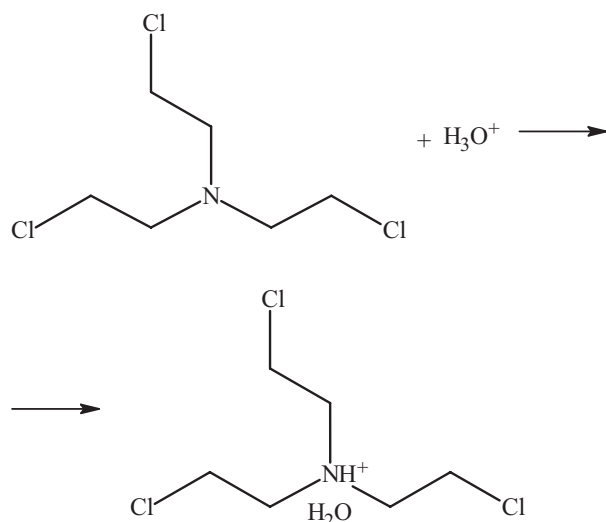(*4*) 0.06 mg/m^3 (yellow line)

(a)

(b)
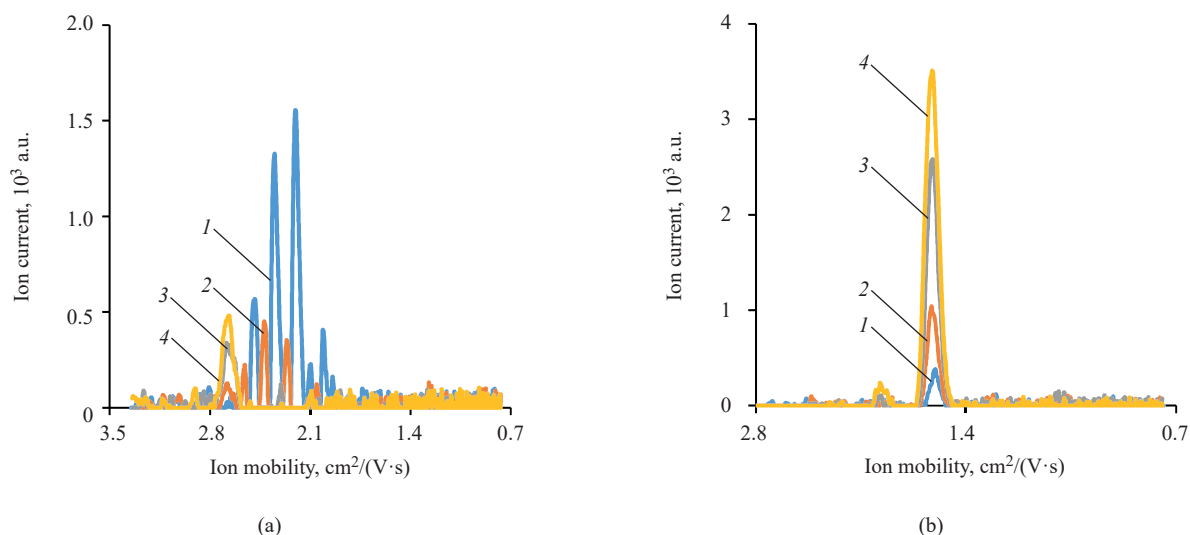
Fig. 5. Ion mobility spectra of tris(2-chloroethyl)amine recorded with the Segment ASGD in
(a) negative and
(b) positive polarity at concentrations of
(*1*) 0.01 mg/m^3 (blue line),
(*2*) 0.025 mg/m^3 (orange line),
(*3*) 0.04 mg/m^3 (gray line), and
(*4*) 0.06 mg/m^3 (yellow line)

Figure 5 shows a series of spectra of tris(2-chloroethyl) amine samples recorded with Segment ASGD.

In negative polarity, with increasing concentration, there is an increase in the signal at a mobility of 2.650 cm^2/(V·s), which can be attributed to the hydrogen chloride ion. Other chlorine signals and a deviation of the background peaks are also present, but are unstable. In positive polarity, there is a pronounced characteristic signal at a mobility of 1.512 cm^2/(V·s), which corresponds to the signal of tris(2-chloroethyl)amine obtained recorded with the Kerber-T IDD.

Ionization in positive polarity is assumed to be at the nitrogen atom by the following mechanism:

Ionization in negative polarity occurs at the chorine atom:
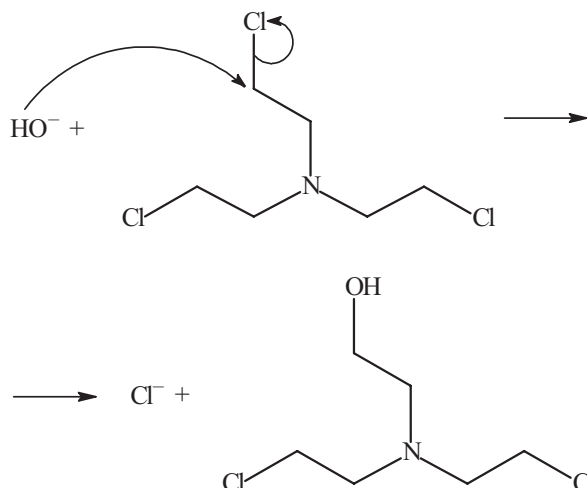
Formation of chlorine dimers and trimers is possible, and so is association with water molecules at the hydrogen atom.

Tris(2-chloroethyl)amine can be used by dissolving its hydrochloride in water and then introducing it into water supply systems. Therefore, aqueous hydrochloride solutions were studied using Kerber-T IDD (Fig. 6): 1 µL of the aqueous solution was applied to a sampling cloth. The cloth was left until water dried and then was placed in the device.

(a)

(b)
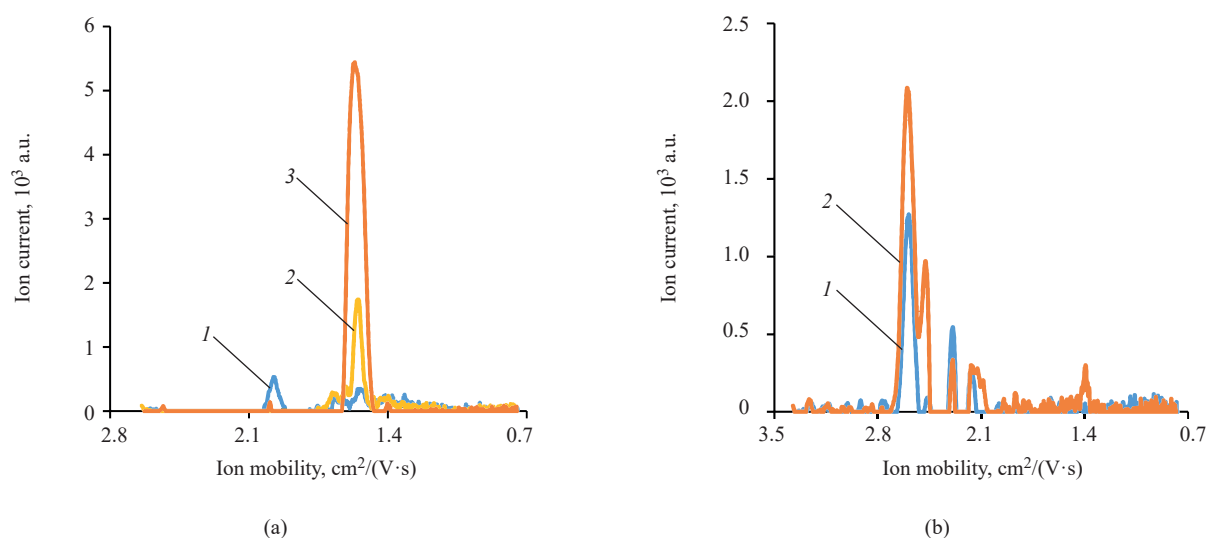
Fig. 6. Ion mobility spectra of tris(2-chloroethyl)amine recorded with the Kerber-T IDD in
(a) negative and
(b) positive polarity at weights of
(*1*) 2 ng (blue line),
(*2*) 70 ng (yelow line), and
(*3*) 200 ng (orange line)

The minimum detection limit on a sampling cloth is 2 ng. With an increase by an order of magnitude, the amplitude of the peaks reaches a maximum value and does not increase further. The minimum detection limit with an amplitude of 300 a.u. in the vapor above an aqueous solution is a solution concentration of 10^{-4} mol/L.

The ion mobilities in positive polarity for the substance, its hydrochloride, the vapor above an aqueous solution, and the sampling cloth are the same: 1.512 cm^2/(V·s).

Study of methanethiol

Figure 7 shows a series of methanethiol spectra recorded with Kerber-T IDD. In negative polarity, there is an increase in the amplitudes of two main peaks at

(a)

(b)
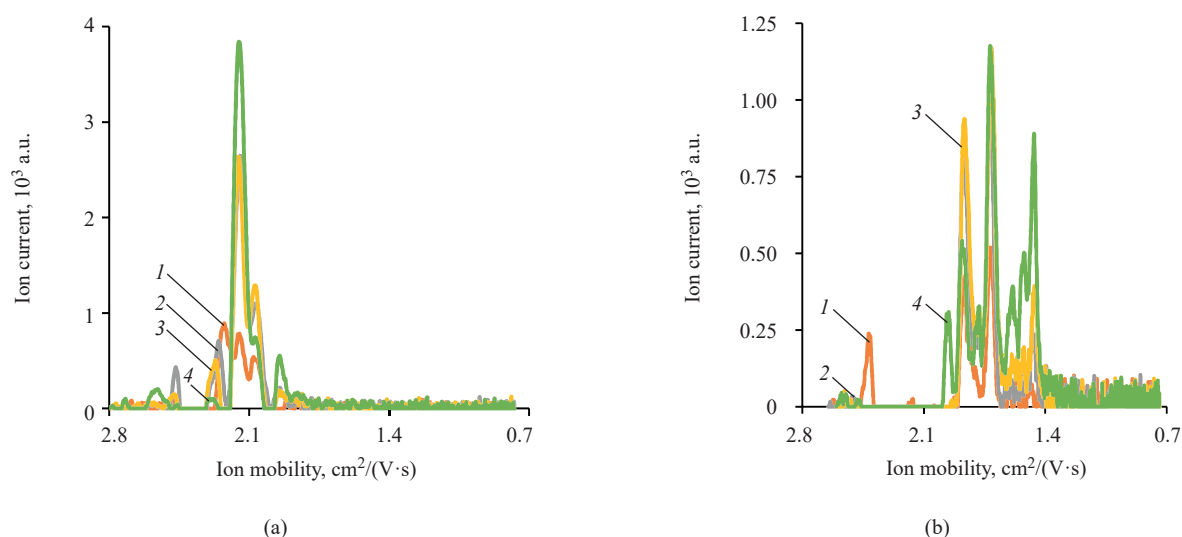
Fig. 7. Ion mobility spectra of methanethiol recorded with Kerber-T IDD in
(a) negative and
(b) positive polarity at concentrations of
(*1*) 1.6 mg/m^3 (orange line),
(*2*) 16 mg/m^3 (gray line),
(*3*) 40 mg/m^3 (yellow line), and
(*4*) 160 mg/m^3 (green line)

mobilities of 2.175 and 2.075 $cm^2/(V·s)$ with an increase in the sample concentration. In positive polarity, up to a concentration of 40 mg/m^3, the signal at a mobility of 1.869 $cm^2/(V·s)$ dominates. With an increase in concentration, signals at mobilities of 1.715 and 1.470 $cm^2/(V·s)$ begin to dominate.

The lower detection limit of methanethiol using Kerber-T IDD is 1.6 mg/m^3. The signal at a mobility of 2.243 $cm^2/(V·s)$ is insufficiently resolved. It merges with the peak at 2.175 $cm^2/(V·s)$ to form a single peak. There is also a flow from the third background peak through 2.243 $cm^2/(V·s)$ to the peak at 2.175 $cm^2/(V·s)$. The complex dynamics of the spectrum makes it difficult to determine methanethiol only in negative polarity. Several peaks for identification in both polarities can be reasonably used simultaneously.

Figure 8 shows a series of methanethiol spectra recorded with Segment ASGD.

The measurements of methanethiol showed good convergence of signals in terms of mobility and peak amplitude. The ion mobility signal value of 2.150 $cm^2/(V·s)$ with a deviation of 0.7% in negative polarity can be used, as well as signals at mobilities of 1.882 and 1.721 $cm^2/(V·s)$ with a deviation of 0.7% in positive polarity. The signals at a mobility of 2.075 $cm^2/(V·s)$ in negative polarity and 1.470 $cm^2/(V·s)$ in positive polarity have small amplitudes, and therefore, they can be considered as additional analytical peaks.

The ion mobility spectra of hydrogen sulfide, methanethiol, and ethanethiol were compared to determine the structures of ions (Fig. 9).

In negative polarity, a separate peak at a mobility of 2.900 $cm^2/(V·s)$ can be observed in the region of light ions, in which the formation of HS^- is most likely. There are also two converging peaks of methanethiol and hydrogen sulfide at mobilities of 2.243 and 2.150 $cm^2/(V·s)$, as well as a separate peak of ethanethiol at a mobility of 2.020 $cm^2/(V·s)$. The signal at a mobility of 2.243 $cm^2/(V·s)$ can be due to the formation of an H–S–S– particle under the influence of a corona discharge.

Since the air in the cylinder is dry and the background of the room is more humid, the connection of the cylinder with the ethanethiol–air mixture to the device gives rise to a signal at a mobility of 2.030 $cm^2/(V·s)$. Therefore, the first signal in positive polarity in the ethanethiol spectrum is not characteristic. The spectra of methanethiol and ethanethiol in positive polarity have a peak with at a mobility of 1.882 $cm^2/(V·s)$, corresponding to hydrogen sulfide. In positive polarity, there are a number of peaks with approximately the same period of ion mobility changes. This forms the basis for the peaks to correspond to the monomer and dimer structure of the methanethiol and ethanethiol ions.

(a)   (b)
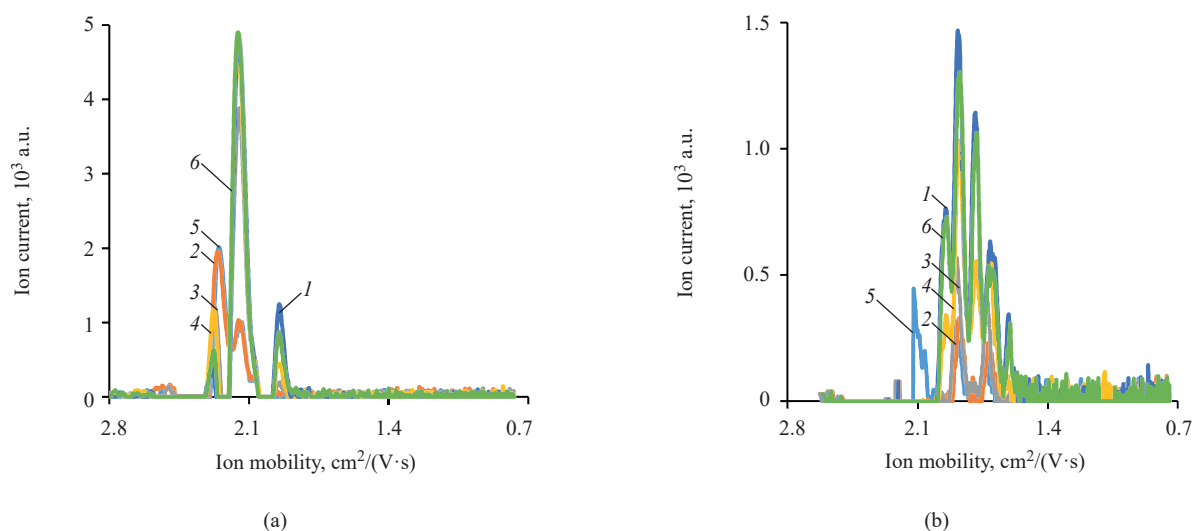
Fig. 8. Ion mobility spectra of methanethiol recorded with the Segment ASGD in
(a) negative and
(b) positive polarity at concentrations of
(*1*) 0.8 mg/m^3 (dark blue line),
(*2*) 1.6 mg/m^3 (orange line),
(*3*) 16 mg/m^3 (gray line),
(*4*) 40 mg/m^3 (yellow line),
(*5*) 80 mg/m^3 (blue line), and
(*6*) 160 mg/m^3 (green line)
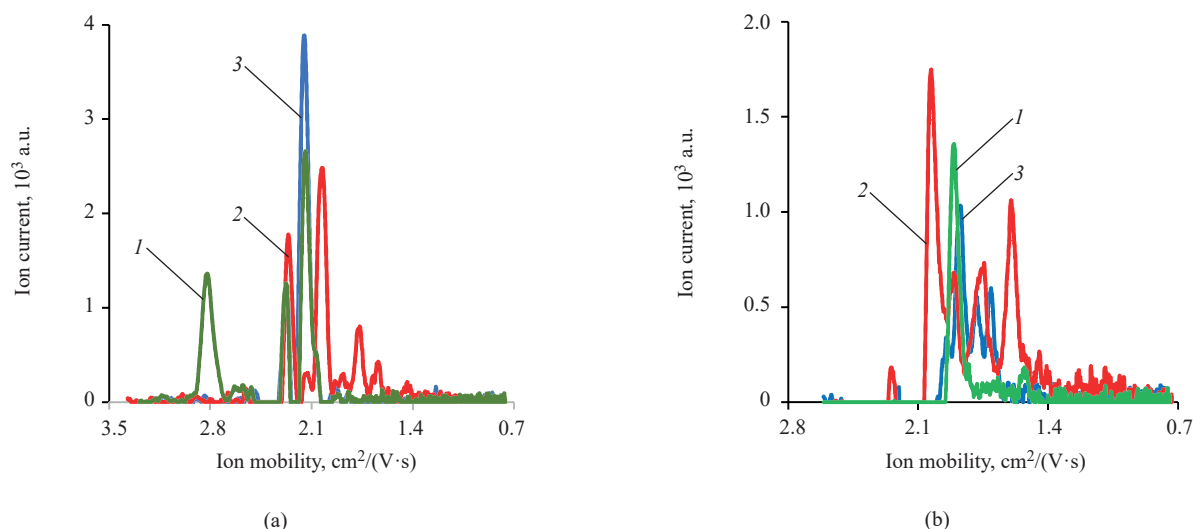
Fig. 9. Comparison of the ion mobility spectra of
(*1*) hydrogen sulfide (green line),
(*2*) ethanethiol (red line), and
(*3*) methanethiol (dark blue line) recorded with the Segment ASGD in
(a) negative and
(b) positive polarity

CONCLUSIONS

In this study, the ion mobility spectra of chloroacetophenone, methanethiol, and tris(2-chloroethyl)-amine were recorded at various vapor concentrations in the gas phase. It was found that the ion mobility values determined by either Kerber-T IDD or Segment ASGD for each of the studied compounds are respectively the same, enabling both of these devices to be used identically for air control. The sensitivity of the Segment ASGD is higher, since the detection limit of substances is lower. All the hazardous chemical substances studied can be detected by ion mobility spectrometers at analytically significant concentrations at the ppm level. Recommendations were given for the use of signals in the Kerber-T IDD and Segment ASGD substance database. Ion mobility spectra and the determination of the ion structure were studied for the first time.

For chloroacetophenone, the ion mobility signal values of 2.650 cm^2/(V·s) with a deviation of 2.5% in negative polarity can be used, as well as signal values at mobilities of 1.706 and 1.478 cm^2/(V·s) with a deviation of 0.7% in positive polarity.

For tris(2-chloroethyl)amine, the ion mobility values can be set in positive polarity at 1.512 cm^2/(V·s) with a deviation of 0.7% and at 2.650 cm^2/(V·s) in negative polarity with a deviation of at least 2.5%. This is because the signal in this region of the spectrum strongly depends on external factors: temperature, humidity, and atmospheric pressure.

For methanethiol, the most characteristic signals are the ion mobility values of 2.150 cm^2/(V·s) with a deviation of 0.7% in negative polarity, and signals at mobilities of 1.882 and 1.721 cm^2/(V·s) with a deviation of 0.7% in positive polarity.

The signals obtained for the compounds allow detection to be set for several peaks simultaneously which can serve as a good filter for false positives.

This work may have practical significance in preventing terrorist attacks, monitoring the air in working areas at production sites, and averting other threats to human life and health. The introduction of new data on ion mobility values of the above substances into the Kerber-T IDD and the Segment ASGD of ion mobility spectrometers is favorable to the replacement of imported analogues of air monitoring devices.

Authors' contributions

D.A. Aleksandrova—methodology development, conducting experiments, analysis of literary sources, writing and editing the text of the article.

T.B. Melamed—methodology development, conducting experiments, processing experimental data, writing and editing the text of the article.

E.P. Baberkina—developing the scientific work concept, methodology development, writing and editing the text of the article.

E.S. Osinova—analysis of literary sources, methodology development.

L.A. Luzenina—conducting experiments, analysis of literary sources.

A.A. Kaplin—conducting experiments.

R.V. Yakushin—offering consultations on methodology and research.

A.E. Kovalenko—offering consultations on the results practical application and research.

G.V. Tsaplin—offering consultations on methodology, properties of organic substances, and organic synthesis.

Yu.B. Sinkevich—offering consultations on methodology, properties of organic substances, and organic synthesis.

A.A. Fenin—offering consultations on methodology and research, calculation of enthalpies of reactions.

Ju.R. Shaltaeva—offering consultations on methodology and research.

V.V. Belyakov—offering consultations on methodology and research.

A.O. Shablya—determination of research objects, provision of equipment, and consultation on the instrument base.

A.G. Sazonov—determination of research objects, provision of equipment, and consultation on the instrument base.

The authors declare no conflicts of interest.

REFERENCES

1. Mäkinen M.A., Anttalainen O.A., Sillanpää M.E. Ion mobility spectrometry and its applications in detection of chemical warfare agents. *Anal. Chem.* 2010;82(23):9594–9600. https://doi.org/10.1021/ac100931n

2. Yamaguchi S., Asada R., Kishi Sh., Sekioka R., Kitagawa N., Tokita K., Yamamoto S., Seto Y. Detection performance of a portable ion mobility spectrometer with [63]Ni radioactive ionization for chemical warfare agents. *Forensic Toxicol*. 2010;28(2):84–95. https://doi.org/10.1007/s11419-010-0092-z

3. Hernandez-Mesa M., Ropartz D., Garcia-Campana A.M., Rogniaux H., Dervilly-Pinel G., Le Bizec B. Ion mobility spectrometry in food analysis: Principles, current applications and future trends. *Molecules*. 2019;24(15):2706. https://doi.org/10.3390/molecules24152706

4. Jafari M.T., Khayamian T., Shaer V., Zarei N. Determination of veterinary drug residues in chicken meat using corona discharge ion mobility spectrometry. *Anal. Chim. Acta.* 2007;581(1):147–153. https://doi.org/10.1016/j.aca.2006.08.005

5. Hashemian Z., Mardihallaj A., Khayamian T. Analysis of biogenic amines using corona discharge ion mobility spectrometry. *Talanta.* 2010;81(3):1081–1087. https://doi.org/10.1016/j.talanta.2010.02.001

6. Allers M., Schaefer Ch., Ahrens A., Schlottmann F., Hitzemann M., Kobelt T., Zimmermann S., Hetzer R. Detection of volatile toxic industrial chemicals with classical ion mobility spectrometry and high-kinetic energy ion mobility spectrometry. *Anal. Chem.* 2022;94(2):1211−1220. https://doi.org/10.1021/acs.analchem.1c04397

7. Smolin Yu.M., Kobtsev B.N., Novoselov N.P. Ion mobility spectrometry technique for chemical environmental contamination detection. *Vestnik TSTU = Transactions TSTU.* 2009;15(3):620–628 (in Russ.).

8. Krylova N., Krylov E., Eiceman G.A., Stone J.A. Effect of moisture on the field dependency of mobility for gas-phase ions of organophosphorus compounds at atmospheric pressure with field asymmetric ion mobility spectrometry. *J. Phys. Chem. A*. 2003;107(19):3648–3654. https://doi.org/10.1021/jp0221136

9. Eiceman G.A., Kapras Z., Hill H.H. *Ion Mobility Spectrometry*. 3rd ed. Boca Raton: CRC Press; 2014. 444 p.

10. Borsdorf H., Eiceman G.A. Ion mobility spectrometry: Principles and applications. *Appl. Spectroscopy Rev.* 2006;41(4):323–375. https://doi.org/10.1080/05704920600663469

СПИСОК ЛИТЕРАТУРЫ

1. Mäkinen M.A., Anttalainen O.A., Sillanpää M.E. Ion mobility spectrometry and its applications in detection of chemical warfare agents. *Anal. Chem.* 2010;82(23):9594–9600. https://doi.org/10.1021/ac100931n

2. Yamaguchi S., Asada R., Kishi Sh., Sekioka R., Kitagawa N., Tokita K., Yamamoto S., Seto Y. Detection performance of a portable ion mobility spectrometer with [63]Ni radioactive ionization for chemical warfare agents. *Forensic Toxicol*. 2010;28(2):84–95. https://doi.org/10.1007/s11419-010-0092-z

3. Hernandez-Mesa M., Ropartz D., Garcia-Campana A.M., Rogniaux H., Dervilly-Pinel G., Le Bizec B. Ion mobility spectrometry in food analysis: Principles, current applications and future trends. *Molecules*. 2019;24(15):2706. https://doi.org/10.3390/molecules24152706

4. Jafari M.T., Khayamian T., Shaer V., Zarei N. Determination of veterinary drug residues in chicken meat using corona discharge ion mobility spectrometry. *Anal. Chim. Acta.* 2007;581(1):147–153. https://doi.org/10.1016/j.aca.2006.08.005

5. Hashemian Z., Mardihallaj A., Khayamian T. Analysis of biogenic amines using corona discharge ion mobility spectrometry. *Talanta.* 2010;81(3):1081–1087. https://doi.org/10.1016/j.talanta.2010.02.001

6. Allers M., Schaefer Ch., Ahrens A., Schlottmann F., Hitzemann M., Kobelt T., Zimmermann S., Hetzer R. Detection of volatile toxic industrial chemicals with classical ion mobility spectrometry and high-kinetic energy ion mobility spectrometry. *Anal. Chem*. 2022;94(2):1211−1220. https://doi.org/10.1021/acs.analchem.1c04397

7. Смолин Ю.М., Кобцев Б.Н., Новоселов Н.П. Метод спектрометрии ионной подвижности для обнаружения химических загрязнений окружающей среды. *Вестник ТГТУ.* 2009;15(3):620–628.

8. Krylova N., Krylov E., Eiceman G.A., Stone J.A. Effect of moisture on the field dependency of mobility for gas-phase ions of organophosphorus compounds at atmospheric pressure with field asymmetric ion mobility spectrometry. *J. Phys. Chem. A*. 2003;107(19):3648–3654. https://doi.org/10.1021/jp0221136

9. Eiceman G.A., Kapras Z., Hill H.H. *Ion Mobility Spectrometry*. 3rd ed. Boca Raton: CRC Press; 2014. 444 p.

10. Borsdorf H., Eiceman G.A. Ion mobility spectrometry: Principles and applications. *Appl. Spectroscopy Rev.* 2006;41(4):323–375. https://doi.org/10.1080/05704920600663469

11. Marquez-Sillero I., Aguilera-Herrador E., Cardenas S., Valcarcel M. Ion-mobility spectrometry for environmental analysis. *TrAC Trends in Analytical Chemistry*. 2011;30(5): 677–690. https://doi.org/10.1016/j.trac.2010.12.007

12. Aleksandrova D.A., Melamed T.B., Baberkina E.P. *et al.* Ion Mobility Spectrometry of Imidazole and Possibilities of Its Determination. *J. Anal. Chem.* 2021;76(11):1282–1289. https://doi.org/10.1134/S1061934821110022
[Original Russian Text: Aleksandrova D.A., Melamed T.B., Baberkina E.P., Kovalenko A.E., Kuznetsov Vl. Vit., Kuznetsov Vit. Vl., Fenin A.A., Shaltaeva Yu.R., Belyakov V.V. Ion Mobility Spectrometry of Imidazole and Possibilities of Its Determination. *Zhurnal Analiticheskoi Khimii.* 2021;76(11):989–996 (in Russ.). https://doi.org/10.31857/S0044450221110025]

13. Aleksandrova D.A., Melamed T.B., Baberkina E.P., Fenin A.A., Osinova E.S., Kovalenko A.E., Yakushin R.V., Shaltaeva Yu.R., Belyakov V.V., Zykova D.I. Ion mobility spectrometry of *N*-methylimidazole and possibilities of its determination. *Tonk. Khim. Technol.* = *Fine Chem. Technol.* 2021;16(6):512–525. https://doi.org/10.32362/2410-6593-2021-16-6-512-525

11. Marquez-Sillero I., Aguilera-Herrador E., Cardenas S., Valcarcel M. Ion-mobility spectrometry for environmental analysis. *TrAC Trends in Analytical Chemistry*. 2011;30(5): 677–690. https://doi.org/10.1016/j.trac.2010.12.007

12. Александрова Д.А., Меламед Т.Б., Баберкина Е.П., Коваленко А.Е., Кузнецов Вл. Вит., Кузнецов Вит. Вл., Фенин А.А., Шалтаева Ю.Р., Беляков В.В. Спектрометрия ионной подвижности имидазола и возможности его определения. *Журн. аналит. химии.* 2021;76(11):989–996. https://doi.org/10.31857/S0044450221110025

13. Александрова Д.А., Меламед Т.Б., Баберкина Е.П., Фенин А.А., Осинова Е.С., Коваленко А.Е., Якушин Р.В., Шалтаева Ю.Р., Беляков В.В., Зыкова Д.И. Спектрометрия ионной подвижности *N*-метилимидазола и возможности его определения. *Тонкие Химические Технологии.* 2021;16(6):512–525. https://doi.org/10.32362/2410-6593-2021-16-6-512-525

About the authors

Daria A. Aleksandrova, Postgraduate Student, Department of Expertise in Doping and Drug Control, Mendeleev University of Chemical Technology of Russia (9, Miusskaya pl., Moscow, 1125047, Russia); Chemical Engineer, Modus (56-2, Varshavskoe sh., Moscow, 117638, Russia). E-mail: dasha-25.2012@yandex.ru. Scopus Author ID 57208706352, RSCI SPIN-code 7704-8764, https://orcid.org/0000-0001-8389-3964

Tatiana B. Melamed, Master Student, Department of Expertise in Doping and Drug Control, Mendeleev University of Chemical Technology of Russia (9, Miusskaya pl., Moscow, 1125047, Russia). E-mail: melamed.tanya@gmail.com. RSCI SPIN-code 8891-1910, https://orcid.org/0000-0002-6457-2417

Elena P. Baberkina, Cand. Sci. (Chem.), Associate Professor, Department of Expertise in Doping and Drug Control, Mendeleev University of Chemical Technology of Russia (9, Miusskaya pl., Moscow, 1125047, Russia). E-mail: bettycka@mail.ru. Scopus Author ID 56636782900, RSCI SPIN-code 3168-3801, https://orcid.org/0000-0002-9226-3478

Ekaterina S. Osinova, Postgraduate Student, Department of Expertise in Doping and Drug Control, Mendeleev University of Chemical Technology of Russia (9, Miusskaya pl., Moscow, 1125047, Russia). E-mail: osinova_kat@mail.ru. RSCI SPIN-code 9063-6384, https://orcid.org/0000-0003-4088-6822

Lidiya A. Luzenina, Student, Mendeleev University of Chemical Technology of Russia (9, Miusskaya pl., Moscow, 1125047, Russia). E-mail: luzenina.l.a@muctr.ru. https://orcid.org/0000-0002-0103-2771

Artem A. Kaplin, Student, Mendeleev University of Chemical Technology of Russia (9, Miusskaya pl., Moscow, 1125047, Russia). E-mail: kaplin.artem@ya.ru. https://orcid.org/0000-0003-1928-5651

Roman V. Yakushin, Cand. Sci. (Eng.), Associate Professor, Department of Organic Chemistry, Dean of the Faculty of Chemical and Pharmaceutical Technologies and Biomedical Products, Mendeleev University of Chemical Technology of Russia (9, Miusskaya pl., Moscow, 1125047, Russia). E-mail: yakushin@muctr.ru. Scopus Author ID 56974245100, ResearcherID A-5116-2014, RSCI SPIN-code 7201-2016, https://orcid.org/0000-0003-2923-5471

Aleksey E. Kovalenko, Cand. Sci. (Eng.), Associate Professor, Department of Expertise in Doping and Drug Control, Mendeleev University of Chemical Technology of Russia (9, Miusskaya pl., Moscow, 1125047, Russia). E-mail: aekov@muctr.ru. Scopus Author ID 57208702823, RSCI SPIN-code 9105-5046, https://orcid.org/0000-0002-8412-0311

Grigory V. Tsaplin, Assistant, Department of Chemistry and Technology of Organic Synthesis, Mendeleev University of Chemical Technology of Russia (9, Miusskaya pl., Moscow, 1125047, Russia). E-mail: tsaplingv@muctr.ru. Scopus Author ID 57202814506, RSCI SPIN-code 2276-9939, https://orcid.org/0000-0001-9469-2682

Yuri B. Sinkevich, Training Master, Department of Chemistry and Technology of Organic Synthesis, Mendeleev University of Chemical Technology of Russia (9, Miusskaya pl., Moscow, 1125047, Russia). E-mail: sinkevich_y@mail.ru. Scopus Author ID 16029689600, https://orcid.org/0000-0001-5987-7673

Anatoliy A. Fenin, Senior Lecturer, Department of High Energy Chemistry and Radioecology, Mendeleev University of Chemical Technology of Russia (9, Miusskaya pl., Moscow, 1125047, Russia). E-mail: fenin@muctr.ru. Scopus Author ID 16202751400, ResearcherID T-9318-2017, https://orcid.org/0000-0002-5193-3607

Julia R. Shaltaeva, Senior Lecturer, Division of Nanotechnologies in Electronics, Spintronics and Photonics, Office of Academic Programs (414), Institute of Nanoengineering in Electronics, Spintronics and Photonics, National Research Nuclear University MEPhI (31, Kashirskoe sh., Moscow, 115409, Russia). E-mail: YRShaltayeva@mephi.ru. Scopus Author ID 56018762000, RSCI SPIN-code 8644-7631, https://orcid.org/0000-0002-9856-6031

Vladimir V. Belyakov, Cand. Sci. (Eng.), Associate Professor, Division of Nanotechnologies in Electronics, Spintronics and Photonics, Office of Academic Programs (414), Institute of Nanoengineering in Electronics, Spintronics and Photonics, National Research Nuclear University MEPhI (31, Kashirskoe sh., Moscow, 115409, Russia). E-mail: VVBelyakov@mephi.ru. Scopus Author ID 7103252626, RSCI SPIN-code 5436-8927, https://orcid.org/0000-0002-0236-1243

Aleksey O. Shablya, Deputy General Director, Modus (56-2, Varshavskoe sh., Moscow, 117638, Russia). E-mail: a.shablya@analizator.ru. https://orcid.org/0000-0002-4605-945X

Andrey G. Sazonov, General Director, Modus (56-2, Varshavskoe sh., Moscow, 117638, Russia). E-mail: kerber@analizator.ru. https://orcid.org/0009-0008-1540-6739

Об авторах

Александрова Дарья Алексеевна, аспирант, кафедра экспертизы в допинг- и наркоконтроле, ФГБОУ ВО «Российский химико-технологический университет им. Д.И. Менделеева» (125047, Россия, Москва, Миусская площадь, д. 9); инженер-химик, ООО «Модус» (117638, Россия, Москва, Варшавское шоссе, д. 56, стр. 2). E-mail: dasha-25.2012@yandex.ru. Scopus Author ID 57208706352, SPIN-код РИНЦ 7704-8764, https://orcid.org/0000-0001-8389-3964

Меламед Татьяна Борисовна, магистрант, кафедра экспертизы в допинг- и наркоконтроле, ФГБОУ ВО «Российский химико-технологический университет им. Д.И. Менделеева» (125047, Россия, Москва, Миусская площадь, д. 9). E-mail: melamed.tanya@gmail.com. SPIN-код РИНЦ 8891-1910, https://orcid.org/0000-0002-6457-2417

Баберкина Елена Петровна, к.х.н., доцент, кафедра экспертизы в допинг- и наркоконтроле, ФГБОУ ВО «Российский химико-технологический университет им. Д.И. Менделеева» (125047, Россия, Москва, Миусская площадь, д. 9). E-mail: bettycka@mail.ru. Scopus Author ID 56636782900, SPIN-код РИНЦ 3168-3801, https://orcid.org/0000-0002-9226-3478

Осинова Екатерина Сергеевна, аспирант, кафедра экспертизы в допинг- и наркоконтроле, ФГБОУ ВО «Российский химико-технологический университет им. Д.И. Менделеева» (125047, Россия, Москва, Миусская площадь, д. 9). E-mail: osinova_kat@mail.ru. SPIN-код РИНЦ 9063-6384, https://orcid.org/0000-0003-4088-6822

Лузенина Лидия Андреевна, студент, ФГБОУ ВО «Российский химико-технологический университет им. Д.И. Менделеева» (125047, Россия, Москва, Миусская площадь, д. 9). E-mail: luzenina.l.a@muctr.ru. https://orcid.org/0000-0002-0103-2771

Каплин Артем Александрович, студент, ФГБОУ ВО «Российский химико-технологический университет им. Д.И. Менделеева» (125047, Россия, Москва, Миусская площадь, д. 9). E-mail: kaplin.artem@ya.ru. https://orcid.org/0000-0003-1928-5651

Якушин Роман Владимирович, к.т.н., доцент, кафедра органической химии, декан факультета химико-фармацевтических технологий и биомедицинских препаратов, ФГБОУ ВО «Российский химико-технологический университет им. Д.И. Менделеева» (125047, Россия, Москва, Миусская площадь, д. 9). E-mail: yakushin@muctr.ru. Scopus Author ID56974245100, ResearcherID A-5116-2014, SPIN-код РИНЦ 7201-2016, https://orcid.org/0000-0003-2923-5471

Коваленко Алексей Евгеньевич, к.т.н., доцент, кафедра экспертизы в допинг- и наркоконтроле, ФГБОУ ВО «Российский химико-технологический университет им. Д.И. Менделеева» (125047, Россия, Москва, Миусская площадь, д. 9). E-mail: aekov@muctr.ru. Scopus Author ID 57208702823, SPIN-код РИНЦ 9105-5046, https://orcid.org/0000-0002-8412-0311

Цаплин Григорий Валерьевич, ассистент, кафедра химии и технологии органического синтеза, ФГБОУ ВО «Российский химико-технологический университет им. Д.И. Менделеева» (125047, Россия, Москва, Миусская площадь, д. 9). E-mail: tsaplingv@muctr.ru. Scopus Author ID 57202814506, SPIN-код РИНЦ 2276-9939, https://orcid.org/0000-0001-9469-2682

Синькевич Юрий Борисович, учебный мастер, кафедра химии и технологии органического синтеза, ФГБОУ ВО «Российский химико-технологический университет им. Д.И. Менделеева» (125047, Россия, Москва, Миусская площадь, д. 9). E-mail: sinkevich_y@mail.ru. Scopus Author ID 16029689600, https://orcid.org/0000-0001-5987-7673

Фенин Анатолий Александрович, старший преподаватель, кафедра химии высоких энергий и радиоэкологии, ФГБОУ ВО «Российский химико-технологический университет им. Д.И. Менделеева» (125047, Россия, Москва, Миусская площадь, д. 9). E-mail: fenin@muctr.ru. Scopus Author ID 16202751400, ResearcherID T-9318-2017, https://orcid.org/0000-0002-5193-3607

Шалтаева Юлия Ринатовна, старший преподаватель, отделение нанотехнологий в электронике, спинтронике и фотонике офиса образовательных программ (414), Институт нанотехнологий в электронике, спинтронике и фотонике, ФГАОУ ВО Национальный исследовательский ядерный университет «МИФИ» (115409, Россия, Москва, Каширское ш., д. 31). E-mail: YRShaltayeva@mephi.ru. Scopus Author ID 56018762000, SPIN-код РИНЦ 8644-7631, https://orcid.org/0000-0002-9856-6031

Беляков Владимир Васильевич, к.т.н., доцент, отделение нанотехнологий в электронике, спинтронике и фотонике офиса образовательных программ (414), Институт нанотехнологий в электронике, спинтронике и фотонике, ФГАОУ ВО Национальный исследовательский ядерный университет «МИФИ» (115409, Россия, Москва, Каширское ш., д. 31) E-mail: VVBelyakov@mephi.ru. Scopus Author ID 7103252626, SPIN-код РИНЦ 5436-8927, https://orcid.org/0000-0002-0236-1243

Шабля Алексей Олегович, заместитель генерального директора, ООО «Модус» (117638, Россия, Москва, Варшавское шоссе, д. 56, стр. 2). E-mail: a.shablya@analizator.ru. https://orcid.org/0000-0002-4605-945X

Сазонов Андрей Гавриилович, генеральный директор, ООО «Модус» (117638, Россия, Москва, Варшавское шоссе, д. 56, стр. 2). E-mail: kerber@analizator.ru. https://orcid.org/0009-0008-1540-6739

Translated from Russian into English by V. Glyanchenko
Edited for English language and spelling by Dr. David Mossop